
We would like to thank the reviewers for their useful comments and suggestions which have helped us to improve the manuscript.

Reviewers' comments

Reviewer 1, Reviewer 2, Reviewer 3

**Authors' response is shown in black and bulleted.
Quotes from the manuscript are in italics.**

Please note:

1. Some figure numbers have been changed in the revised version of the manuscript. New figure numbers are referenced in any related comments.
2. There has been some substantial restructuring of the article following the comments of the reviewers. This has made the track-changed document very difficult to read. Therefore, we strongly suggest reading the revised manuscript and only consulting the track-changed version for specific alterations. **Any line numbers referenced in the authors' response refer to this revised version of the manuscript.**

It has been brought to our attention that the dropsondes used to initialise the model were affected by a dry bias, leading to an underestimation of the humidity in the model. Given that we initialise the cloud fields in each simulation from an assumed adiabatic profile, this has had little impact on our conclusions. Nevertheless, we have acknowledged this dry bias in the manuscript, and have provided profiles of the revised data, and an example simulation for justification, in the Supplement. The reasons behind this bias are detailed at the following link:

[https://www.eol.ucar.edu/system/files/software/Aspen/Windows/W7/documents/Tech%20Note%20Dropsonde Dry Bias 20160527_v1.3.pdf](https://www.eol.ucar.edu/system/files/software/Aspen/Windows/W7/documents/Tech%20Note%20Dropsonde%20Dry%20Bias%2020160527_v1.3.pdf)

Reviewer 1:

Review of “Microphysical sensitivity of coupled springtime Arctic stratocumulus to modelled primary ice over the ice pack, marginal ice and ocean” by Young et al. This paper uses LES simulations of mixed phase Arctic clouds in order to determine the sensitivity of the microphysical structure and lifetime of single-layer mixed phase stratocumulus clouds in the Arctic to three different ice nucleation parameterizations. Overall, I think this is an excellent paper that would be a great fit for ACP, and honestly all I think the authors need to do is to improve the presentation in some of the figures. The uncertainties in the model simulations and data are very thoroughly discussed, the procedures they used are well documented, and I think that it is interesting to find that small uncertainties in Nice can lead to drastically different simulations, which further adds to our need to better characterize the microphysical observations of mixed phase stratocumulus.

I have some minor comments that would improve the paper. In general, I do think Figures 5,6, and 8 do need to be more readable, as many of the sub panels are quite small and can be difficult to read at points.

- We have made Fig. 5 clearer, and split Figs. 6 and 8 into 3 separate figures for each case study. These new figures show each of the 5 implemented parameterisations split over sea ice (Fig. 6), MIZ (Fig. 9), and ocean (Fig. 10).

I also think that Figures 7a,b,c are not needed as the conclusions reached by those figures could be misleading since you are comparing modelled Nice to observed Nice >100 , which are not the same quantity since they cover different size ranges of particles. Particles with sizes less than 100 microns can vastly outnumber those at larger sizes, so it is crucial to make sure that the number concentrations being compared cover the same size range.

- Figure 7a-c has been removed following Reviewer 1’s concerns.

Secondary ice production processes also occur in Arctic mixed phase stratocumulus, such as in Rangno and Hobbs 2001. I think it would be a benefit to mention them in the introduction when you introduce primary nucleation. You can then mention that the focus of your study is on primary nucleation rather than secondary production.

- The beginning of this paragraph (page 2, lines 20-22) has been updated to reflect Reviewer 1’s comment:

“Ice crystals may form through primary or secondary processes in Arctic MPS (Rangno and Hobbs, 2001). Here, we focus on primary ice formation as secondary ice production has been shown to be less influential in the springtime MPS we shall consider (e.g. Jackson et al., 2012; Young et al., 2016a).”

Reviewer 2:

The authors simulate three cases of mixed-phase cloud near Svalbard, based on observations conducted during March 23 and 29 of 2013 as part of the ACCACIA campaign. The focus of this work is on how ice nucleation parameterizations influence results from the UKMO LEM model in comparison with the observations. The authors use three basic parameterizations: Copper 1986; DeMott 2010; another empirical parameterization (ACC) based on the observations they evaluate against. They also evaluate some extremes of the D10 parameterization and the D10*0.1 is one of the better performers for the ocean case. Overall, D10 and C86 produce more ice, which leaves less liquid water, and ACC produces less ice and more liquid water. In general, ACC compares better with the number concentrations of measured ice particles larger than 100 μm , where the latter is used to put the observations and simulations on the same footing. It is perhaps expected and unfair to say ACC performs better, since it is based on the observations being compared against, but it provides an important perspective on the number concentrations of ice particles.

- We agree that the “performance” of ACC is poor wording as this would likely agree best with the observations due to its derivation from these. We have updated the language throughout the manuscript to use ACC as an “empirically-derived” comparison to the 2 established parameterisations. However, we do feel it is important that the ACC relationship is able to produce both the persistent mixed-phase conditions in each case and a comparable ice phase to the observations as well.

The authors identify a “sweet spot” in the number concentration of ice particles, represented by either the ACC or D10*0.5 parameterizations, at which the balance of liquid and ice in these cold clouds over ocean is able to maintain a persistent mixed phase without glaciation or generating too much convection. In general, the study points to the strong sensitivity of Arctic mixed phase clouds to ice crystal number concentrations. Also, for the three cases studied, the authors show that ice nucleation under water saturated conditions must be implemented.

The paper is long and a little difficult because of the many tests and the bouncing back and forth among figures 6 through 9, but it is otherwise well organized, the discussions are good and the results are interesting and important. The paper is appropriate for ACP.

- We agree that the paper includes a lot of comparisons and can be complicated to follow. We have made efforts throughout the manuscript to make it easier for the reader to follow our arguments.

Specific comments:

1) Section 2.2 - Some clarification of the context of the model and observations is needed. The dropsonde data are used for model initialization. The model then simulates cloud for 24 hours, with the first 3 hours considered as “spin-up”. During the 21 hours of simulation, is the model maintaining the same underlying surface: i.e. ice for case 1, mixed ice and water for case 2 and water for case 3? It would seem that in reality the MIZ cloud may have moved from over the MIZ to open water during the time equivalent to the simulation period.

- For simplicity, the same surface conditions are maintained throughout the full duration of each model run. We acknowledge that this approximation is idealistic and, instead, it is likely that surface temperatures would increase. We have made this clearer in the manuscript (page 4, lines 24-25).

“These surface conditions were kept constant throughout each simulation.”

Were the in-situ microphysical observations conducted near the locations of the dropsondes or farther downwind? There appear to be differences in the heights of the clouds between the microphysical measurements and the dropsondes with the microphysics suggesting deeper cloud.

-
- The in-situ observations were conducted geographically close to the dropsonde measurements; however, they were carried out at a later time (case 1 ~ 3 h, case 2 ~ 5 h, case 3 ~ 5 h). We are aware that cloud structure will have changed between these measurement times. As mentioned, this is particularly clear in case 2 where the cloud has deepened between the times of the sonde and in situ measurements. We were limited to the data we had from the campaign, so unfortunately measurements closer in time were not made. We have made it clearer in the manuscript (page 8, lines 6-12) that these measurements are co-located spatially, but not strictly temporally. Additionally, as summarised at the top of this document, a potential dry bias in the dropsonde measurements was brought to our attention after our study was completed. We have addressed this bias in the manuscript, and included details – and additional simulations – in the supplementary material.

“These aircraft observations sampled the same geographical location approximately 3-5 hours after the dropsonde measurements; therefore, some evolution in cloud properties between the two data is expected. These dropsonde data were affected by a potential dry bias, as discussed by Young et al. (2016a): corrections were applied after this study was completed, and the revised profiles are shown in Figs. S1 and S2. Whilst the general properties of the modelled clouds are mostly unchanged with these corrections imposed, the development of precipitation is affected (examples shown in Figs. S4, S5). Our conclusions are unaffected by this bias; however, these revised profiles highlight an additional sensitivity to humidity in the three cases considered here (see the Supplementary Material for further details).”

2) Presumably, changes in the numbers and sizes of the cloud droplets will also affect the WBF process. Why did you use a cloud droplet number concentration of 100/cc, when you have the measurements from the CDP that you could have used?

- We used a consistent cloud droplet number concentration across all simulations to ensure the differences between each case were due to the changes in primary ice number alone. Measured N_{drop} for cases 1, 2, and 3 were $110 \pm 36 \text{ cm}^{-3}$, $141 \pm 66 \text{ cm}^{-3}$, $63 \pm 30 \text{ cm}^{-3}$. Cloud droplet number concentrations for cases 1 and 3 have been previously reported in Young et al., 2016a. We have now reported these values in the manuscript (page 5, lines 6-8).

“A prescribed droplet number of 100 cm^{-3} , approximated from the measured values of $110 \pm 36 \text{ cm}^{-3}$, $141 \pm 66 \text{ cm}^{-3}$, and $63 \pm 30 \text{ cm}^{-3}$ (Young et al., 2016a) for cases 1, 2, and 3 respectively, is applied in all simulations.”

3) For case 1, how are you sure the liquid phase existed? The CDP is a one dimensional probe. What were the droplet number concentrations?

- N_{drop} for case 1 was $110 \pm 36 \text{ cm}^{-3}$. These observations have been detailed previously in Young et al., 2016a; therefore, we did not wish to go into detail in order not to encroach on that study. The observations suggest that there was indeed liquid in the case 1 cloud, but the cloud droplets were very small in size (~5 μm effective radius). We have now quoted the number concentrations in the manuscript for completeness (see above).

4) Section 4.1, line 12 – at or below 500 m?

- This should read “below 500 m”, thank you for highlighting this mistake. We have updated the manuscript accordingly (page 10, line 24).

5) Page 12, line 1 – provide a reference for the 2DS statement.

- References have been included as requested (page 12, line 4 – page 13, line 2):
-

“2DS data has poor resolution at small sizes (<80 μm), preventing the particle shape factor from being accurately determined at these sizes (Crosier et al., 2011; Taylor et al., 2016; Young et al., 2016a); therefore, the number concentration of small ice crystals is not a reliable measure with this instrument.”

6) Page 14, line 1 – among rather than between.

- We feel that this change would have changed the meaning of the sentence, and would be incorrect. We acknowledge that this sentence was not clear; therefore, it has been changed to the following (page 12, line 4):

“The poor resolution of 2DS data at small sizes (<80um) prevents the particle shape factor from being accurately determined”

7) Page 18, lines 1-3 - In figure 7, D10 produces the highest ice numbers for >100um. Even using the total measured ice numbers, D10 is still high. D10 appears to do relatively well in case 1, and it is closer to the observations than C86 in case 3. Is your reference to case 2 a mistake? If not, please explain how you arrive at this statement. The statement on lines 2-3 of page 19 appears to contradict.

- The reference to case 2 was not a mistake. When considering the values quoted in Table 3, D10 produces lower N_{ice} than C86 in every case, and therefore provides better agreement with the low N_{ice} observed. We realise that this statement is confusing when, in Fig. 7, D10 was shown to give the highest N_{ice} at the chosen time step.

Following Reviewer 1's comment, Fig. 7(a-c) has been removed to avoid misleading conclusions. The comparison of large ice (new version of Fig. 7, panel b) also shows that D10 gives the highest, and thus compares the worst, with observations. This suggests that a large fraction of the modelled N_{ice} by D10 is growing too efficiently in the model with comparison to the observations. With less (total) ice than C86, the ice particles are allowed to grow larger.

8) Page 19, line 7 – There may be fewer sources, but so little is known about INP in the Arctic that I think this sentence would be better removed.

- This sentence has been removed as requested.

9) Possibly of interest to the authors, INPs measured at Alert, Nunavut (Mason et al., Atmos. Chem. Phys., 16, 1637–1651, 2016) during spring to early summer vary from 0.2 per litre to 1 per litre for temperatures from 20oC to 25oC, which covers the range of average ice particle number concentrations you report for the three cases.

- We thank Reviewer 2 for bringing this study to our attention, we have included a reference to it in Sect. 5.4.3 (page 24, line 14 onwards):

“ These concentrations compare well with INP measurements made at the Alert station in the Canadian Arctic in the spring of 2014, where mean INP number concentrations of 0.05 L⁻¹, 0.2 L⁻¹ and 1 L⁻¹, at -15 °C, -20 °C, and -25 °C respectively, were measured by Mason et al., 2016.”

Reviewer 3:

The paper "Microphysical sensitivity of coupled springtime Arctic stratocumulus to modelled primary ice pack, marginal ice, and ocean" by Young et al. 2016 investigates the sensitivity of three Arctic mixed-phase clouds (at different surface conditions) to primary ice concentrations for three different types of primary ice parameterisations. The simulated microphysical properties of the three case-clouds are compared to field observations. The setup of the study is interesting and provides some nice insights about the modelling of Arctic mixed-phase clouds. However, some parts of the discussion are quite circuitous and could be a bit better organised to transport the main message of the paper in a more compromised way. In total the study is suitable to be published in ACP.

General comments:

- Some sentences of the abstract are not very clear for readers who haven't looked at the paper yet. More specifically in line 7 it is not very clear what kind of key sensitivities (of what to what) you are referring to. It also reads as if the key sensitivities emerge from the comparison to the observations, but they already emerge from the sensitivity simulations itself (or from a combination of both).

- We have updated the language to specifically refer to cloud ice number concentrations (page 1, lines 7-8):

"Three key dependencies on N_{ice} are identified from sensitivity simulations and comparisons with observations over the sea ice pack, marginal ice zone (MIZ), and ocean."

In line 11 it is not specified what kind of parameterisations you are talking about. You should add "for primary ice nucleation" (or something similar).

- We have included this information as requested (page 1, lines 10-12):

"We show that warm supercooled (-13°C) mixed-phase clouds over the MIZ are simulated to reasonable accuracy when using both the DeMott et al., 2010 and Cooper 1986 primary ice nucleation parameterisations."

In line 16 you could add half a sentence what "cloud break up" is.

- We have lengthened this sentence (page 1, line 17) to read:

"... promoting cloud break up through a depleted liquid phase"

- The terming "primary ice crystals/primary ice number concentration" is not always consistent, e.g. on page 5, line 11 it is written "pristine ice crystals". It is also not clear how different the terming is meant in the different parameterisation schemes. In DeMott et al. 2010 the parameterisation scheme refers to INP, but INP translate directly to primary ice crystals (the way they mean it) and therefore the parameterisation schemes should technically be the same. If that is not the case, a better explanation (also of how it is differently implemented in the model) would be needed.

- We have used the terms as they appear in the parent articles to be distinct in their meaning, as the parameterisations predict subtly different things. Cooper 1986 was derived from measurements of ice number concentrations, whilst DeMott et al., 2010 was derived from INP measurements. The ice number concentration is the key quantity of importance to our study. For the analysis presented, we have chosen to refer to primary ice number concentrations. We felt it was important to highlight the fact that DeMott et al., 2010 was derived from INP measurements, and therefore should only be used to predict INP number concentrations. We are assuming that these all activate and, whilst this is potentially the
-

case, it is possible that the conditions attained were not suitable for all to do so. It is therefore an assumption that our D10 INP all activate. This is discussed in Sect. 5.4.

Following this comment, we decided to be more explicit in the manuscript when referring to ice number concentrations. N_{ice} is used to refer to ice number concentrations; for example, from evaluated parameterisations or observations. N_{isg} is used to refer to the total frozen (ice+snow+graupel) number concentrations simulated with the model. This distinction has been made to make it clearer what parameters are being compared at each step.

The terming "primary ice nucleation" does sound tautologous (nucleation always leads to primary ice).

- We agree that it is repetitive phrasing; however, it is often referred to in this manner and we wish to make the clear distinction that only primary processes are being considered.

- It would also be interesting to add a simulation where the different freezing pathways (immersion freezing and deposition nucleation) can compete and look at the importance of the different pathways acting in different S/T-regimes. I was missing this discussion or the discussion of this aspect in the manuscript. Of course it is interesting to look at the resulting ice crystal concentrations of both pathways separately but in reality both pathways could take place in parallel or rather compete with each other depending on the environmental conditions.

- The influence of deposition-condensation, immersion- and contact-freezing acting together is discussed in the Supplement, using Cooper 1986, Bigg 1953, and Meyers et al., 1992 respectively. When using these three parameterisations combined, the modelled microphysics is unrepresentative of the observations (Fig. S7). In case 1, no liquid is modelled when using all three parameterisations, and the ice phase agrees poorly with observations (similar to the C86-only cases presented in Sect. 4.1). Including Bigg immersion-freezing and Meyers et al., 1992 contact-freezing increases the ice number concentrations in case 2 to quantities much larger than observed ($\sim 2 \text{ L}^{-1}$). In case 3, the inclusion of these immersion- and contact-freezing parameterisations causes a sharp increase in the modelled ice number concentrations; an increase which causes cloud glaciation. When immersion-freezing is represented by the Bigg parameterisation for freezing rain drops, the ice number concentrations are increased, thus producing poorer agreement with observations. A summary of these findings have been added to Sect. 4.1; however, the majority of the discussion has been kept in the Supplement.

We are not directly referring to immersion-freezing with our method, instead we are stating that water saturation must be attained before ice nucleation can occur. This simply means that we only allow ice crystals to form when there are also cloud droplets present. We do not specify a nucleation mechanism, instead we are assuming that any of condensation-, immersion-, or contact-freezing could be occurring under these conditions to give the resulting ice crystal number concentrations. If we were to assume that our limitation is representative of immersion-freezing alone, and used this additionally within the Morrison et al., 2005 microphysics scheme, we would simply get two sources of ice (from the deposition parameterisation and the immersion parameterisation) instead of just one. The Morrison et al., 2005 scheme therefore is not tailored to investigating the competition between different modes of freezing, as the represented modes simply add to the ice fields when these parameterisations are satisfied, independent of each other.

To investigate the competition between different freezing modes, the composition of aerosol would need to be explicitly represented to take into account the dominance of one freezing mode over another in different environmental conditions for different aerosol particle species. A spectral microphysics scheme may therefore be more appropriate to conduct this pathway of investigation; however, such schemes are rarely included in 3D models due to computational cost. To investigate the competition between the modes of freezing, we

suggest that a different scheme, which explicitly resolves aerosol composition and size distributions, would be necessary to provide an accurate representation of the competition between the microphysical processes occurring in these clouds.

- The result that ACC provides the best agreement with the observations (e.g. page 11, line 3) is trivial since the parameterisation is based on the observations. However, it is interesting to have an empirical parameterisation in the comparison, but maybe a bit more critical discussion on this could be added.

- We agree that the “performance” of the ACC relationship is poor phrasing, and have updated its use in the manuscript to be an “empirically-derived” comparison for the two established parameterisations. Reviewer 2 also highlighted this issue, and it has been addressed throughout the manuscript. We feel it is important to include the ACC results as it shows that persistent mixed-phase conditions can be attained with its use across all three cases. We address the limitations of this relationship in Sect. 5.5, but have included more critical discussion as requested. Specifically, we have focussed on the over predicted liquid phase and potential overestimation of cloud stability (i.e. would this relationship allow for cloud break up downstream?).

- The first part of the paper is quite lengthy, especially the comparison of every single case. Some plots do not seem very interesting at the first point but are very interesting later in the discussion when you explain some of the details behind some features (e.g. Fig. 8). I also had the feeling that later in the discussion many things are repeated (e.g. in section 5.4.3). The discussion itself was (just looking at the headers of the sections) not very intuitively organised, it is quite difficult to see where this now leads to/what the main points are/will be (before reaching the conclusions). It could help to restructure the paper/think again how to organise it so that the focus is clear and the paper interesting to read without losing interest in the first part.

- We had originally structured the article into distinct Results and Discussions sections to adhere to ACP’s manuscript preparation policies. However, we agree that some restructuring would help to keep the reader motivated and emphasise the focus of the article. We have therefore restructured the Results and Discussions sections to make the focus of the article clearer to the reader throughout.

I had the feeling that most of the description on page 22 and also section 5.4.3 could already be moved to the case description and make this part more interesting to read. Also the comparison of the cases within each other came quite late (before they seemed to be quite isolated in the analysis). However, this point might be subjective and a matter of taste.

- Comparisons between simulations that were detailed in Sect. 5.4.3 have now been moved to the relevant case results section to make the focus clearer.

Specific comments:

- Page 2, line 15: Add which kind of parameterisations you are talking about.

- Sentence has been updated to refer specifically to ice nucleation:

“...commonly-used mid-latitude parameterisations for primary ice formation, such as...”

- Page 2, line 20: You should add in brackets the name of the four ice nucleation modes you talk about. You could also add a bit more explanation (or more structured explanation) about the different ice nucleation modes. You mention that partly later, but maybe it would help the inexperienced reader if you have short explanations first before you elaborate the pathways and their representation in models in detail.

-
- This paragraph has been expanded to reflect Reviewer 3's comments. A sentence giving an approximate description of each nucleation mode has been included. This paragraph has also been reorganised to accommodate these changes (page 2, lines 22 - 30).

- Page 2, line 20: In most models not all four ice nucleation modes are represented. It is a bit miss leading to say "commonly represented". Many models only treat immersion freezing, on the contrary contact freezing is very rarely explicitly modelled.

- This section has been reworded to describe the modes physically instead of in a modelling context (page 2, lines 22-25).

“Primary ice particles may be nucleated heterogeneously through four different modes of action; deposition, condensation, immersion, and contact (Pruppacher and Klett, 1997). These modes describe the deposition of water vapour onto an INP, forming ice directly (deposition) or freezing upon condensation (condensation), or the freezing of a cloud droplet through activation from within (immersion) or collision with an INP (contact).”

- Page 2, line 26: Your example does not fit to the argumentation before (referring to deposition nucleation instead of immersion freezing).

- The argument was correct, but we agree that not enough information was included. By suppressing the deposition mode, we were implying that the immersion mode would likely occur. In our reorganisation of the manuscript, we decided to remove this discussion from the manuscript as the introduction had become quite lengthy and this information was not strictly necessary to our study.

- Page 2, line 28: You write that deposition nucleation and condensation freezing are experimentally difficult to distinguish but most instrument have rather difficulties to distinguish immersion and condensation freezing since in both cases the liquid phase is involved. Deposition nucleation takes place at a different saturation ratio/temperature regime compared to condensation freezing. Many models use immersion freezing as a surrogate for immersion and condensation freezing. I was surprised to read that deposition nucleation should be often related to condensation-freezing- are you referring to pore-condensation? Maybe this issue is related to the definition used of the nucleation modes and more a matter of phrasing/language but it could be confusing to other readers as well, so it might be better to add more explanation.

- We were referring to measurements made in the past through which parameterisations have been derived (e.g. Cooper 1986, Meyers et al., 1992). These articles refer to deposition-condensation nucleation as they could not guarantee one mode was occurring without the other. We agree that the immersion-condensation freezing argument is similar, especially with the most up-to-date INP counters which utilise water saturated conditions within their chambers. We are not specifying which nucleation mode we are referring to as we are simply making ice nucleation occur at water saturation; in reality, this could encompass immersion-, condensation-, and/or contact-freezing. For the purpose of this article, we simply wish to acknowledge the difficulties in measuring specific ice nucleation modes and knowing how others have done it in the past. We agree that in its current state this argument could be confusing; therefore, we have adapted the language to make this distinction clearer (page 2, lines 26-28).

“Due to their similarities, it can be difficult to differentiate between these mechanisms in measurements; for example, deposition or immersion nucleation are often quoted to occur alongside condensation-freezing processes (e.g. Cooper 1986; Meyers et al., 1992; de Boer et al., 2010; Fan et al., 2016).”

- Page 2, line 10: What do you mean when you say "ice number concentrations will be suppressed under these conditions"? So deposition nucleation is also only allowed to take place at water saturation? That does not make sense physically.

- As above, we are not specifying a nucleation mode. We are using the location of the deposition-condensation parameterisation in the microphysics scheme to input an ice nucleation parameterisation; this parameterisation is not always used under deposition conditions, in fact we restrict the parameterisation to water-saturated conditions for the majority of the model runs presented. We used this language so that those familiar with the scheme could follow, but we agree that this may have been misleading. We have updated the language (page 3, lines 12-14) to make this clearer.

"We hypothesise that ice number concentrations will be suppressed and liquid fractions will be enhanced under this restriction, thus reducing the influence of the WBF mechanism and prolonging cloud lifetime."

- Page 4, line 20: What is a sub-Arctic McClatchy profile? Either explain or generalise?

- A McClatchey dataset includes historical measurements of stratospheric transmittance. These profiles allow the optical properties of the simulated atmosphere to be representative of the region modelled, and are used to determine the attenuation of radiation by the atmosphere. Vertical profiles of tropospheric temperature, pressure, water vapour, and ozone were imposed. The sub-Arctic versions used are relevant to this region alone and differ, for example, from similar measurements in the tropics. Additionally, the spelling of McClatchey has been rectified (page 4, lines 26-28).

"Sub-Arctic McClatchey profiles of tropospheric temperature, pressure, water vapour, and ozone -- based on historic measurements of stratospheric transmittance -- were imposed in all simulations to ensure the initialised vertical profiles were representative of the environment modelled."

- Page 4, section 2.2: What is the time step of the simulations? 150 seconds?

- The time step is variable to satisfy CFL criteria and varies between case studies. For cases 1, 2, and 3, Δt was approximately 0.3 sec, 0.4 sec, and 0.2 sec respectively. This information has been included in the manuscript (page 4, line 25-26).

- Page 5, line 3-7: You can skip this explanation since you switch of Bigg 1953 and Meyers 1992 in the final simulations. That is confusing (especially when readers watch out for B53 and M92).

- We wish to keep this information in, again, for those familiar with the microphysics scheme. It is important to the study to know that these have been specifically switched off. We have removed the short-hand for the parameterisations and reworded this paragraph to reflect this comment. We have moved this discussion to Sect. 4.1 (page 10, lines 3-17).

- Page 6, line 11: It is good that you point out the limitations of this study. However, it would also be nice to add how realistic this idealistic study is and under which conditions you would have a similar system in reality.

- The model setup is idealistic in terms of the surface conditions and the representation of ice nucleation; therefore, we wished to stress this to the reader. However, the model is able to produce cloud microphysics comparable to the observations in some cases, simulating clouds which persist for lengths suggested by previous observations. This suggests that our assumptions may be credible, creating an environment that is more representative of reality than first thought.
-

Whilst INP depletion may be more applicable to clean environments susceptible to INP plumes, INP recycling below cloud and/or a source of INP at the surface/aloft could act to continually supply INP to the cloud via advection or entrainment. This study could act to represent such an environment with a consistent source of INP.

We have added information to this effect into the manuscript (page 6, lines 12-14):

“However, this setup can give an approximation of the cloud microphysics that may form in the vicinity of an INP source; for example, a local source at the surface or a long-range transported INP population aloft.”

- Why did you only add an ice crystal number concentration sensitivity for DeMott et al. 2010? Is there a reason you picked this parameterisation and did not add it for all of them (computational costs?)?

- Yes this was predominantly due to computational cost and time constraints. We wished to include sensitivity tests, and decided to choose the most recent parameterisation for these, which is based on measurements using updated techniques. This has been added into the manuscript for clarification (page 6, lines 19-20):

“We chose D10 for this sensitivity study as this is the more up-to-date of the two established parameterisations used.”

- Fig. 1: You should plot the parameterisation only in the temperature range where they are valid or make them transparent in the temperature regime beyond their validity. Or do you extrapolate the parameterisations schemes over the whole temperature range in your model setup (then I miss interpreted it wrong before)?

- We have updated Fig. 1 to show the parameterisations in their valid temperature ranges only. Reviewer 3 is correct, these are not extrapolated outwith this range (except for ACC in case 3, this is discussed in Sect. 5.5 as being a point to note about this simulation).

- Fig. 1: Instead of having three line for D10 and the corresponding variations, you could only plot D10 and add a shaded area around the line. The D10 Fit is not needed. You also do not really discuss it in detail later. The D10x0.5 line is not really needed here, you already describe it later (and no visualisation is necessary). However, of course you can keep it, it would just make the figure a bit less busy.

- Figure 1 has been updated following Reviewer 3's comments. We were unsure of what shaded area was requested; therefore, we have opted to show the variability (due to different aerosol loadings) in each version of D10 (D10x0.1, D10, and D10x10).

- Fig. 2: You could increase the figure to enable better readability. Remove the doubled red altitude axis on the right (or colour it black), that is miss leading. It would be useful to add the cloud extent in the figure. Would you still need the grey boxes when you add the cloud extent to the figure (since the altitudes without sampling seem to be always below cloud)? Would it be possible to use the same scale for all cases?

- Reviewer 3's comments did not apply to Fig. 2, so we assumed (through their comments) that they were referring to Fig. 4. We would like the current grey boxes to remain as, although these altitudes do appear to be below cloud across the three cases, we cannot say for certain what was present at these altitudes because we didn't sample there. We would like to illustrate that surface fog or a low-altitude cloud layer, for example, cannot be ruled out. We have removed the red axis and have altered the scales as requested. Cloud extent is inferred by the measurements, as only in-cloud measurements are shown.
-

- Page 10, line 14 and line 17: At which altitudes are the ice crystal concentrations estimated?

- For case 2, the concentrations are taken from approximately 1000m, at the end of the simulation. For case 3, these are taken from ~1450m. This information has been added to the manuscript (page 10, lines 27-28, lines 29-30).

“Modelled N_{isg} over the MIZ ($\sim 1.0 L^{-1}$ at 1000 m, Fig. 5b) is in reasonable agreement with the mean observed ($0.35 \pm 0.20 L^{-1}$, Table 2).”

“Such conditions are also attained in case 3 (Fig. 5c); modelled N_{isg} peaks at $3.7 L^{-1}$ at ~1450 m, whereas only $0.55 \pm 0.95 L^{-1}$ was observed.”

- Fig. 5: You could increase the figure to enable better readability. The scale is not reasonable (there should not be negative Q_{liq}).

- Figure size and scale amended as requested.

- Page 12, line 6: Can you further explain this?

- The shaded areas in Fig. 7 represent the variability in the Q_{liq} profile over the given time window. In contrast to the $N_{ice>100um}$ data, clear contours of shading are not present around the plotted profile. This is what we were alluding to with our analysis; however, we felt this comment is not necessary (and confusing) and so have removed it from the manuscript

- Page 12, line 8/Figure 8: Again is the D10 Fit really needed here?

- The D10 simulation shown in Fig. 8 is the D10 run for each case, not the fit from DeMott et al., 2010 that was shown in Fig. 1. Figure 8 has now been dissected to show each parameterisation for each case (Figs. 6 and 8 now make up Figs. 6, 9, and 10); therefore, this query should no longer be an issue.

- Page 12, line 14: Why does IWP decrease subsequently?

- The IWP decreases once the ice number concentration begins to be depleted in the cloud layer, through fallout as snow (page 13, lines 11-12).

“... the simulated IWP increases initially (between approximately 17 h and 20 h), but subsequently decreases as the N_{isg} falls out from the cloud layer.”

- By how much is $N_{\{ice > 100 \mu m\}}$ still clearly related to the ice nucleation parameterisations in your model? Which other processes might influence this variable? Is it fair to compare this variable among the different parameterisations (since that is not the size of primary ice formation)?

- $N_{\{ice > 100 \mu m\}}$ is the number concentration of ice crystals larger than 100um in size only. We believe this is a robust parameter to compare with observations as we can be confident that we are comparing ice crystals over the same size range. As for the comparisons between simulations, the only differences are the parameterisations themselves; therefore, any additional processes which act in one simulation will act in all of the simulations. We feel that $N_{\{ice > 100 \mu m\}}$ is the best parameter to compare with the observations, whilst N_{isg} (total ice+snow+graupel number concentration) is more suited for comparisons between the model simulations. We have altered the language throughout the manuscript to make this distinction clearer.

- Fig. 6: Would it be possible to use the same scale for all cases?

-
- Figure 6 has been dissected into each separate case following comments from the other reviewers. In each separate case, the 5 simulations (for each parameterisation) are shown on the same colour scale.

- Fig. 7: It is very difficult to compare the single lines. It would help to increase the size of the figure. It would also be possible to cut Fig. 7 a, b, d, e, g, h to the relevant altitudes (leaving away everything above 1000 m). It is unclear over which time span the mean was taken and why. What was the availability of the observations? Did you choose to calculate the mean as described to temporally collocate the data?

- Following Reviewer 2's comments, the first row (7a-c) has been removed, making the 6 remaining sub-figures clearer. For the observations, the mean is taken over all measurements of the relevant cloud layer. The mean at each altitude bin was taken over approximately one full hour of data; however, each altitude was sampled differently due to constraints on the flight track (i.e. vertical profiles were not taken, a selection of straight-and-level runs and sawtooth profiles makes up the data from which the mean is calculated). This observed mean (at each altitude) was then subtracted from the modelled mean (per hour) for the full 24h simulation to find which time step gave the best agreement with the observations, allowing for the best possible comparison for each case. The time step selection is detailed in the supplement.

- Page 15, line 3: Why do the glaciation events take place every 3h? What is driving that?

- High concentrations of ice crystals are produced which use up the water vapour in the air through depositional growth, causing the ice supersaturation to decrease. Therefore, large number concentrations of ice crystals are produced when ice supersaturation is reached, these deplete the vapour, fall out of the cloud and sublimate, and the ice crystals form again when ice supersaturation is reached (which occurs readily due to the cold temperatures modelled). This explanation has been included in the manuscript for clarity (page 17, lines 20-23).

“Due to the strong dependence of N_{ice} on temperature, high N_{isg} are created which readily undergo depositional growth, deplete the vapour field, and fall from the cloud once the particles transition to the snow category. The vapour field recovers due to the moisture fluxes from the surface, and the process repeats once water and ice supersaturation are attained.”

- Page 15, line 13 + page 15, line 17: You do not really mention or explain the spikes here which is a bit irritating. You also do not explain (here) why only D10 has these glaciation peaks. It is also unclear (here) why in case of C86 the glaciation leads to a decrease of IWP and not an increase. You could think of reorganising your paper so that you add already part of the discussion here.

- As above, these sections have been reorganised to make these points clearer to the reader.

- Page 15, line 22: Explain what W is.

- W represents the vertical velocity. This has been updated in the manuscript (page 18, lines 11-12):

“... and the vertical velocity, W , is chosen at approximately cloud top (1500 m).”

- Fig. 8: Was more interesting later for the discussion but at this part of the paper it does not seem so interesting, you might want to shift either the figure or the discussion (see general remarks). Fig. 9: The features (peaks) are not really clear until the discussion. You could add the periods at the time scale when the cloud had a mixed-phase structure/when there was a cloud. Fig. 10: The

differences of the last three lines did not get very clear before the discussion also includes the precipitation (Fig. 11)- it could help to reorganise the discussion here.

- As above, we have restructured the article to include some discussion in the same section as the figure to motivate the reader.

- Page 15, line 33: The unit for the precipitation is a bit confusing here (is clear in Fig. 11). Fig. 11: It would be an interesting information to also add the total amount of precipitation for all the cases (mm/m^2).

- This may be misleading, as the rain produced is effectively virga as it evaporates below cloud and does not reach the surface. We consider large particles, which are falling relative to the cloud layer, to be precipitation, and it is the number concentration of these particles that is of interest to our analysis. We agree that using the term “precipitation” here may be misleading; therefore, we have adapted our language throughout to refer to “precipitable particles” and “large hydrometeors”.

- Page 21, line 2: You could elaborate here why it is so different in case 3. What is different in that case?

- The dropsonde data used to initialise the model gives a moist boundary layer in which cloud forms immediately. This cloud is unsustainable due to its mixed-phase, high N_{ice} nature, and it begins to decay by the WBF mechanism (added to page 16, lines 1-2).

“Cloud forms and begins to decay immediately in case 3, as shown by the decreasing LWPs modelled (Fig. 8c), caused by the moist BL and a high N_{isg} which acts as an efficient sink for liquid by the WBF mechanism.”

- Page 21, line 14: It is good that the modelled N_{ice} is in reasonable agreement. However, if that is due to colder temperatures than observed, it would indirectly mean that the temperature dependence of the parameterisation schemes used (or the temperature regime where they are efficient) is not correct. You could add some critical thoughts about this issue.

- As Fig. 7 has now changed, we have rephrased this argument to avoid confusion. Whilst the absolute number concentration of total ice particles is in reasonable agreement with observations (Tables 2, 3), it is important to note that the $N_{\{\text{ice}>100\mu\text{m}\}}$ agreement is poor (Fig. 7b). We have addressed this issue in the manuscript, and added some critical discussion as requested (page 22, lines 9-13):

“As a result, the $N_{\text{ice}>100\mu\text{m}}$ modelled with the temperature-dependent parameterisations considered is greater than observed (Fig. 7b). Overall, the N_{isg} is in reasonable agreement with the observed N_{ice} (Tables 2, 3), likely due to the low concentrations of snow and graupel produced at the warm sub-zero temperatures considered, and it is probable that this agreement would improve further if the modelled temperature was accurate. In contrast to cases 1 and 3, the reasonable agreement of N_{isg} and poorer agreement of $N_{\{\text{ice}>100\mu\text{m}\}}$ suggests that the ice crystal growth rates are too efficient in case 2.”

- Page 23, line 12: I did not understand what you meant by “sweet spot” here when you mentioned it the first time. However, it was clear later on.

- This reference has been updated to be clearer (page 21, lines 12-13):

“...there is an optimal N_{ice} for cloud persistence in this case...”

The “sweet spot” reference in the Conclusions has been kept the same to emphasise its importance.

- Page 25, line 5: Add the order of magnitude.

- We have restructured this paragraph and the comment in question has been removed as a result. We have ensured a range for ice number is quoted in the revised paragraph. This discussion is now Sect. 5.6, on page 24.

- Page 26, line 2-4: Could the less pronounced difference in case 2 (compared to 1 and 3) be a result of the higher cloud top temperature and the onset temperature of freezing? It would be an interesting aspect to add to the discussion.

- Yes, with a higher CTT, less ice will form in the cloud in the absence of secondary ice production. We have included this aspect in our discussion in Sects. 5.3 and 5.7.

Technical corrections:

- Page 1, line 12: The Cooper (1986) parameterisation...

- Changed as requested.

- The ice nucleation pathway deposition nucleation is commonly not named deposition freezing, since it does not involve the liquid phase (and freezing refers to the liquid phase).

- Changed throughout the manuscript as requested.

- Page 3, line 14: Replace guide by guidance.

- Changed as requested (now page 3, line 18).

- Page 3, line 32: You could exchange the second with the first sentence.

- Changed as requested (now page 4, lines 3-5).

- Page 4, line 18: The numbering of the cases is wrong in this case (here it reads as if the ocean case is number 2 and the marginal ice zone case is number 3). You should check if the case-numbering is consistent everywhere.

- Thank you for highlighting this mistake, we had missed it. Case 2 is indeed the MIZ case, and case 3 is over the ocean. We have checked the rest of the document and all other references are correct.

- Page 5, line 2: You write that you vary the form of the deposition-condensation freezing parameterisation but you only use C86 and compare it to D10, which refers to immersion freezing. You should therefore change this here to prevent confusion.

- We were referring to the location of the changed relationship in the Morrison microphysics scheme for those who are familiar with it. As stated, primary ice nucleation is included as three separate parameterisations in this scheme: we removed the separate immersion- and contact-freezing relationships so that the ice could only be formed by the parameterisation that we chose. This change occurred in the position of the deposition-condensation nucleation parameterisation in the code. We see how this may be misleading, however, so we have made this more explicit in the manuscript. This discussion has been moved to Sect. 4.1 (page 10, lines 7 - 17).
-

- The equations have the unit and the dependence in the same bracket, which is a bit strange. It would be more correct to write the unit and the dependence in separate bracket, e.g. $N_{ice}(T_k)$ [m^{-3}].

- Equations 1-3 have been updated with Reviewer 3's suggestions.

- Page 5, line 19: It would read better if you have the text first and then the formula.

- This section has been re-ordered as requested.

- What does the Index k means for the temperature? Why do you not write T?

- The subscript K refers simply to Kelvin. Given that temperature is referred to in both Kelvin and Degrees in the article, we felt it necessary to specify which is being used in the evaluation of each relationship. This has been made clearer in the manuscript.

- Page 7, line 5: Replace These by The (otherwise the reference is missing).

- Changed as requested (now page 8, line 4).

- Page 7, line 12: Skip "over the".

- Changed as requested (now page 8, lines 18-19).

- Page 9, caption Fig. 4: Replace mixed-phase cloud by mixed-phase clouds.

- Changed as requested.

- The numbering/organisation of the figures is not always consistent (e.g. Fig. 7 does not use i/ii for the columns). It would be great to have the explanation of the numbering of the different columns as in the caption of Fig. 10 in the caption of Fig. 1 (you do not need it then in Fig. 10). In Fig. 12 you use the labels i/ii in a different way then before.

- Line plot subpanels are labelled a-f. Colour plot subpanels have an additional label of (1-4) for different data presented from the same simulation. These colour figures are labelled in this way to make it clear that these subpanels are related, e.g. a(1) and a(2) are related and from the same simulation. Figure labels have been updated to follow these guidelines. We have also shortened the figure captions of later figures as requested, by referencing earlier figures.

- Page 20, line 11: Replace , before Mason by ;.

- Changed as requested (now page 23, line 25).

- Page 20, line 30: More accurately would be mixed-phase formation phase instead of formation phase.

- We agree with this requested change; however, on reordering the manuscript, we have removed this reference as it was not necessary to our arguments.

- Page 24, line 30: Move also in between are and not.

- This statement has been moved to Sect. 4.2.3, and re-worded so that the requested change is no longer necessary (page 15, lines 10-13):

"ACC produces comparable $N_{\{ice>100\mu m\}}$ and Q_{liq} to observations as expected – when not considering the shattering event at cloud base (Fig. 4c) – and predicts $0.54 L^{-1}$ at the

case 3 CTT. D10x0.1 produces reasonable agreement with the Q_liq observations at 7 h (Fig. S11); however, the rapidly increasing cloud top height and Q_liq with time are not representative of the observations.”

- Page 26, line 7: Replace microphysical structure by microphysical structure of MPS.

- Changed as requested (now page 25, line 26).

Microphysical sensitivity of coupled springtime Arctic stratocumulus to modelled primary ice over the ice pack, marginal ice, and ocean

Gillian Young¹, Paul J. Connolly¹, Hazel M. Jones¹, and Thomas W. Choullarton¹

¹Centre for Atmospheric Science, School of Earth and Environmental Sciences, University of Manchester, Manchester, UK.

Correspondence to: Gillian Young (gillian.young@manchester.ac.uk)

Abstract.

This study uses large eddy simulations to test the sensitivity of single-layer mixed-phase stratocumulus to primary ice number concentrations in the European Arctic. Observations from the Aerosol-Cloud Coupling and Climate Interactions in the Arctic (ACCACIA) campaign are considered for comparison with cloud microphysics modelled using the Large Eddy Model (LEM, UK Met. Office). We find that cloud structure is very sensitive to ice number concentrations, N_{ice} , and small increases can cause persisting mixed-phase clouds to glaciate and break up.

Three key ~~sensitivities are identified with comparison to in-situ cloud observations~~ dependencies on N_{ice} are identified from sensitivity simulations and comparisons with observations made over the sea ice pack, marginal ice zone (MIZ), and ocean. Over sea ice, we find deposition-condensation ice formation rates are overestimated, leading to cloud glaciation. When ice formation is limited to water-saturated conditions, we find microphysics comparable to ~~the~~ aircraft observations over all surfaces considered. We show that warm supercooled (-13°C) mixed-phase clouds over the MIZ are simulated to reasonable accuracy when using both the DeMott et al. (2010) and Cooper (1986) primary ice nucleation parameterisations. Over the ocean, we find a strong sensitivity of Arctic stratus to ~~ice number concentrations. Cooper (1986) N_{ice} . The Cooper (1986) parameterisation~~ performs poorly at the lower ambient temperatures, leading to comparatively higher ice number concentrations a comparatively higher N_{ice} (2.43 L^{-1} at the cloud top temperature, approximately -20°C) and cloud glaciation. A small decrease in the predicted N_{ice} (2.07 L^{-1} at -20°C), using the DeMott et al. (2010) parameterisation, causes mixed-phase conditions to persist for 24 h over the ocean. However, this representation leads to the formation of convective structures which reduce the cloud liquid water through snow precipitation, promoting cloud break up through a depleted liquid phase. Decreasing the ~~ice crystal number concentration N_{ice}~~ further (0.54 L^{-1} , using a relationship derived from ACCACIA observations) allows mixed-phase conditions to be maintained for at least 24 h with more stability in the liquid and ice water paths. Sensitivity to N_{ice} is also evident at low number concentrations, where $0.1 \times N_{ice}$ predicted by the DeMott et al. (2010) parameterisation results in the formation of rainbands within the model; rainbands which also act to deplete the liquid water in the cloud and promote break up.

1 Introduction

The significant uncertainties associated with global climate model (GCM) predictions may be largely attributed to the inadequate treatment of sub-grid scale, such as cloud microphysical, parameterisations (Boucher et al., 2013). These uncertainties are predicted to enhance discrepancies in temperature forecasts at the polar regions of our planet (ACIA, 2005; Serreze and Barry, 2011; Stocker et al., 2013). The accuracy of these forecasts can be improved by developing the modelled representation of the physical processes involved through comparisons with in situ observations (Curry et al., 1996).

Various observational studies have shown that single-layer mixed-phase stratocumulus (MPS) clouds are common in the Arctic (e.g. Pinto, 1998; Shupe et al., 2006; Verlinde et al., 2007; Morrison et al., 2012). These clouds have been observed to persist for ~ 12 h (Shupe et al., 2006) – with some ~~lasting~~ persisting longer than 100 h (Shupe et al., 2011) – whilst maintaining cloud top temperatures as low as -30°C (Verlinde et al., 2007). Single-layer Arctic MPS typically form at low altitudes and maintain a liquid layer at cloud top which facilitates ice formation and precipitation below (Rangno and Hobbs, 2001; Shupe et al., 2006; Verlinde et al., 2007; McFarquhar et al., 2011; Jackson et al., 2012; Morrison et al., 2012, amongst others). The Wegener-Bergeron-Findeisen (WBF) mechanism strongly influences MPS and initiates a continually-changing microphysical structure. Moderate vertical motions maintain these clouds, where mixing ensures that the proximity between ice crystals and cloud droplets is variable whilst sustaining supersaturated conditions (Korolev and Isaac, 2003).

Models do not reproduce the microphysical structure and radiative interactions of these persistent Arctic mixed-phase clouds well (e.g. Tjernström et al., 2008; Klein et al., 2009; Morrison et al., 2009; Morrison et al., 2012; de Boer et al., 2014). Detailed cloud resolving model (CRM) simulations have previously shown that commonly-used mid-latitude parameterisations for primary ice formation, such as Cooper (1986) or Meyers et al. (1992), overestimate the cloud ice number concentration, N_{ice} , in Arctic MPS, causing the rapid depletion of liquid and cloud glaciation (Harrington et al., 1999; Prenni et al., 2007). Modelled MPS are particularly sensitive to N_{ice} , with small decreases in simulated ice number causing significant increases in modelled liquid water path (Harrington and Olsson, 2001).

~~Four ice nucleation modes are commonly represented in models, and three (immersion-, contact-, and condensation-freezing) require the presence of cloud droplets for initiation (Pruppacher and Klett, 1997). Immersion-freezing occurs when a cloud droplet is nucleated by an aerosol particle of mixed composition; mixing which likely incorporates both soluble and insoluble fractions. Solubility is a crucial property of an efficient cloud condensation nuclei (CCN) whilst efficient ice nucleating particles (INPs) are insoluble (Pruppacher and Klett, 1997; Murray et al., 2012). The inclusion of an insoluble fraction would allow a CCN to obtain some ability as an INP (de Boer et al., 2010). In the atmosphere, soluble coatings on previously CCN-inactive particles, like desert dusts, promote ice nucleation via this pathway (Bigg and Leek, 2001). For example, organic coatings can suppress the ability of an INP to nucleate via the deposition mode (Möhler et al., 2008; Primm et al., 2016). Deposition-freezing results from the direct deposition of water vapour onto an INP, and is often linked with condensation-freezing due to difficulties in distinguishing~~ Ice crystals may form through primary or secondary processes in Arctic MPS (Rangno and Hobbs, 2001). Here, we focus on primary ice formation as secondary ice production has been shown to be less influential in the springtime MPS we shall consider (e.g. Jackson et al., 2012; Young et al., 2016a). Primary ice particles may be nucleated heterogeneously

through four different modes: deposition, condensation, immersion, and contact (Pruppacher and Klett, 1997). These modes describe the deposition of water vapour onto an ice nucleating particle (INP), forming ice directly (deposition) or freezing upon condensation (condensation), or the freezing of a cloud droplet through activation from within (immersion) or collision with an INP (contact). Due to their similarities, it can be difficult to differentiate between these mechanisms in measurements-

5 ~~Deposition-freezing~~; for example, deposition or immersion nucleation are often quoted to occur alongside condensation-freezing processes (e.g. Cooper, 1986; Meyers et al., 1992; de Boer et al., 2010; Fan et al., 2016). Three of these mechanisms (~~immersion-~~, ~~contact-~~, and condensation-freezing) require the presence of cloud droplets for initiation (Pruppacher and Klett, 1997), whereas deposition nucleation may occur in ~~both water- and ice-~~supersaturated conditions.

The frequency of MPS in the Arctic suggests that ice formation in these clouds is tied to the liquid phase, as preferential
10 nucleation via ~~deposition-freezing the deposition mode~~ may, in theory, result in a higher proportion of fully glaciated clouds than are observed (de Boer et al., 2011; Vihma et al., 2014). Consequently, recent studies (e.g. de Boer et al., 2011) suggest that liquid-dependent modes of nucleation are dominant in Arctic MPS at sub-zero temperatures greater than -25°C .

Liquid-dependent freezing may be inferred by observations in the Arctic. ~~Previous~~, as ~~previous~~ studies have found correlations between the number concentrations of ice crystals and large ($>23\ \mu\text{m}$) cloud drops (and drizzle drops; Hobbs and Rangno, 1998; Rangno and Hobbs, 2001). These large liquid particles have an increased likelihood of containing a partially-insoluble nucleus, or colliding with one, due to aerosol scavenging; therefore, they may nucleate via ~~the~~ immersion- or contact-freezing
15 ~~modes~~ respectively. Arctic aerosol particles are often well-mixed due to long-range transport (Young et al., 2016b); therefore, they ~~can provide a may provide an~~ efficient platform for immersion-freezing (Bigg and Leck, 2001; de Boer et al., 2010). Similarly, mixed particles can promote ice nucleation through collisions with cloud droplets; however, contact-freezing nuclei
20 are generally thought to be predominantly insoluble and ice-active, with little ~~CCN-ability-ability to act as a cloud condensation nuclei (CCN)~~ (Young, 1974).

Investigating the sensitivity of ~~springtime Arctic~~ MPS to ice crystal number concentrations will help to improve our understanding of the microphysical limitations of these clouds. Here, we test if primary ice formation under ~~water-saturation water-saturated~~ conditions improves the modelled microphysical structure with comparison to ~~deposition-condensation-freezing;~~
25 ~~with the hypothesis the commonly-used deposition conditions (below water saturation). We do not specify a nucleation mode: simply, ice formation can only occur when liquid cloud droplets are present, producing a number concentration specified by the chosen parameterisation. We hypothesise~~ that ice number concentrations will be suppressed ~~and liquid fractions will be enhanced~~ under this restriction, ~~thus reducing the influence of the WBF mechanism and prolonging cloud lifetime~~. Modelling studies which ~~specifically~~ utilise immersion-freezing have successfully simulated the persistence of Arctic stratocumulus
30 clouds, producing sustained liquid water in the presence of ice crystals for up to 12 h (de Boer et al., 2010).

Here, we use in situ cloud observations of Arctic MPS, from the Aerosol-Cloud Coupling and Climate Interactions in the Arctic (ACCACIA) campaign of 2013, ~~as a guide for guidance~~ to infer the microphysical sensitivity of modelled clouds to both ice number and surface conditions. We use the Large Eddy Model (LEM, UK Met Office, Gray et al., 2001) to simulate cloud microphysics observed over the sea ice, marginal ice zone (MIZ), and ocean. The UK's BAe-146-301 Atmospheric
35 Research Aircraft was used during the springtime (Mar-Apr) campaign, collecting high-resolution in situ observations of the

cloud microphysics encountered (Lloyd et al., 2015; Young et al., 2016a). Several dropsondes were launched from the aircraft during these cases to provide vertical profiles of the boundary layer (BL) structure. By combining dropsonde and in situ measurements, the sensitivity of modelled cloud microphysics to changes in predicted ice number concentrations is tested to infer the microphysical limitations of persistent springtime MPS in the European Arctic.

5 2 Methodology

2.1 Aircraft ~~Instrumentation~~instrumentation

Measurements from instruments on-board the Facility for Airborne Atmospheric Measurements' (FAAM) BAe-146 aircraft during three chosen case studies are presented to test the ability of the LEM to reproduce the Arctic mixed-phase clouds observed. Specifically, data from two wing-mounted instruments – the 2-Dimensional Stereo Particle imaging probe (2DS, Lawson et al., 2006) and Cloud Droplet Probe (CDP-100 Version 2, Droplet Measurement Technologies (DMT), Lance et al., 2010) – are used to investigate the mixed-phase clouds, as these probes can measure the sizes and number concentrations of ice crystals (80-1280 μm) and cloud droplets (3-50 μm) respectively. Details on the functioning of these probes, data analysis, and subsequent particle phase discrimination have been discussed previously by Crosier et al. (2011, 2014) and Taylor et al. (2016). The use of these instruments during ACCACIA is discussed by Lloyd et al. (2015) and Young et al. (2016a).

~~Aerosol particle data are used for the evaluation of the DeMott et al. (2010) ice nucleation parameterisation.~~ Data from the Passive-Cavity Aerosol Spectrometer Probe (PCASP 100-X, Droplet Measurement Technologies, Rosenberg et al., 2012) are used to size and count aerosol particles from sizes 0.1 μm to 3 μm . Aerosol particle data are used for the evaluation of the DeMott et al. (2010) ice nucleation parameterisation. Additionally, dropsondes released during each case are used to provide representative vertical profiles of potential temperature, water vapour mixing ratio, and wind fields to initialise the model.

20 2.2 Large Eddy Model (LEM)

The LEM allows cloud microphysics to be studied in isolation from large scale meteorological features. Cloud microphysical interactions, wind velocities, and turbulent motions within the boundary layer are simulated to allow a detailed investigation of cloud formation and evolution over ~~the~~ a 3-D domain (Boucher et al., 2013). Here, we consider three case studies of observations over the sea ice, marginal ice zone (MIZ), and ocean ~~;~~ cases 1, 2, and 3 respectively.

25 A 16 km \times 16 km domain was used, centred on the respective dropsonde release points in each case, with a spatial resolution of 120 m and a model height of 3 km applied. A vertical resolution of 20 m was imposed from the surface to above the altitude of the boundary layer temperature inversion (1500 m), above which it was reduced to 50 m. The LEM was run for 24 hours to simulate the respective observations. The first 3 hours of each simulation was not considered due to model spin-up. For all cases, cyclic lateral boundary conditions were imposed. A sponge layer was applied to the top 500 m of the domain, allowing 30 the fields to revert back to their initial conditions in this region. Long- and shortwave radiation was modelled using the Edwards and Slingo (1996) scheme and was called every 150 seconds within the model. Dropsonde profiles of potential temperature,

wind speed, and water vapour mixing ratio were used ~~to initialise the model~~ for initialisation. An adiabatic liquid water profile was assumed up to the first temperature inversion (approximately 600 m, 350 m, and 1150 m for cases 1, 2, and 3 respectively).

Over the ~~ocean and marginal ice zone~~ MIZ and ocean (cases 2 and 3), surface fluxes were calculated by the model, which assumes a water-saturated ~~,~~ ocean surface. Small sensible heat fluxes (1 W m^{-2}) were imposed to simulate the sea ice surface (case 1), as studies have measured such values adjacent to the ice pack (e.g. Sotiropoulou et al., 2014). ~~A sub-Arctic McClatchey profile was imposed in all simulations to ensure the initialised vertical~~ These surface conditions were kept constant throughout each simulation. A variable time step was imposed to satisfy Courant-Friedrichs-Lewy (CFL) criteria (Courant et al., 1967), and dt was approximately 0.3 s, 0.4 s, and 0.2 s for cases 1, 2, and 3, respectively. Sub-Arctic McClatchey profiles of tropospheric temperature, pressure, water vapour, and ozone were ~~based on historic measurements of stratospheric transmittance~~ – were imposed in all simulations to ensure the initialised vertical profiles were representative of the environment modelled.

No large-scale subsidence was imposed in these simulations to allow the microphysical effect of ice number and surface fluxes to be studied in isolation. Imposed subsidence would affect the microphysical structure of the modelled clouds, and the effect of including large-scale subsidence is discussed in Sect. 5.3.

2.2.1 Primary ~~Ice Nucleation~~ ice nucleation

The ~~double-moment microphysics scheme by Morrison et al. (2005)~~ Morrison et al. (2005) microphysics scheme is used within the LEM to test the sensitivity of the simulated mixed-phase Arctic clouds to ice number concentration. This scheme represents single-moment liquid, with a prescribed droplet number, and double-moment ice, snow, graupel, and rain. Quoted $N_{\text{ice-igg}}$ in this article represents the summed contributions of the ice crystal, ~~graupel, and snow~~ snow, and graupel number concentrations simulated. 2DS measurements are not segregated into such categories; therefore, bulk, "total ice" number concentrations are compared. A ~~mean-prescribed~~ droplet number of 100 cm^{-3} , approximated from the ~~aircraft observations, measured values of~~ $110 \pm 36 \text{ cm}^{-3}$, $141 \pm 66 \text{ cm}^{-3}$, and $63 \pm 30 \text{ cm}^{-3}$ (Young et al., 2016a) for cases 1, 2, and 3 respectively, is applied in all simulations. The sensitivity of the ice phase to this number is not considered here.

~~Deposition-condensation, immersion, and contact-freezing are all represented within the Morrison microphysics scheme. The form of the deposition-condensation-freezing parameterisation is varied in this study to test the cloud microphysical response. Immersion-freezing is included as the Bigg parameterisation (Bigg 1953 – hereafter, B53) and contact-freezing is represented by the Meyers parameterisation (Meyers et al. 1992 – hereafter, M92). The influence of these parameterisations on simulated ice number concentrations is detailed in the Supplement. To investigate the sensitivity of the modelled microphysics to predictable primary ice number concentrations, B53 immersion and M92 contact-freezing were switched off within the microphysics scheme, and the sole contribution to N_{ice} from one implemented parameterisation was considered.~~

Three distinct ice nucleation parameterisations were imposed in this study (Fig. 1). Firstly, the deposition-condensation ice nucleation parameterisation proposed by Cooper 1986 (hereafter, C86) was tested against the ACCACIA observations. This relationship is commonly used within the Morrison microphysics scheme in the Weather Research and Forecasting (WRF) model, amongst others. In Eq. 1, N_{ice} represents the ~~number concentration of pristine ice crystals~~ primary ice number concentration,

and $T_0 - T_K$ defines the sub-zero temperature. This parameterisation is used to simulate ice number concentrations below 265 K only.

$$N_{ice}[m^{-3}, T_K] = 5 \cdot \exp\left(0.304 [T_0 - T_K]\right) N_{ice}(T_K)[m^{-3}] = 5 \cdot \exp\left(0.304 [T_0 - T_K]\right) \quad (1)$$

Secondly, an approximation of the DeMott et al. 2010 (hereafter, D10) parameterisation was applied ~~-(Eq. 2)~~. This study derived a detailed relationship between INP number, temperature, and aerosol number concentration based on an amalgamation of different INP field data. D10 was imposed at temperatures below 264 K and at water-saturation (in accordance with DeMott et al., 2010).

$$N_{INP}[m^{-3}, T_K] = 0.0594 \left(273.16 - T_K\right)^{3.33} \left(n_{aer,0.5}\right)^{0.0264(273.16 - T_K) + 0.0033}$$

Equation 2 predicts the number concentration of INPs active at the given temperature (in Kelvin), T_K . As input, it requires $n_{aer,0.5}$: the number concentration of aerosol particles with diameter, D_P , greater than 0.5 μm . These aerosol data were averaged using PCASP measurements in the close vicinity to the observed cloud, producing input concentrations of 1.13 cm^{-3} , 1.77 cm^{-3} , and 2.20 cm^{-3} over the sea ice, MIZ, and ocean respectively. Below-cloud data were solely used over the ocean, whereas above-cloud measurements were included in the sea ice and MIZ calculations as the observed clouds had sub-adiabatic liquid water profiles, making entrainment processes - from the lateral or top boundaries of the clouds - likely.

$$N_{INP}(T_K)[m^{-3}] = 0.0594 \left(273.16 - T_K\right)^{3.33} \left(n_{aer,0.5}\right)^{0.0264(273.16 - T_K) + 0.0033} \quad (2)$$

Additionally, a curve was fitted to the observed ice crystal number concentrations during ~~ACCACIA~~ the ACCACIA campaign and used within the model ~~-(Eq. 3)~~. Data from ACCACIA flights B761, B762, B764, B765, and B768 ~~are~~ were included in the derivation of this curve. Microphysical data from B762, and B761/B768, have been previously detailed by Young et al. (2016a) and Lloyd et al. (2015) respectively. Young et al. (2016b) illustrate the corresponding flight tracks of each of these cases. Bulk number concentrations from these flights were plotted against temperature and the following relationship was derived from these data:

$$N_{ice}[m^{-3}, T_K] = \frac{0.068 \left(273.5 - T_K\right)^{3.3}}{\exp\left(0.05(273.16 - T_K)\right)} N_{ice}(T_K)[m^{-3}] = \frac{0.068 \left(273.5 - T_K\right)^{3.3}}{\exp\left(0.05(273.16 - T_K)\right)} \quad (3)$$

This curve is valid below 265 K. Temperatures greater than this were subject to minor secondary ice production ~~(see Young et al., 2016a)~~; therefore, the primary ice component could not be cleanly extracted from ~~these~~ those data. These observed ice data spanned 252 K to 265 K. ~~This curve somewhat mirrors the shape of D10 (Fig. 1); however, it is weighted by an~~

Table 1. Predicted number concentrations of ice crystals, $N_{\text{ice}} [\text{L}^{-1}]$, using each parameterisation considered in this study at the observed cloud top temperatures in each case.

Case Number	Temperature ^a [K (°C)]	D10 ^b × 10	C86	D10 ^b	ACC	D10 ^b × 0.1
1	253.4 (-19.8)	<u>13.1</u>	2.03	1.31	0.51	0.13 <u>13.1</u>
2	260.5 (-12.7)	<u>3.37</u>	0.23	0.34	0.17	0.03 <u>3.37</u>
3	252.8 (-20.4)	<u>20.7</u>	2.43	2.07	0.54	0.21 <u>20.7</u>

^aCloud top temperature (CTT)

^b $N_{\text{INP}} [\text{L}^{-1}]$

~~exponential term to provide better agreement with the observations at low temperatures.~~ In this article, this curve will be abbreviated to ACC. We expect this empirically-derived relationship to perform well with comparison to the observations; therefore, ACC is used to assess how well the two established parameterisations, C86 and D10, reproduce the cloud microphysics observed.

5 INPs are not depleted in this study; however, ice crystal number concentrations are prognostic within the Morrison et al. (2005) microphysics scheme. Aerosol particles are not strictly represented in the LEM and the microphysical representation is bulk, not binned. These simulations are only representative of a system with a replenishing source of INPs, and are therefore idealistic representations of the modelled clouds. However, this setup can give an approximation of the cloud microphysics that may form in the vicinity of an INP source; for example, a local source at the surface or a long-range transported INP population aloft.

10 The primary objective of this study is to identify the sensitivity of cloud stability to ice crystal number concentration. DeMott et al. (2010) suggest that INP number concentrations need to be predicted to within a factor of 10 to avoid an unrealistic treatment of mixed-phase cloud microphysics. Therefore, D10×10 and D10×0.1 were considered – in addition to C86, D10, and ACC – to additionally test sensitivity of simulated mixed-phase cloud microphysics to large changes in ice crystal number concentration. We chose D10 for this sensitivity study as this is the more up-to-date of the two established parameterisations considered. Figure 1 illustrates the performance of each parameterisation considered: the C86 and ACC cases, dependent only on temperature, are valid across the three observational studies chosen, whilst the D10 parameterisation – and variations thereof – is variable between cases given its dependence on observed aerosol particle number concentrations.

3 Aircraft observations

20 In situ observations of cloud microphysics over the sea ice and ocean during ACCACIA flight B762 (23 Mar 2013), and over the ~~marginal ice zone (MIZ)~~ MIZ during flight B764 (29 Mar 2013), are considered for model comparison. Microphysical observations from flight B762 have been detailed previously by Young et al. (2016a). The corresponding flight tracks are illustrated in Fig. 2. ~~These~~ The case studies were chosen due to the availability of dropsondes for model initialisation and temporally-close

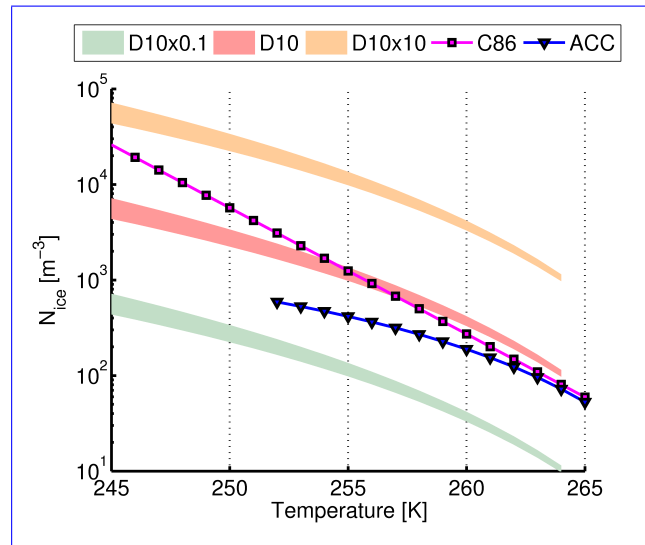


Figure 1. Evaluation of the five parameterisations used (C86, D10, ACC, D10×0.1, and D10×10) in the three cases considered with respect to temperature. **Case 1: sea ice, case 2: marginal ice zone (MIZ), and case 3: ocean.** The black line depicts the temperature-dependent fit of DeMott et al. (2010) for reference. The C86 parameterisation and ACC are valid for all cases, whereas the different aerosol particle loadings, and thus, variability, are accounted for with the D10 parameterisation. D10×0.5 is implemented in the ocean case in Sect. 5.2.

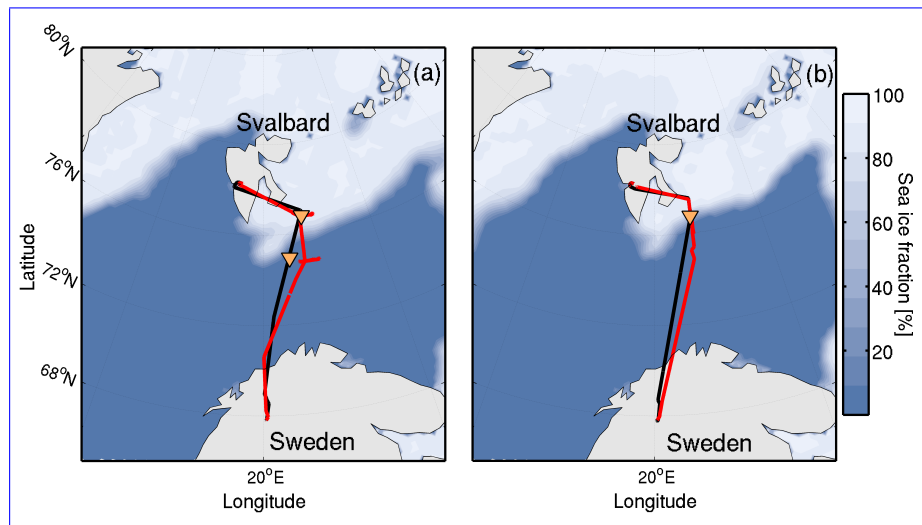


Figure 2. Flight track of (a) B762 and (b) B764, with section 1 (black) and section 2 (red) indicated. Dropsondes were released during section 1, whilst in situ observations were made during section 2. Dropsonde release locations are marked (orange triangles). (a) Case 1 (sea ice, north) and case 3 (ocean, south) are from flight B762, whilst (b) case 2 (MIZ) is from B764. Sea ice fraction is shown in shading.

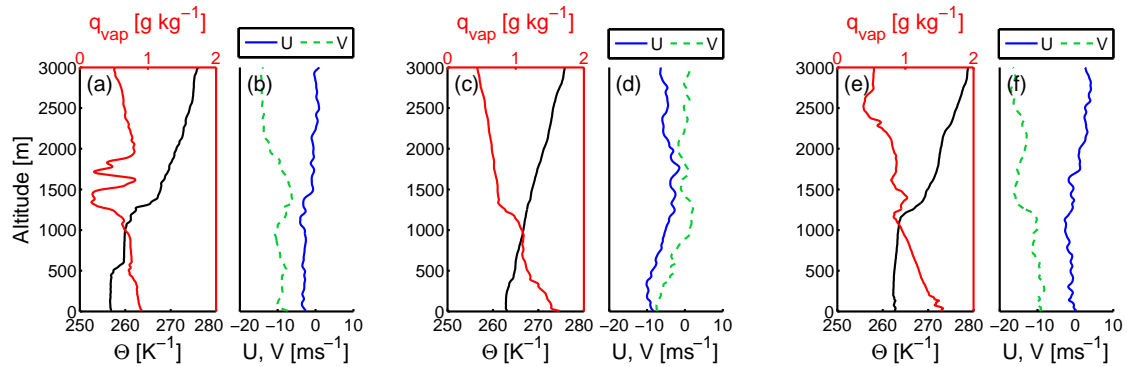


Figure 3. Potential temperature, vapour mixing ratio, and wind speed profiles measured by the three dropsondes used to initialise the LEM in this study. **(a-b):** dropsonde 1 released over the sea ice during flight B762. **(c-d):** dropsonde 2 released over the MIZ during flight B764. **(e-f):** dropsonde 3 released over the ocean during flight B762.

in situ aircraft observations. These aircraft observations sampled the same geographical location approximately 3-5 hours after the dropsonde measurements; therefore, some evolution in cloud properties between the two data is expected. These dropsonde data were affected by a potential dry bias, as discussed by Young et al. (2016a); corrections were applied after this study was completed, and the revised profiles are shown in Figs. S1 and S2. Whilst the general properties of the modelled
 5 clouds are mostly unchanged with these corrections imposed, the development of precipitation is affected (examples shown in Figs. S4, S5). Our conclusions are unaffected by this bias; however, these revised profiles highlight an additional sensitivity to humidity in the three cases considered here (see the Supplementary Material for further details).

Dropsondes from B762 distinctly sampled either the sea ice or ocean (as shown in Fig. 2a). The ocean dropsonde was far from the sea ice edge (~ 140 km). The B764 dropsonde (Fig. 2b) was dropped over the MIZ. As in Young et al. (2016a), the
 10 MIZ was is defined as sea ice fractions $>10\%$ and $<90\%$ based on NSIDC data (National Snow and Ice Data Centre, Fig. 2). These three cases were conducted over similar longitudes ($\sim 27^\circ$ E) and approximately the same latitude range ($\sim 75\text{-}77^\circ$ N).

Figure 3 shows the potential temperature, vapour, and wind speed profiles measured by each dropsonde used to initialise the LEM. In all cases, the net wind direction was north-easterlynorth-northeasterly, bringing cold air from over the sea ice pack to the over the comparatively warm ocean. The potential temperature profile for the sea ice case (case 1) displays a double
 15 inversion; the first at ~ 600 500 m and the second at ~ 1100 1200 m. The latter inversion is at approximately the same altitude as that measured in the ocean case downstream over the ocean (case 3). The MIZ case shows a subtle inversion at approximately 500350 m; however, it is not as prominent as the other two cases.

In situ measurements for all cases show a distinct, mixed-phase cloud from approximately 300 m to 700 m (case 1), 200 m to 900 m (case 2) and 700 m to 1500 m (case 3, Fig. 4). These measurements are summarised in Table 2. Liquid water mass
 20 mixing ratios (LWMLWMRs), derived from CDP measurements, provide a direct comparison with the LEM: the liquid measurements in the sea ice case are low, of the order of ~ 0.05 g kg $^{-1}$, whereas the MIZ and ocean cases have larger mixing ratios (~ 0.1 -0.3-0.2 g kg $^{-1}$). 2DS ice number concentrations are consistently low within the cloud layer in all cases, on the order of

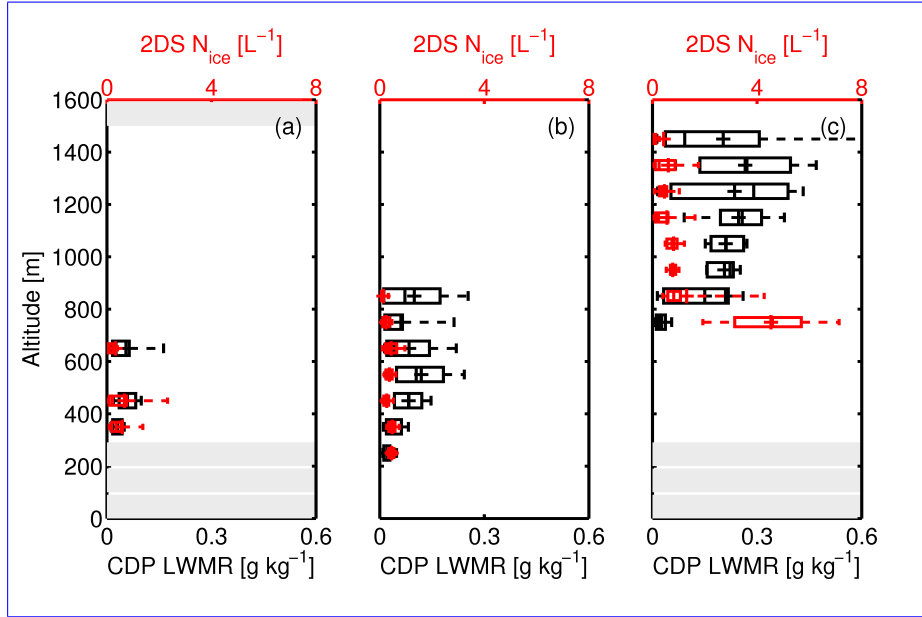


Figure 4. Observations of 2DS ice number concentration (red) and CDP liquid water mixing ratio (LWMR, black). **(a):** Sea ice, case 1. **(b):** MIZ, case 2. **(c):** Ocean, case 3. Only observations from mixed-phase [cloud-clouds](#) are included, with a derived CDP liquid water content threshold of $\geq 0.01 \text{ g m}^{-3}$ distinguishing in-cloud measurements. Box edges: 25th and 75th percentiles, Median: |, and Mean: +. Altitudes not sampled by the aircraft are indicated with grey boxes.

Table 2. Summary of cloud observations for each of the three cases considered. Values quoted are averaged quantities, with 1σ in brackets.

Case Number	Flight	Date [2013]	Surface Conditions	Cloud Extent [m]	LWMR ^a [g kg ⁻¹]	N _{ice} ^b [L ⁻¹]
1	B762	23 Mar	Sea ice	300-700	0.05 (0.04)	0.47 (0.86)
2	B764	29 Mar	MIZ/Ocean	200-900	0.09 (0.07)	0.35 (0.20)
3	B762	23 Mar	Ocean	700-1500	0.24 (0.13)	0.55 (0.95)

^aLiquid water mixing ratio

^bIce crystal number concentration

approximately $0.2\text{-}1.5 \text{ L}^{-1}$. High ice number concentrations at cloud base in case 3 are thought to be minor contributions of secondary ice due to crystal fragmentation (Young et al., 2016a). Cloud top temperatures (CTTs) were approximately -20°C , -13°C and -20°C respectively (Table 1). Such temperatures are too cold for efficient secondary ice production and too warm for homogeneous ice nucleation (Hallett and Mossop, 1974; Pruppacher and Klett, 1997). For this study, modelled microphysics

5 below 1500 m is focused upon as this is directly comparable with these aircraft observations.

4 Results

4.1 Control simulations

Within the Morrison et al. (2005) bulk microphysics scheme, primary ice nucleation is represented by three separate parameterisations: one each for deposition-condensation, immersion (Bigg, 1953), and contact (Meyers et al., 1992) nucleation. By default, the
5 C86 ice nucleation parameterisation is used to ~~simulate the heterogeneous~~ represent the deposition-condensation nucleation of ice. ~~Onset~~ When used together, these three modes of ice formation – in their represented forms – overpredict ice number concentrations over all surfaces, producing unrepresentative microphysics (not shown, Fig. S7). High ice number concentrations
glaciate case 3 and completely suppress the liquid phase in case 1. The influence of each of these modes of nucleation is discussed further in the Supplement.

10 To investigate the sensitivity of the modelled microphysics to predictable primary ice number concentrations, the Bigg (1953) immersion- and Meyers et al. (1992) contact-freezing parameterisations were switched off within the microphysics scheme, and the sole contribution to $N_{\text{ice-ig}}$ from one implemented parameterisation was considered. This relationship was varied in this study to test the cloud microphysical response. Deposition-condensation onset conditions commonly used in the WRF model ($T < -8^\circ\text{C}$ and $S_w > 0.999$, or $S_i > 1.08$) were applied as a control simulation for each case. Figure 5 shows the total
15 ice number concentrations, $N_{\text{ice-ig}}$, and liquid water mixing ratios, Q_{liq} , modelled over the sea ice (case 1), MIZ (case 2), and ocean (case 3). ~~In case 1, no liquid water is modelled~~

Using C86 to represent deposition-condensation nucleation as a control for each case, the mixed-phase conditions observed over the MIZ (case 2) and the ocean (case 3) are captured by the model; however, no liquid is modelled over the sea ice (case 1, Fig. 5a). Ice number concentrations of $\sim 3 \text{ L}^{-1}$ are simulated at an altitude of approximately 1000 m for the first 10 h of the
20 run, peaking at 3.4 L^{-1} . This ice then dissipates, after which $N_{\text{ice-ig}} \sim 1 \text{ L}^{-1}$ is maintained at below 500 m for the remainder of the simulation. This sustained number concentration is ~~within the range observed of the same order of magnitude as the observations~~ ($0.47 \pm 0.86 \text{ L}^{-1}$, Table 2); however, mixed-phase conditions are not modelled.

In contrast, co-existing regions of liquid and ice are simulated in cases 2 and 3. Modelled $N_{\text{ice-ig}}$ over the MIZ ($\sim 1.0 \text{ L}^{-1}$
at 1000 m, Fig. 5b) is in reasonable agreement with the mean observed ($0.35 \pm 0.20 \text{ L}^{-1}$, Table 2). Persistent mixed-phase
25 conditions are simulated in case 2 for approximately 16 h. Such conditions are also attained in case 3 (Fig. 5c), ~~with modelled ice number concentrations much greater than observed; modelled $N_{\text{ice-ig}}$; however, modelled $N_{\text{ice-ig}}$ peaks at 3.7 L^{-1} ; compared with at $\sim 1450 \text{ m}$, whereas only $0.55 \pm 0.95 \text{ L}^{-1}$ was observed.~~ This case glaciates after approximately 15 h.

Cases 2 and 3 impose surface fluxes from the simulated ocean surface below; fluxes which induce turbulence in the modelled clouds. The lack of strong surface sensible and latent heat fluxes in case 1 restricts the formation of liquid water in the
30 model as the second imposed criterion of ice supersaturation ($S_i > 1.08$) is attained first. This modelled microphysics is unrepresentative of the observations during case 1. It is unlikely that the nucleation mechanisms involved in these clouds would differ substantially between the sea ice, MIZ, and ocean. Therefore, under the conditions commonly used in the WRF model, C86 overpredicts $N_{\text{ice-ig}}$ and unsuccessfully reproduces the observed mixed-phase conditions over all three surfaces

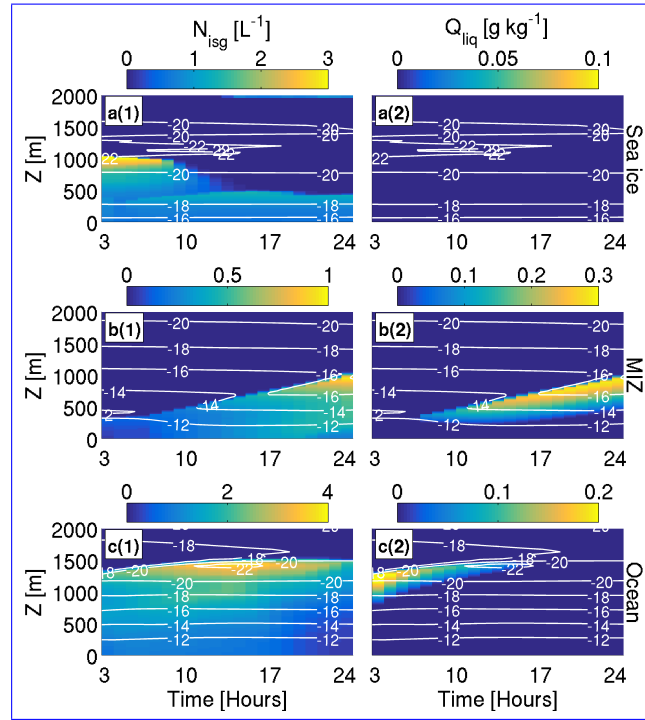


Figure 5. Simulated ice number concentrations ($N_{ice,sg}$, (1)) and liquid water mixing ratios (Q_{liq} , (2)) using the C86 parameterisation under default WRF conditions ($T < -8^{\circ}\text{C}$, $S_w > 0.999$, or $S_i > 1.08$). **a:** Sea ice (case 1), **b:** MIZ (case 2), **c:** Ocean (case 3). Run length 24 hours. Temperature ($^{\circ}\text{C}$) contours are overlaid in white. Note changing colour bar for each subfigure.

considered. To force the formation of persistent liquid in all cases, we restrict the formation of primary ice to water-saturated conditions in our subsequent [model runs simulations](#).

4.2 Ice nucleation at water-saturation

4.2.1 Case 1: Sea ice

5 [Figure 6](#) shows modelled $N_{ice,sg}$ and liquid water mixing ratio, Q_{liq} , using the [three main five](#) parameterisations – [D10×10](#), C86, D10, [and ACCACC](#), and [D10×0.1](#) – over the sea ice. Vertical (Z-Y) slices of $N_{ice,sg}$, Q_{liq} , and W at 21 h are included in the Supplement (Fig. S8).

[No liquid water is simulated when using D10×10](#). A mixed-phase cloud is simulated [at ~500 below 600 m](#) after 17 h [in the remaining four simulations](#), with a liquid layer at cloud top with ice formation and precipitation below. Peak Q_{liq} varies from C86 at the smallest (0.09 g kg^{-1}), through D10 (0.1 g kg^{-1}), [to ACC and ACC](#) (0.14 g kg^{-1}), to D10×0.1 at the largest ($0.140.16 \text{ g kg}^{-1}$, Table 3). $N_{ice,sg}$ and Q_{liq} , [with the exception of D10×10](#), both increase with time as [the each](#) cloud evolves. Modelled N_{ice} [is of the same](#) $N_{ice,sg}$ [varies through an](#) order of magnitude [using each parameterisation](#), with maximum values of

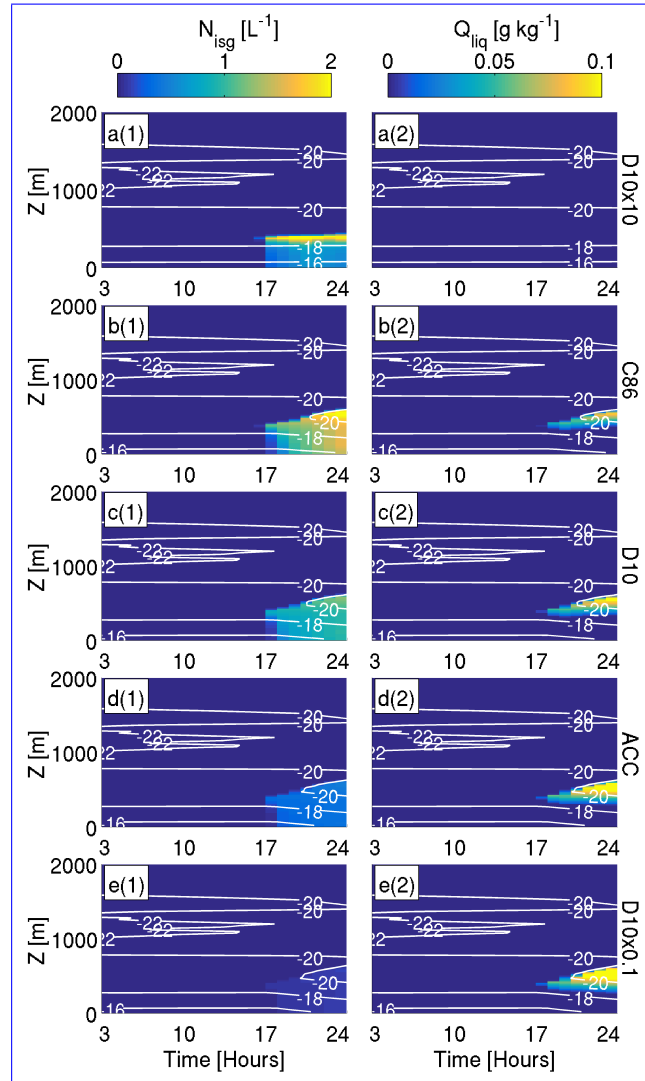


Figure 6. Simulated total ice number concentrations (N_{ice} , 1) and liquid water mixing ratios (Q_{liq} , 2) using the (a) D10×10, (b) C86, (c) D10, (d) ACC, and (e) D10×0.1 parameterisations for case 1 (sea ice). All are restricted to water-saturation. Run length 24 hours. Temperature ($^{\circ}$ C) contours are overlaid in white. Runs are arranged such that the simulation which produced the most ice (D10×10, a) is on the top row, and that which produced the least ice (D10×0.1, e) is on the bottom row. Note changing colour bar at the top of each column, which corresponds to data in that column only.

$2.89 L^{-1}$, $2.32 L^{-1}$, $1.29 L^{-1}$, and $0.47 L^{-1}$ attained by -, and $0.13 L^{-1}$ attained by D10×10, C86, D10, and ACC, ACC, and D10×0.1 respectively.

Figure 7 shows a comparison between measured and modelled (total) N_{ice} , $NN_{ice>100\mu m}$, and Q_{liq} for each case when using these three parameterisations. Comparisons including D10×10 and D10×0.1 are included in the Supplement (Fig. S11). Mean

Table 3. Maximum modelled values during each case for each parameterisation implemented at water-saturation.

Case	Parameter	<u>D10×10</u>	C86	D10	ACC	D10×10 <u>D10×0.1</u>
Sea ice (case 1)	$N_{ice-issg} [L^{-1}]$	<u>2.89</u>	2.32	1.29	0.47	2.89 0.13
	$Q_{liq} [g kg^{-1}]$	<u>0</u>	0.09	0.10	0.14	0 0.16
MIZ (case 2)	$N_{ice-issg} [L^{-1}]$	<u>6.57</u>	1.09	1.03	0.36	6.57 0.11
	$Q_{liq} [g kg^{-1}]$	<u>0.12</u>	0.29	0.28	0.34	0.12 0.39
Ocean (case 3)	$N_{ice-issg} [L^{-1}]$	<u>15.5</u>	3.83	3.01	0.71	15.5 0.37
	$Q_{liq} [g kg^{-1}]$	<u>0.10</u>	0.32	0.32	0.36	0.10 0.38

parameters modelled at 21 h during case 1 are shown in Fig. 7(a, d, g). The method for choosing these time steps is detailed in the Supplement (Figs. S12). C86 produces the greatest ice number concentration, with D10 producing the second-greatest and ACC producing the least (Fig. 7a). ACC provides the best agreement with the mean observed N_{ice} , simulating approximately 0.4 L⁻¹, and ACC.

- 5 Software for processing the 2DS data ~~cannot distinguish between liquid and ice~~ has poor resolution at small sizes (<80 μm), preventing the particle shape factor from being accurately determined at these sizes (Crosier et al., 2011; Taylor et al., 2016; Young et al., 2016). therefore, the number concentration of small ice crystals is not a reliable measure with this instrument. For this reason, the observed number concentration of ice crystals greater than 100 μm are ~~also compared with those modelled~~ directly compared with modelled ice and snow particles in this size range. Figure 7da shows this comparison using the C86, D10, and ACC parameterisations for case 1. ~~Again, ACC performs well, with approximately 0.2 L⁻¹ simulated.~~ D10 and C86 produce a larger ~~h during case 1 are shown in Fig. 7(a, d). The empirically-derived ACC relationship produces~~ $N_{ice>100\mu m}$ than observed. Figure 7g shows the comparison of observed LWMR and modelled and Q_{liq} . ~~Modelled variability is not as clear as with the N_{ice} data, and most of the variability occurs at the same altitude (500 m). In contrast to N_{ice} and $N_{ice>100\mu m}$, ACC produces the greatest Q_{liq} , while C86 and D10 produce profiles comparable to the mean observed as expected (Fig. 7a, d), suggesting that ice particle growth rates are adequately represented, whilst D10 underestimate with respect to the observations.~~

Modelled N_{ice} and C86 overpredict $N_{ice>100\mu m}$ and marginally underpredict Q_{liq} for. Comparisons including D10×10 and D10×0.1 are shown in Fig. 8(a, g), and D10 is again included (Fig. 8d) for comparison. D10×0.1 produces N_{ice} values which are approximately a factor of 2 too low. As a consequence of these lower ice number concentrations, Q_{liq} is enhanced, with maximum of 0.16 g kg⁻¹ modelled. In contrast, no liquid water is simulated when using D10×10, with peak ice number concentrations of 2.89 L⁻¹ produced at approximately 400 m. and the method for choosing these time steps are detailed in the Supplement (Figs. S11, S12).

Liquid and ice water paths (LWP and IWP, respectively) using each parameterisation are shown in Fig. 8(a, d). Both increase with model time when using each of the parameterisations. D10×0.1 produces the highest LWP and lowest IWP. D10×10 produces no liquid – giving a LWP of zero – and the simulated IWP increases initially (between approximately 17 h and 20 h),

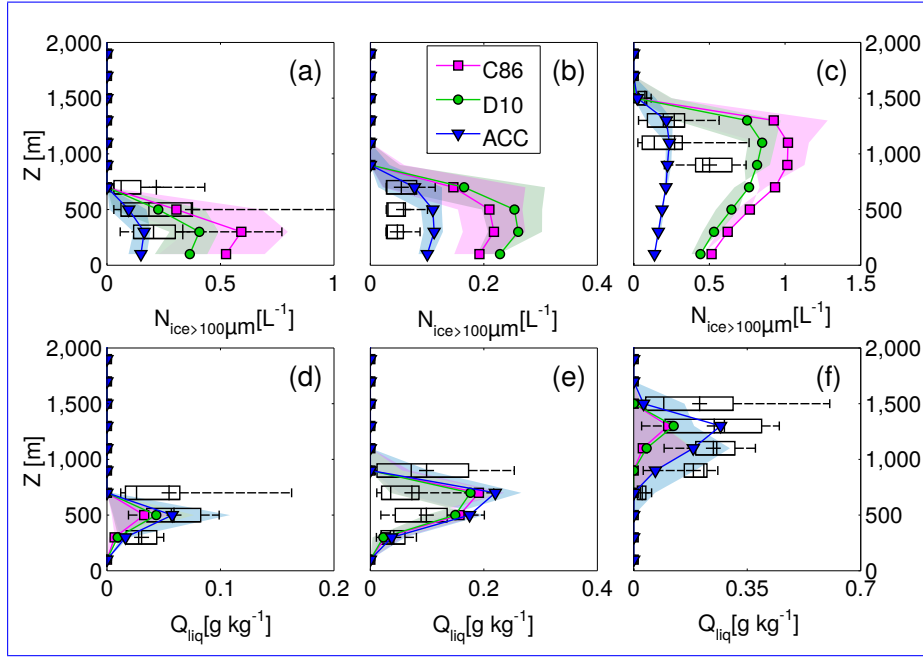


Figure 7. Observed $N_{ice>100\mu m}$ and Q_{liq} for the sea ice (column 1), MIZ (column 2), and ocean (column 3) cases. Observations are shown as black boxes, similar to Fig. 4. Mean modelled concentrations of ice and snow particles greater than $100\mu m$, using the C86 (magenta), D10 (green), and ACC (blue) parameterisations, are overlaid. Model time steps of 21 h, 17 h, and 7 h are used for the sea ice, MIZ, and ocean cases respectively, as these time steps offer the best comparison with the observations. Shading (in pink, green, or blue for C86, D10, and ACC respectively) indicates variability in the model parameters from ± 3 h in cases 1 and 2, and ± 4 h in case 3, where a larger interval is implemented in the latter case as the chosen parameters showed little variability over the shorter time step. In panel (f), the variability illustrated is always less than the mean modelled profile shown using each parameterisation as the Q_{liq} is at its greatest at the chosen time step. Observed $N_{ice>100\mu m}$ data from noted shattering event (Young et al., 2016a) are excluded in panel c, so that only primary contributions of ice are considered.

but subsequently decreases as the N_{isg} falls out from the cloud layer. The D10 and C86 parameterisations produce similar trends in the LWP and IWP traces, resulting in approximately $15\text{-}20\text{ g m}^{-2}$ and $2\text{-}3\text{ g m}^{-2}$ respectively by 24 h.

5 Negligible surface fluxes were applied in this case; therefore, cloud dynamics was driven primarily by longwave radiative cooling (similar to Ovchinnikov et al., 2011). In the observations, a lack of strong turbulent motions within this mixed-phase cloud layer caused a suppressed LWMR in the vicinity of moderate ice number concentrations (Young et al., 2016a). The LEM reproduces these conditions well in the absence of strong surface fluxes, as a small Q_{liq} and a reasonable N_{isg} are modelled under the restriction of water-saturated ice nucleation.

4.2.2 Case 2: Marginal ice zone

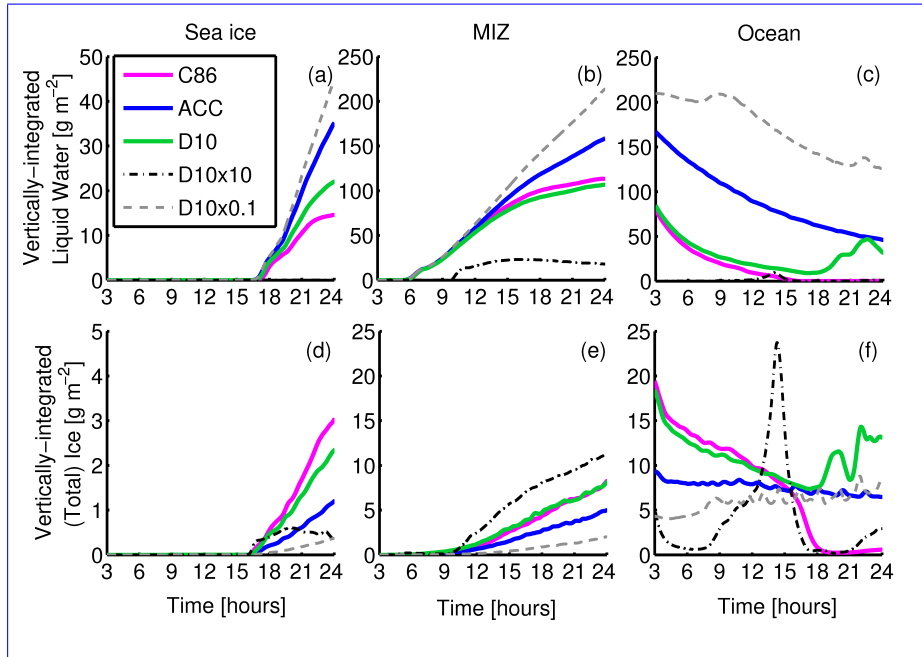


Figure 8. Vertically-integrated liquid (a-c) and ice water paths (d-f) for the sea ice, MIZ, and ocean cases when implementing each of the C86, ACC, D10, D10×10, and D10×0.1 parameterisations under water-saturated conditions.

All parameterisations produce a mixed-phase, sustained cloud layer over the MIZ (case 2, Fig. 9). Modelled LWPs and IWPs are larger in case 2 than in case 1. Strong surface fluxes are implemented in case 2 to represent a comparatively-warm ocean at the surface, allowing turbulent motions to sustain a greater Q_{liq} within the mixed-phase cloud layer (Morrison et al., 2008).

Figure 9 shows that there is little variation between the simulations over the MIZ (case 2, except when implementing D10×10. N_{isg} of up to $6.6 L^{-1}$ are simulated using D10×10, with a suppressed Q_{liq} (Fig. 9a). C86 and D10 produce perform similarly, predicting a N_{ice} of $0.23 L^{-1}/0.34 L^{-1}$ respectively at the CTT (Table 1), and producing comparable peak N_{ice}^{isg} and Q_{liq} values (Table 3). These parameterisations also produce a similar LWP when implemented in the model. Similar liquid ($\sim 100 g m^{-2}$) and IWP ice water paths ($\sim 7 g m^{-2}$) are also modelled by the end of each simulation (Fig. 8b, e). More liquid and less ice is simulated with ACC (Fig. 6h, Table 3). Q_{liq} agrees reasonably well with observations when implementing C86 and D10 (7e); however, both overpredict $N_{ice>100\mu m}$, suggesting that the modelled ice is growing too efficiently. This overprediction of $N_{ice>100\mu m}$ may be due to the modelled temperature being lower than was observed (see Table 1).

D10×0.1 produces the lowest N_{ice} overall ($0.11 L^{-1}$, Fig. 8h). This allows ACC also produces a sustained, mixed-phase cloud layer in case 2; however, a significantly greater Q_{liq} to be greater than in the other simulations (0.39 is modelled than is observed ($0.22 g kg^{-1}$, Table 3) and the simulated LWP and IWP increase steadily with time (Fig. 8b, e). D10×0.1 produces the lowest IWP, whilst D10×10 produces the greatest. N_{ice} of up to 6.6 compared with $0.07 L^{-1}$ are simulated using D10×10, with a suppressed Q_{liq} (Fig. 8b).

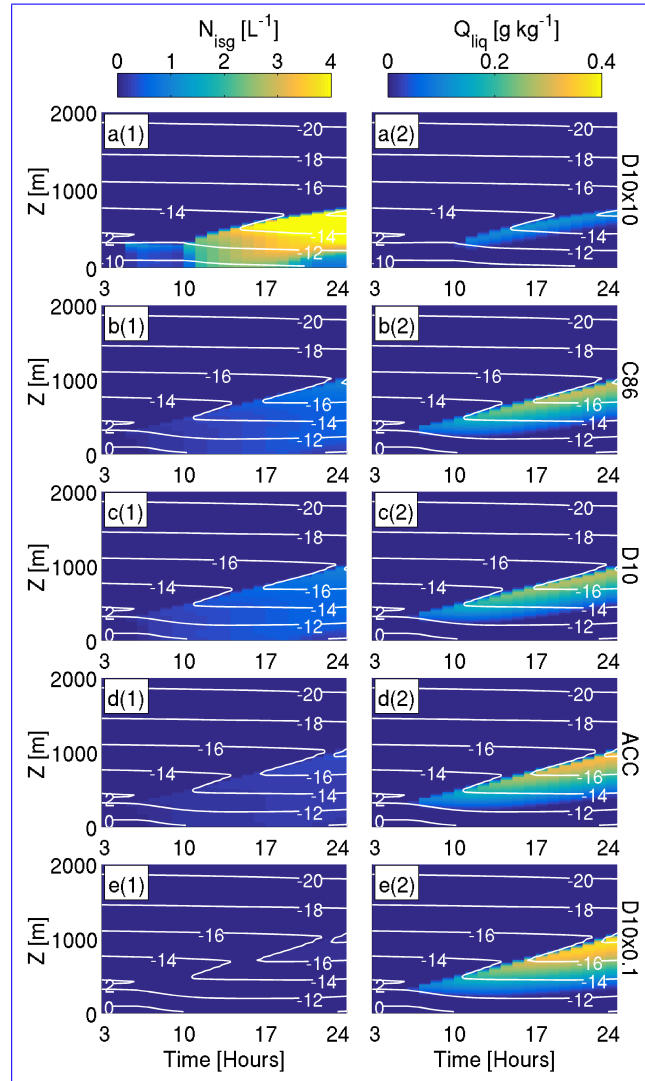


Figure 9. MIZ (case 2) simulations, presented similarly to Fig. 6.

At 17g h, N_{ice} modelled using ACC are lower ($0.2 L kg^{-1}$) in comparison to the mean observed at each altitude bin (, at 700 m in Fig. 7be). However, ACC This suggests that the simulated ice number concentration is not sufficient enough to suppress the formation of liquid with this relationship. ACC marginally overpredicts $N_{ice>100\mu m}$ compared to observations ($0.13 L^{-1}$ versus $0.03 L^{-1}$, Fig. 7eb) .D10 produces the greatest N_{ice} in this case, yet whereas, the greater $N_{ice>100\mu m}$ concentrations modelled by C86 produces a similar concentration. Again, D10 and C86 both overpredict $N_{ice>100\mu m}$ and variability in D10 suppress the Q_{liq} more effectively, improving agreement with the observations. D10x0.1 produces the lowest N_{isg} overall ($0.11 L^{-1}$, Fig. 9e), producing the greatest Q_{liq} is limited to the same altitude (700 out of all of the simulations ($0.39 m$, Fig. 7hg kg^{-1} , Table 3).

Simulated ice number concentrations (N_{ice} , (i)) and liquid water mixing ratios (Q_{liq} , (ii)) using the (a-e) C86, (d-f) D10, and (g-i) ACC parameterisations. All are restricted to water saturation. (a, d, g): Sea ice (case 1), (b, e, h): MIZ (case 2), (c, f, i): Ocean (case 3). Run length 24 hours. Temperature ($^{\circ}C$) contours are overlaid in white. Colour bar at the top of each column corresponds to data in that column only.

5 Observed N_{ice} , $N_{ice>100\mu m}$, and Q_{liq} for the sea ice (column 1), MIZ (column 2), and ocean (column 3) cases. Observations are shown as black boxes. Box edges represent the 25th and 75th percentiles, and the median and mean values are denoted by | and + respectively. Mean modelled values using the C86 (magenta), D10 (green), and ACC (blue) parameterisations are overlaid. Model time steps of 21 h, 17 h, and 7 h are used for the sea ice, MIZ, and ocean cases respectively, as these time steps offer the best comparison with the observations. Shading (in pink, green, or blue for C86, D10 and ACC respectively) indicates
 10 variability in the model parameters from ± 3 h in cases 1 and 2, and ± 4 h in case 3, where a larger interval is implemented in the latter case as the chosen parameters showed little variability over the shorter time step (a-e): N_{ice} ; (d-f): $N_{ice>100\mu m}$; and (g-i): Q_{liq} . Observed N_{ice} data from noted shattering event (Young et al., 2016a) are excluded in panels e and f, so that only primary contributions of ice are considered.

4.2.3 Case 3: Ocean

15 Over the ocean (case 3), strong sensitivities to N_{isg} emerge (Fig. 10). D10 \times 10 simulates a high N_{isg} , producing repetitive glaciating events occur. Little liquid water is produced throughout (~ 0.1 g kg $^{-1}$); however, small increases are modelled alongside the glaciating bursts. C86 causes cloud glaciation at allows a mixed-phase cloud layer to form for some time, approximately 17 h, after which it glaciates due to an accumulated N_{isg} . Liquid water is only simulated at cloud top until this point. Glaciation does not occur with D10 produces a, despite predicting only ~ 0.4 L $^{-1}$ less N_{ice} at the CTT than C86 (Table 1). D10
 20 allows for mixed-phase cloud layer conditions to be maintained for the full 24 h duration of the run. Again, however, Q_{liq} is underestimated (Fig. 7f). As with cases 1 and 2, both C86 and D10 overpredict $N_{ice>100\mu m}$ at the chosen time step (Fig. 7c).

ACC and D10 \times 0.1 also produce a mixed-phase cloud layer; however, more liquid and less ice is modelled using ACC (Table 3) in these simulations. ACC produces comparable $N_{ice>100\mu m}$ and Q_{liq} to observations as expected – when not considering the shattering event at cloud base (Fig. 4c) – and predicts 0.54 L $^{-1}$ at the case 3 CTT. D10 \times 0.1 produces peak
 25 N_{ice} reasonable agreement with the Q_{liq} observations at 7 h (Fig. S11); however, the rapidly increasing cloud top height and Q_{liq} with time are not representative of the observations. D10 \times 0.1 produces peak N_{isg} values that are almost a factor of 2 lower than observed for case 3 (0.37 L $^{-1}$), allowing the greatest peak Q_{liq} to form out of the five parameterisations considered (0.38 g kg $^{-1}$, Fig. 810ie, Table 3). This Q_{liq} is high with comparison to the ACCACIA observations (Table 2); however, N_{ice}
 30 N_{isg} is in better agreement than the D10 simulations in this case. In contrast, D10 \times 10 causes rapid glaciating events to occur (Fig. 8c). These repeat every ~ 3 h of the model simulation. Little liquid water is produced throughout (~ 0.1 g kg $^{-1}$); however, small increases are modelled alongside the glaciating bursts.

Substantial differences can be identified between the three main parameterisations considered. At 7 h, C86 produces the highest N_{ice} , with D10 producing the second greatest and ACC producing the least. Cloud forms and begins to decay immediately in case 3, as shown by the decreasing LWPs modelled (Fig. 78c). D10 and C86 overpredict $N_{ice>100\mu m}$, as with cases 1 and

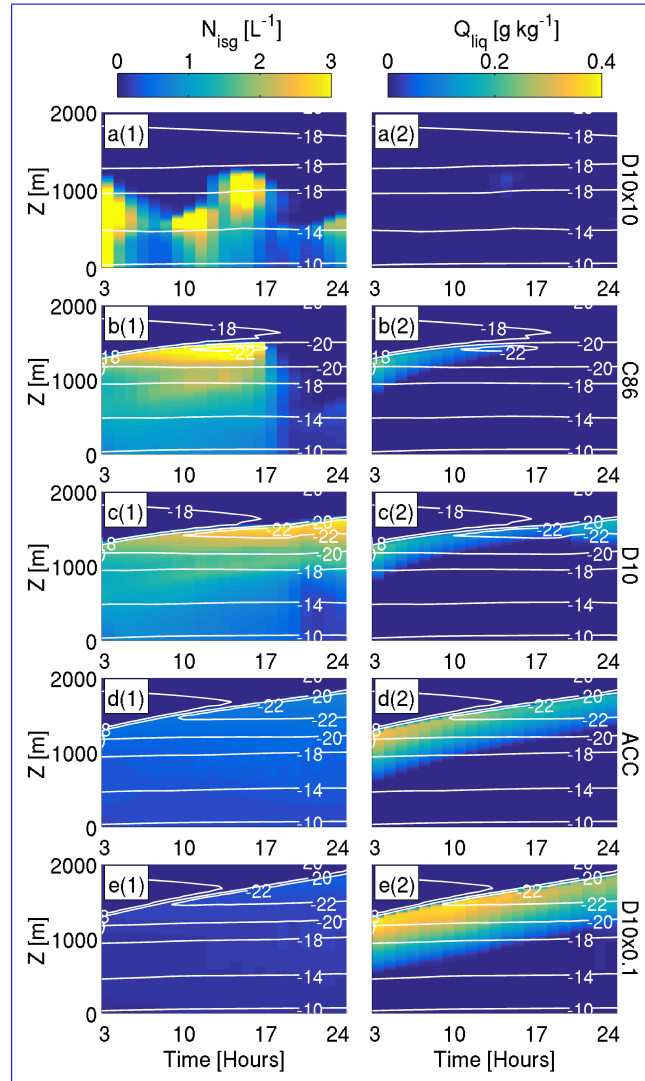


Figure 10. Ocean (case 3) simulations, presented similarly to Figs. 6 and 9.

2. ACC provides the best agreement with the mean N_{ice} observed, simulating approximately $0.4 L^{-1}$. ACC also produces a comparable $N_{ice>100\mu m}$ ($\sim 0.2 L^{-1}$, Fig. 7f). A more complex picture occurs in Fig. 7i: Q_{liq} is at its greatest at the chosen time step (7 h, Fig. S14), therefore the ± 4 h variability illustrated is always less than the mean modelled profile shown using each parameterisation. As with case 1, C86 and D10 underestimate Q_{liq} , and ACC performs well, with comparison to the observations.

The steady increase of IWP and LWP seen in cases 1 and 2 is not modelled in case 3: all simulations produce a decreasing LWP with time, whilst the majority caused by the moist BL and a high N_{isg} which acts as an efficient sink for liquid by the WBF mechanism. Most of the simulations also produce a decreasing IWP (Fig. 8e, f). A consistent IWP and steadily decreasing

LWP are; however, a consistent IWP is modelled with ACC and D10×0.1. The rapid glaciating events modelled with D10×10 (shown in Fig. 810ea) can again be seen in the IWP, with a maximum value of nearly 25 g m⁻² attained at approximately 14 h (Fig. 8f). The LWP is zero for the majority of this simulation; however, a small amount of liquid also forms at 14 h. As with case 2, D10 and C86 produce similar IWP and LWPs in case 3 for the majority of the simulations; however, these diverge at approximately 17 h when the C86 case glaciates (Fig. 8c, f).

During the D10 simulation, peculiar trends form in both the LWP and IWP traces at approximately 19 h. Peaks and troughs in the IWP trace correspond with peaks in the LWP at approximately 20 h and 22 h. To investigate these LWP and IWP trends further, Fig. 11 shows X-Y planar views of each simulated parameterisation at 21 h: LWP and IWP are total integrated values over the full height of the domain, and W is chosen at approximately cloud top (1500 m). Little variation can be seen in D10×10 (Fig. 11a) and C86 (Fig. 11b) at this time as Due to the strong dependence of N_{ice} and Q_{iq} have dissipated and not reformed yet. Co-located hot spots of IWP, LWP, and vertical velocity can be seen in the D10 simulation (Fig. 11c). Strong updraughts are modelled in close vicinity to enhanced downdraughts. Regions of high LWP or IWP are not seen in the ACC case (Fig. 11d); however, similar activity can be identified in the D10×0.1 (Fig. 11e) case. This structure is most visible in the LWP as little ice is simulated.

The parameterisations represented in Fig. 11(c, d, e) were considered further: the D10 case produces the most ice and least liquid of the three, with D10×0.1 vice versa. Hot spots of LWP, IWP, and W form with D10, but not with ACC. Defined structure can be seen in the LWP of D10×0.1, and this shape mirrors a region of isolated downdraughts (Fig. 11e). These features may be linked to precipitation from the simulated cloud, and Fig. 12 shows the solid (snow + graupel) and liquid (rain) precipitation modelled in the D10, ACC, and D10×0.1 simulations for case 3. With D10, a greater number concentration of solid precipitation (up to 1 L⁻¹) is modelled than in the ACC (0.29 L⁻¹) or D10×0.1 (0.17 L⁻¹) simulations. Similarly, significantly more rain is modelled (up to 27 L⁻¹) in the D10×0.1 simulation in comparison to ACC (17 L⁻¹) or D10 (12 L⁻¹). With comparison to D10 on temperature, high N_{isg} are created which readily undergo depositional growth, deplete the vapour field, and D10×0.1, ACC produces less solid and less liquid precipitation respectively. Precipitation modelled during cases 1 and 2 are shown in the Supplement (Fig. S15).

Sensitivity of cloud structure to ice crystal number. (a-c): D10×10, (d-f): D10, (g-i): D10×0.1. As previous, N_{ice} and Q_{iq} are shown, and columns indicate sea ice, MIZ, and ocean from left to right. Run length 24 hours. Temperature (°C) contours are overlaid in white. Note changing colour bars for each subfigure.

Vertically-integrated liquid (a-c) and ice water paths (d-f) for the sea ice, MIZ, and ocean cases when implementing each of the C86, ACC, D10, D10×10, and D10×0.1 parameterisations under water-saturated conditions.

Liquid and ice water path (first (i) and second (ii) columns) and vertical velocity at approximately 1500 m (third (iii) column) for each of the five ice nucleation parameterisation scenarios in the ocean case. Planar X-Y slices are shown at 21 h. Runs are arranged such that the simulation which produced the most ice (D10×10, a) is on the top row, and that which produced the least ice (D10×0.1, e) is on the bottom row. Colour bar at the top of each column corresponds to data in that column only.

Summed snow and graupel number concentrations (N_{s+g} , (i)) and rain number concentration (N_{rain} , (ii)) using (a) D10, (b) ACC, and (c) D10 \times 0.1 during case 3. Run length 24 hours. Temperature ($^{\circ}$ C) contours are overlaid in white. Colour bar at the top of each column corresponds to data in that column only.

5 Discussion

5 4.1 Ice nucleation at water saturation: Cooper (1986)

Using in situ observations for reference, we have shown that ice nucleation under water-saturated conditions allows mixed-phase conditions to be modelled over the sea ice, marginal ice zone (MIZ), and ocean. Using C86 deposition-condensation freezing in the Morrison microphysics scheme (Morrison et al., 2005) as a control for each case, the mixed-phase conditions observed over the MIZ (case 2) and the ocean (case 3) are captured by the model; however, no liquid is modelled over the sea ice (case 1).
10 Cases 2 and 3 impose surface fall from the cloud once the particles transition to the snow category. The vapour field recovers due to the moisture fluxes from the simulated ocean surface below; fluxes which induce turbulence in the modelled clouds. The lack of strong surface sensible and latent heat fluxes in case 1 restricts the formation of liquid water in the model as the second imposed criterion of ice supersaturation ($S_1 > 1.08$) is attained first. This modelled microphysics is unrepresentative of the observations during case 1. It is unlikely that the nucleation mechanisms involved in these clouds would differ substantially
15 between the sea ice, MIZ, and ocean. Therefore, we suggest that deposition-condensation freezing is ineffective at ubiquitously reproducing Arctic MPS over the range of surfaces possible.

4.1 Relationship with predicted INPs: DeMott et al. (2010)

Of the two established parameterisations considered (Cooper 1986 and DeMott et al. 2010), D10 produces the best agreement with the observed ice and liquid in all cases. In particular, it reproduces the low ice number concentrations observed during
20 case 2.

D10 predicts the number of INPs—not ice crystals—active at a given temperature, T_K . Though reasonable agreement is found with observations, D10 still produces too many ice crystals in each case (Fig. 6d, e, f). D10 predicts approximately double and quadruple the number of ice crystals observed at the respective CTFs in cases 1 and 3 (Tables 1 and 2). Young et al. (2016b) found a large fraction of super-micron sea salt particles over the sea ice (case 1) and below the MIZ cloud (case 2). No filter data
25 were available for the ocean case (case 3); however, it can be assumed that a similar fraction of these aerosol particles may also be sea salt, given they were found upstream over the sea ice under the same meteorological conditions (Young et al., 2016a). Given these results, it is not surprising that D10 overestimates the quantity of super-micron INPs available to nucleate ice in these conditions, as sea salt is an inefficient INP and constitutes a large fraction of $n_{aer, > 0.5 \mu m}$ surface, and the process repeats once water and ice supersaturation are attained.

30 Additionally, an approximation of D10 was applied. The average aerosol number concentration ($0.5 < D_p \leq 1.6 \mu m$, DeMott et al., 2010) in each case was used to evaluate Eq. 2 to give a temperature-dependent function.

This idealised scenario would only be representative of a region where the aerosol particle number concentration was being replenished and INPs were not depleted. Such replenishment is likely unrepresentative of the Arctic, as there are few in situ sources of INP in this region. Additionally, a constant input of aerosol particle number concentration was used in Eq. 2, irrespective of altitude in the model; therefore, spatial variability of INPs in the boundary layer is not represented. Particle number concentrations typically decrease with altitude away from local surface sources; therefore, this approximation of vertical homogeneity may also be positively influencing the number concentration of ice crystals predicted by D10.

4.1 ACCACIA observational fit: ACC

For the three case studies considered, the ACC relationship performs well. Cloud temperatures are colder and cloud top is higher than in the C86. The LWP is zero for the majority of this simulation; however, D10, or D10×10 simulations, due to strong radiative cooling from the heightened Q_{liq} . The liquid-dominated clouds modelled display enhanced cloud-driven convection across the full domain (Figs. 11, S8-S10). Only the D10×0.1 simulations produce colder temperatures and a higher cloud top. ACC produces the best microphysical agreement with observations for cases 1 and 3 (Fig. 7g, i); however, too much Q_{liq} is modelled in case 2 (Fig. 7h). Too few ice crystals are modelled to sufficiently deplete the liquid phase via the WBF mechanism. Ice crystal habits are not explicitly resolved in the microphysics scheme, which could influence the modelled Q_{liq} . Habits which undergo efficient vapour growth (e.g. stellar dendrites or sector plates, Mason, 1993) would allow increased ice mass to be modelled, with a consistent N_{ice} and a suppressed Q_{liq} .

The ACC relationship was derived from 2DS ice number concentration data from five springtime ACCACIA flights. The small sample size restricted the range over which a relationship could be established. Ice observations between 252 a small amount of liquid also forms at 14 K and 265 K were collected; therefore, the dependence of ice number concentration on temperatures outwith this range could not be established. Further observations in this temperature range could allow this relationship to be validated and potentially extended further; however, based on these ACCACIA data, this curve is not applicable beyond $252\text{ K} < T_k < 265\text{ K}$. Temperatures colder than this limit are modelled in case 3 due to increasing cloud top height and strong radiative cooling; therefore, these results must be interpreted with caution.

4.1 Ice number sensitivity

4.0.1 Cloud microphysics

As shown by previous studies (Harrington and Olsson, 2001; Morrison et al., 2011; Ovchinnikov et al., 2011, amongst others), the microphysical structure of Arctic MPS is highly sensitive to ice crystal number. Greater ice number concentrations enhance the efficiency of the WBF process – leading to the depletion of liquid water within the cloud – whilst lower number concentrations allow liquid droplets to persist under moderate vertical motions. D10 sensitivity tests for cases 1 and h. As with case 2 behave as would be expected: D10×0.1 produces significantly less ice, allowing liquid to dominate and cloud top height to increase, whilst D10×10 produces high ice number concentrations which glaciates case 1 and strongly suppress the liquid of case 2

(Fig. 8). Mixed-phase conditions are maintained in case 2; however, N_{ice} is much larger than observed using this parameterisation (Fig. 4, Table 2). Additionally, in case 3, $D10 \times 10$ causes rapid glaciating events to occur.

To compare between our water-saturated simulations, we define two stages of cloud evolution: a formation phase, characterised by an increasing LWP, and a decaying phase, with a decreasing LWP. In cases 1 and 2, each parameterisation causes the simulated clouds to remain in the formation phase by the end of each run (Fig. 8c, f). Both the LWP and IWP typically increase during these simulations. The LWP of case 2 begins to plateau towards 24 h in these cases, indicating the possible start of the decaying phase. Case 3 attained this phase immediately, as shown by the decreasing LWPs modelled.

Modelled LWPs and IWPs are smaller in case 1 than in both cases 2 C86 produce similar IWP and 3. Case 1 imposed negligible surface fluxes; therefore, cloud dynamics was driven primarily by longwave radiative cooling (similarly to Ovchinnikov et al., 2011). In the observations (Young et al., 2016a), a lack of strong turbulent motions within this cloud layer caused a suppressed LWMR in the vicinity of moderate ice number concentrations. The LEM reproduces these conditions well in the absence of strong surface fluxes (sensible heat fluxes of 1 LWPs in case 3; however, these diverge at approximately 17 W m⁻² imposed). The ocean surface cases (2 and 3) implement strong surface fluxes, allowing turbulent motions to sustain a greater Q_{liq} within the mixed-phase cloud layer (Morrison et al., 2008).

Cloud top height clearly increases with model time in cases 1 and 2, and more subtly in case 3. Large-scale subsidence, which would act to suppress cloud top ascent, was not imposed in these simulations. This increasing cloud top was observed by Young et al. (2016a) over the transition from sea ice to ocean; therefore, the modelled cloud structure is in good agreement with observations without large-scale subsidence imposed. However, the temperatures simulated in case 2 (Figs. 6, 8b, e, h) are colder than observed (Table 1). Despite this, N_{ice} modelled with the temperature-dependent parameterisations considered is in reasonable agreement with the observations (Fig. 7b). Case 2 occurred on a different day to cases 1 and 3; therefore, different synoptic conditions were influencing the sampled cloud systems. Increasing the modelled large-scale subsidence acts to increase the modelled temperatures (not shown, Fig. S16); however, a substantial subsidence would be required to match the observations. Given that imposing large-scale subsidence increases the temperature and suppresses Q_{liq} , without greatly affecting N_{ice} , we suggest that a greater imposed subsidence may improve the agreement with the observations in case 2.

Cloud top reaches higher altitudes in the ACC and $D10 \times 0.1$ simulations — across all surfaces — compared to $D10$, h when the C86, and $D10 \times 10$, due to a greater liquid water content; as more liquid forms from the vapour field, more heat is released, pushing the cloud top higher. These liquid-dominated cases are also shown to experience enhanced convection across the full domain in case 3 case glaciates (Fig. 11). With increased cloud top height, enhanced radiative and evaporative cooling enforce downdraughts whilst increased latent heat release from droplet formation and growth strengthens updraughts. In the C86, $D10$, and $D10 \times 10$ simulations, a greater N_{ice} suppresses efficient droplet growth, latent heat release, cloud top ascent, and strong radiative cooling through the WBF mechanism. This finding is in agreement with Harrington and Olsson (2001), who showed that high N_{ice} produced weaker BL convection and a shallower BL, whilst liquid-dominated mixed-phase clouds promote a higher cloud top and deeper BL. 8c, f).

4.0.1 ~~Cloud glaciation or break up~~

5 Discussion

5.1 Cloud glaciation

Over the ocean (case 3), C86 leads to cloud glaciation when freezing is implemented under both deposition-condensation (Fig. 5c) and water-saturated (Fig. 610eb) conditions. This cloud glaciation is tied to the number of ice crystals produced: over the temperature range shown in Fig. 1, D10×10 and C86 typically produce the most ice, ~~and so therefore~~ rapid ice formation is simulated once the onset thresholds are reached. ~~This~~ The high N_{isg} suppresses the liquid phase within the cloud layers, either immediately (D10×10) or after an accumulation period (C86). However, D10 produces a similar N_{ice} (2.07 L^{-1}) to C86 (2.42 L^{-1} , Table 1) at the CTTs considered. This subtle difference in predicted ice number allows the D10 cloud to persist, whilst the C86 cloud glaciates. Similarly, D10×10 does not allow liquid water to ever form in case 1, whilst it allows for mixed-phase conditions, albeit with a highly suppressed Q_{liq} , to be modelled in case 2.

~~While~~

5.2 Cloud break up

Whilst D10 produces a persistent mixed-phase cloud for the full duration, peculiar trends appear at times >20 h. Figure 8 shows the development of peaks and troughs in the IWP, with corresponding peaks in the LWP, after this time. From To investigate these LWP and IWP trends further, Fig. 11 e, localised hot spots of LWP, IWP, and vertical velocity shows X-Y planar views of each simulated parameterisation at 21 h: LWP and IWP are total integrated values over the full height of the domain, and the vertical velocity, W , is chosen at approximately cloud top (1500 m). Little variation can be seen in D10×10 (Fig. 11a) and C86 (Fig. 11b) at this time as N_{isg} and Q_{liq} have dissipated and not yet reformed.

Co-located hot spots of IWP, LWP, and W can be seen in the D10 simulation (Fig. 11c). These localised regions of increased ice and/or liquid result from isolated convective cells within the cloud. The formation of these cells forces the cloud top higher (Fig. 610fc), with renewed liquid and ice formation. Similar Strong updraughts are modelled in close vicinity to enhanced downdraughts. Similar defined structures can be seen in the D10×0.1 simulations (Fig. 11e); however, these appear mostly in the LWP field and have an elongated, banded shape in comparison to the compact, almost circular, structures which evolve in D10. These localised regions of enhanced convection This elongated band of increased LWP in D10×0.1 mirrors a region of isolated downdraughts. In contrast, regions of high LWP or IWP are not seen in the ACC case (Fig. 11d)

The simulations presented in Fig. 11(c, d, e) were considered further. The D10 case produces the most ice and least liquid of the three, with D10×0.1 vice versa. The convective regions of D10 and D10×0.1 can be linked to increased precipitation an increased number concentration of large precipitable particles (Fig. 12). Specifically, increased greater number concentrations of large solid (snow + graupel) precipitation is hydrometeors are modelled using D10, whilst increased more large liquid (rain) precipitation is modelled in hydrometeors are modelled in D10×0.1. Rain particles evaporate below cloud in all simulations and do not reach the surface. With D10, a greater number concentration of solid precipitating particles (up to 1 L^{-1}) is modelled

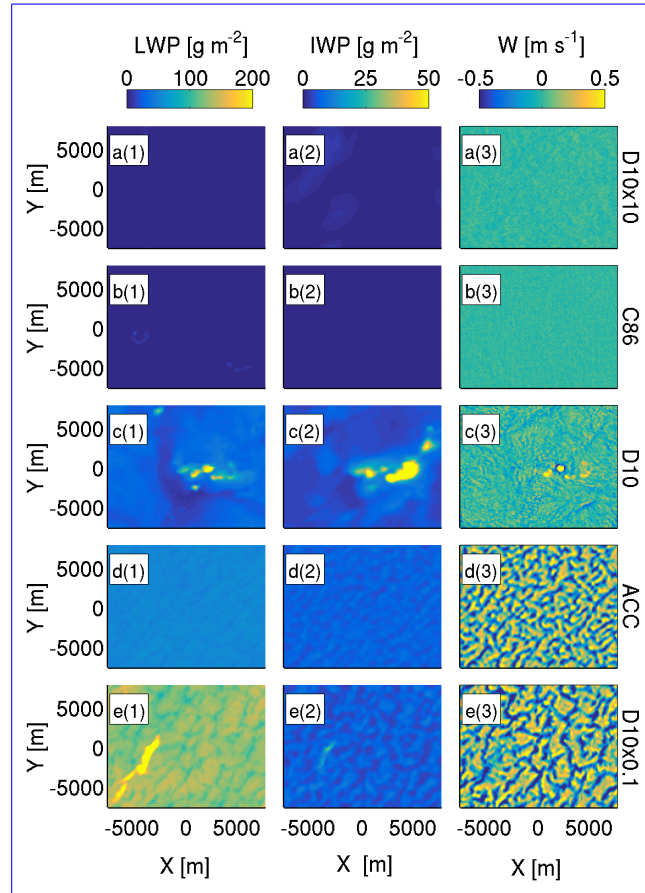


Figure 11. LWP (1), IWP (2) and vertical velocity (W, 3) at approximately 1500 m for each simulation in the ocean case. Planar X-Y slices are shown at 21 h. Note changing colour bar at the top of each column, which corresponds to data in that column only.

than in the ACC (0.29 L^{-1}) or D10 \times 0.1 (0.17 L^{-1}) simulations. Similarly, significantly larger concentrations of rain particles are modelled (up to 27 L^{-1}) in the D10 \times 0.1 simulation in comparison to ACC (17 L^{-1}) or D10 (12 L^{-1}). With comparison to D10 and D10 \times 0.1, ACC produces less solid and less liquid precipitating particles respectively. Number concentrations of large precipitable particles modelled during cases 1 and 2 are shown in the Supplement (Fig. S15).

- 5 The formation of convective cells in the ocean case mirrors cold air outbreak observations: as cold air moves from over the sea ice to the ocean, the boundary layer becomes thermodynamically unstable, allowing temperature perturbations to cause strong positive feedbacks on the cloud structure. Mixed-phase clouds are sustained by moderate vertical motions (e.g. Shupe et al., 2008a, b), driven by latent heating from hydrometeor growth within the cloud and radiative cooling at cloud top (Pinto, 1998; Harrington and Olsson, 2001). At the cold temperatures considered (approximately $-20 \text{ }^\circ\text{C}$), ice grows favourably by
- 10 vapour growth in the vicinity of liquid droplets and, given a high enough $N_{\text{ice,ig}}$, updraughts are enhanced through latent heat release. With enforced updraughts, water supersaturations are sustained, more cloud droplets form, and cloud top is forced to

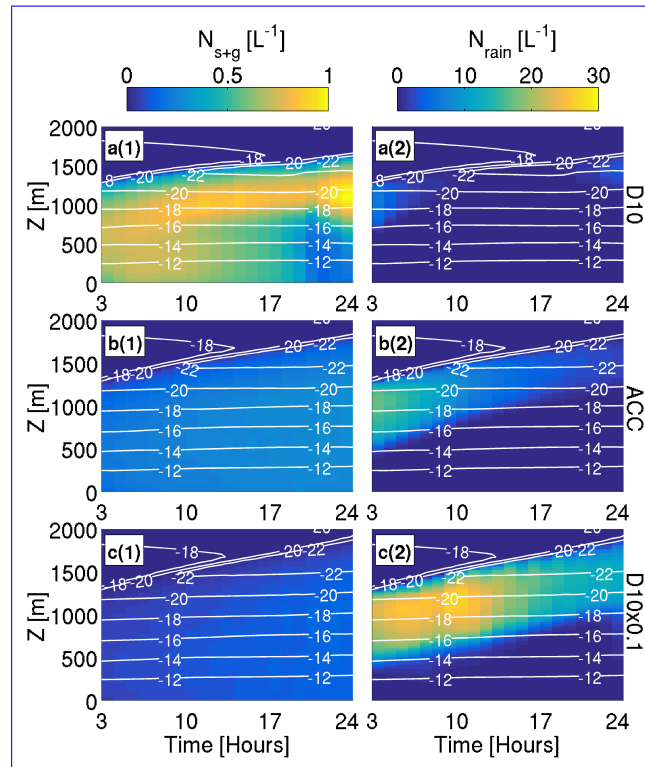


Figure 12. Summed snow and graupel number concentrations (N_{s+g} , 1) and rain number concentration (N_{rain} , 2) using (a) D10, (b) ACC, and (c) D10x0.1 during case 3. Run length 24 hours. Temperature (°C) contours are overlaid in white. Note changing colour bar at the top of each column, which corresponds to data in that column only.

higher altitudes. With more liquid and a higher cloud top, enhanced radiative cooling strengthens downdraughts adjacent to the updraught columns. With a deeper cloud layer, precipitation can form by an increased likelihood of collision-coalescence of droplets, or ice crystal growth and aggregation, within the downdraughts. The formation of precipitation warms and dries the cloud, reinforcing the updraughts and recycling the process. In the D10 ocean case – with high ice number concentrations, but not high enough for glaciation – the accumulation of $N_{ice_i\text{sg}}$ promotes this pathway, with the development of precipitation being the key factor in the localised, runaway convection that occurs.

With precipitation as snow or rain, the development of precipitable particles – as snow and graupel, or rain – Q_{liq} is depleted from the cloud layer. The D10 case produces high number concentrations of snow, which depletes Q_{liq} efficiently. Once the convective activity starts in this case, the cloud liquid is depleted; however, it is also partially restored through sustained supersaturations in the strong updraughts. In the D10x0.1 case, the Q_{liq} depletion is slower as rain is less efficient at removing droplets than snow. Both of these precipitation pathways would therefore likely lead to cloud break up if the simulation time was extended further.

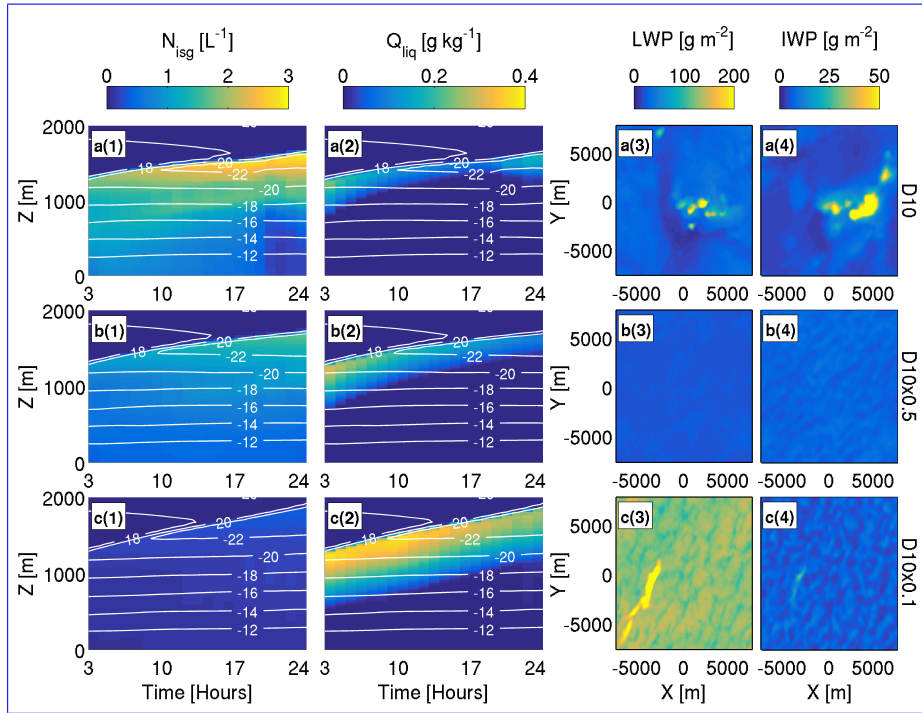


Figure 13. $N_{ice_{issg}}$ (1), Q_{liq} (2), LWP (3), and IWP (4) modelled in the D10 (a-b), D10, (b) D10 \times 0.5 (c-d), and (c) D10 \times 0.1 (e-f) simulations over the ocean (case 3). N_{ice} and Q_{liq} Data are shown in the first and second columns, plotted against time and altitude as previously presented similarly to Figs. LWP_10 and IWP (third and fourth columns) are X-Y planar views at 21 h, as also shown in Fig. 11. (a, c, e): Temperature ($^{\circ}$ C) contours overlaid in white in panels 1 and 2. Colour Note changing colour bar at the top of each column, which corresponds to data in that column only.

Given the two pathways of precipitation identified by Fig. 12, a question arose: do these structures form as a result of the functional form of D10, or are they related simply to ice number? ACC produced an $N_{ice_{issg}}$ between D10 and D10 \times 0.1, and no heterogeneous structures were observed. Therefore, to address this question, D10 \times 0.5 was imposed in the LEM (see Fig. 1). For comparison with Table 1, D10 \times 0.5 predicts $1.04 L^{-1}$ at the CTT. Figure 13 illustrates modelled $N_{ice_{issg}}$ and Q_{liq} for the D10, D10 \times 0.5, and D10 \times 0.1 simulations over the ocean. LWP and IWP modelled at 21 h are also shown. D10 \times 0.5 produces less ice than D10 and less liquid than D10 \times 0.1: this simulation behaves as expected to also give the microphysical mid-point between the D10 and D10 \times 0.1 these scenarios. Therefore, the modelled cloud persistence and stability is not just a feature of ACC. A homogeneous cloud structure is modelled with D10 \times 0.5 and the localised hot-spots of the D10 and D10 \times 0.1 cases is not seen are not present. Such hot-spots never do not form in the D10 \times 0.5 simulation. Modelled precipitation number concentrations of precipitating particles using this parameterisation (Fig. S17 in the Supplement) using this parameterisation is are significantly less than D10 (snow + graupel) and D10 \times 0.1 (rain), and the simulated cloud persists for the full 24 h duration with no break up.

Additionally, a larger domain size was imposed to test if these convective cells were related to the imposed cyclical boundary conditions: both similar structures and LWP/IWP trends formed (not shown, Figs. S18, S19), suggesting these convective cells are not simply a result of the domain configuration. Within the time scales imposed in this study (24 h), these cells are only observed over the ocean (case 3). Given more time (33 h), case 2 also develops convective cells and ~~precipitation increased~~
5 ~~concentrations of large hydrometeors~~ when D10 and D10×0.1 are imposed (not shown, Figs. S20– S23). Therefore, we conclude that – in two of the ACCACIA cases considered, which occurred on different days, under different synoptic conditions, with different air mass histories (Young et al., 2016b) – model simulations using the D10 ice nucleation parameterisation can produce localised cellular structure within the mixed-phase cloud layer, given enough time to do so.

~~Here, the~~ The development of appreciable precipitation is particularly sensitive to ice number in this study. ACC and D10×0.5 maintain mixed-phase conditions for 24 h over the ocean, with no cell development and little precipitation (Fig. 13), suggesting there is ~~a "sweet spot" for N_{ice}~~ an optimal N_{jsg} for cloud persistence in this case. Glaciation occurs with C86, persistence is achieved with D10×0.5 and ACC, and convective cells form in D10 and D10×0.1: ~~it~~. It is unclear which representation is correct in this environment, as observations do show the development of roll convection in cold air outbreak scenarios as the cold air masses move over the warm ocean (e.g. Hartmann et al., 1997). Additionally, snow precipitation was
15 observed by Young et al. (2016a) in this case. It cannot be stated whether the time scales of convection development modelled here are good representations of this phenomenon.

5.2.1 ~~Cloud persistence~~

5.3 Cloud top height

~~Mixed-phase conditions are sustained for at least 8 h in all three cases when imposing the three main parameterisations; ACC, D10, Cloud top height clearly increases with model time in cases 1 and C86. By additionally considering the sensitivity tests (C86, D10, ACC, D10×10, and D10×0.1), we can suggest limitations of N_2 , and more subtly in case 3. Large-scale subsidence, which would act to suppress cloud top ascent, was not imposed in these simulations. This increasing cloud top was observed by Young et al. (2016a) over the transition from sea ice to ocean; therefore, the modelled cloud structure is in reasonable agreement with observations without large-scale subsidence imposed. However, the temperatures simulated in case 2 (Fig. 9) are colder than observed (Table 1). As a result, the $N_{ice>100\mu m}$ modelled with the temperature-dependent parameterisations considered is greater than observed (Fig. 7b). Overall, the N_{jsg} is in reasonable agreement with the observed N_{ice} which maximise cloud persistence in each case, based on the predictions at the cloud top temperature (Table 1). Over the sea ice (Tables 2, 3), likely due to the low concentrations of snow and graupel produced at the warm sub-zero temperatures considered, and it is probable that this agreement would improve further if the modelled temperature was accurate. In contrast to cases 1 and 3, the reasonable agreement of N_{jsg} and poorer agreement of $N_{ice>100\mu m}$ suggests that the ice crystal growth rates are too efficient in case 1), ACC compares particularly well (producing $0.51 L^{-1}$ at the CTT) and produces a comparable 2. Additionally, case 2 occurred on a different day to cases 1 and 3; therefore, different synoptic conditions were influencing the sampled cloud systems. Increasing the modelled large-scale subsidence acts to increase the modelled temperatures slightly~~
20
25
30

(not shown, Fig. S16); however, a substantial subsidence would be required to match the observations in this case. Given that imposing large-scale subsidence increases the temperature and suppresses Q_{liq} , without greatly affecting N_{isg} , we suggest that a greater imposed subsidence may improve the agreement with the observations in case 2.

5 Cloud top reaches higher altitudes in the ACC and D10×0.1 simulations – across all surfaces – compared to D10, C86, and D10×10, due to a greater liquid water content: as more liquid forms from the vapour field, more heat is released, pushing the cloud top higher. These liquid-dominated cases are also shown to experience enhanced convection across the full domain in case 3 (Fig. 7a, g)–11). With increased cloud top height, enhanced radiative and evaporative cooling enforce downdraughts whilst increased latent heat release from droplet formation and growth strengthens updraughts. In the C86, D10 only marginally overpredicts N_{ice} ($1.31 L^{-1}$, Table 1), and D10×0.1 produces too few ice crystals and simulated Q_{liq} is too high with comparison to the observations–10 simulations, a greater N_{isg} suppresses efficient droplet growth, latent heat release, cloud top ascent, and strong radiative cooling through the WBF mechanism. This finding is in agreement with Harrington and Olsson (2001), who showed that a high N_{isg} produces weaker BL convection and a shallower BL, whilst liquid-dominated mixed-phase clouds promote a higher cloud top and deeper BL.

5.4 Relationship with predicted INPs: DeMott et al. (2010)

15 Of the two established parameterisations considered (Cooper 1986 and DeMott et al. 2010), D10 produces better agreement with the observed ice and liquid in all cases (Table 3). C86 predicts too much ice ($2.03 L^{-1}$, Table 1), peaking at $2.32 L^{-1}$ when implemented in the model (Table 3). Given these results, optimal mixed-phase cloud persistence, and comparable microphysics, are simulated with $0.51 L^{-1} < N_{ice(CTT)} < 1.31 L^{-1}$ over the sea ice, where the upper limit is more than twice the mean observed throughout the cloud layer ($0.47 \pm 0.86 L^{-1}$, Table 2), but is still within In particular, it does reasonably well at predicting the lower ice number concentrations observed during cases 1 and 2.

20 Over the MIZ D10 predicts the number of INPs – not ice crystals – active at a given temperature, T_K . Though reasonable agreement is found with observations, D10 still produces too much N_{isg} in each case (Figs. 6c, 9c, and 10c). D10 predicts approximately double and quadruple the number of ice crystals observed at the respective CTTs in cases 1 and 3 (Tables 1 and 2). Young et al. (2016b) found a large fraction of super-micron sea salt particles over the sea ice (case 1) and below the MIZ cloud (case 2), all parameterisations produce a mixed-phase, sustained cloud layer. Without observations to compare to, it may not have been possible to identify which has a more realistic grounding. However, we have shown that C86 and No filter data were available for the ocean case (case 3); however, it can be assumed that a similar fraction of these aerosol particles may also be sea salt, given they were found upstream over the sea ice under the same meteorological conditions (Young et al., 2016a). Given these results, it is not surprising that D10 perform similarly and produce marginally higher ice number concentrations than are observed (Fig. 7b). These relationships predict ice/INP number concentrations of $0.23 L^{-1}/0.34 L^{-1}$ respectively at the CTT of case 2. Q_{liq} also agrees well with observations when implementing these parameterisations. However, both C86 and overestimates the quantity of super-micron INPs available to nucleate ice in these conditions, as sea salt is an inefficient INP and constitutes a large fraction of $n_{aer,0.5}$.

Additionally, an approximation of D10 overpredict $N_{ice>100\mu m}$, suggesting the majority of modelled ice is growing too efficiently. This is likely representative of this case, as the warm, sub-zero cloud temperatures (-13°C) would not promote efficient ice crystal growth was applied. The average aerosol number concentration ($0.5 < D_p < 1.6 \mu\text{m}$, DeMott et al., 2010) in each case was used to evaluate Eq. 2 to give a temperature-dependent function. This idealised scenario would only be representative of a region where the aerosol particle number concentration was being replenished and INPs were not depleted. Additionally, a constant input of aerosol particle number concentration was used in Eq. 2, irrespective of altitude in the model; therefore, spatial variability of INPs in the boundary layer is not represented. Particle number concentrations typically decrease with altitude away from local surface sources; therefore, this approximation of vertical homogeneity may also be positively influencing the number concentration of ice crystals predicted by D10. ACC also produces a sustained,

5.5 ACCACIA observational fit: ACC

For the three case studies considered, the empirically-derived ACC relationship produces a similar number concentration of large ice crystals ($>100\mu\text{m}$) as are observed. This suggests that the efficiency of ice growth is well represented by the microphysics scheme. As this relationship is a fit to our observations, a good comparison between total ice number concentrations are expected, and the N_{ice} predicted at the CTT agrees well with the mean observed (Tables 1, 2). Modelled N_{isg} allows for stable mixed-phase cloud layer in case 2 conditions to be simulated in each case; however, a significantly greater Q_{liq} is modelled than is observed (0.22 g kg^{-1} , compared with 0.07 g kg^{-1} , at 700 m in the liquid phase of the cloud is overpredicted with comparison to observations in each case (Table 3). This is particularly clear in case 2 (Fig. 7he). This suggests that the simulated ice number concentration is not sufficient enough to suppress the formation of liquid with this relationship. Too few ice crystals are modelled to sufficiently deplete the liquid phase via the WBF mechanism. The modelled ice crystal growth rates – which allow for the good comparison between modelled and observed large ice number concentrations – do not act to adequately suppress the liquid phase in this case. Ice crystal habits are not explicitly resolved in the microphysics scheme, and the resultant variable growth rates could act to suppress the modelled Q_{liq} . Habits which undergo efficient vapour growth (e.g. stellar dendrites or sector plates; Mason, 1993) would allow increased ice mass to be modelled, with a consistent N_{isg} and a suppressed Q_{liq} . Optimal mixed-phase cloud persistence and comparable microphysical structure is modelled when 0.23

This relationship was derived using data from five springtime ACCACIA flights; therefore, the small sample size restricted the range over which a relationship could be established. Further observations could allow this relationship to be validated and potentially extended further; however, based on these ACCACIA data, this curve is not applicable beyond $252 \text{ L}^{-1} \text{ K} < N_{ice(CTT)} T_k < 0.34265 \text{ L}^{-1}$ over the MIZ, where the upper limit is in good agreement with the mean observed and the lower limit is within one standard deviation (0.35 ± 0.20 , Table 2).

Over the ocean (K. Temperatures colder than this limit are modelled in case 3), strong sensitivities to N_{ice} emerge. D10 $\times 10$ simulates a high N_{ice} ; therefore rapid, repeating glaciating events occur. This is not representative of the persistent, due to increasing cloud top height and strong radiative cooling; therefore, these results must be interpreted with caution. ACC produces stable mixed-phase MPS of interest. C86 allows a mixed-phase cloud layer to form for some time, approximately 17 conditions in all cases; however, it could potentially be overpredicting this stability and it may not adequately allow for

cloud break up downstream. This could have implications for the radiative budget of the region; therefore, the ability of ACC to allow for eventual cloud break up should be tested in further work.

5.6 Cloud persistence

As shown by previous studies (Harrington and Olsson, 2001; Morrison et al., 2011; Ovchinnikov et al., 2011, amongst others), the microphysical structure of Arctic MPS is highly sensitive to ice crystal number. Greater ice number concentrations enhance the efficiency of the WBF process – leading to the depletion of liquid water within the cloud – whilst lower number concentrations allow liquid droplets to persist under moderate vertical motions. Mixed-phase conditions are sustained for at least 8 h, after which it glaciates due to accumulated ice concentrations. This glaciating event does not occur within all three cases when imposing the three main ice nucleation parameterisations – ACC, D10, even though only ~ 0.4 , and C86 – under water-saturated conditions. By additionally considering the sensitivity tests (D10 \times 10, and D10 \times 0.1), we can suggest limitations of N_{ice} which maximise cloud persistence in each case, based on the predictions at the cloud top temperature (Table 1).

Optimal mixed-phase cloud persistence, and comparable microphysics, is modelled in case 1 with $0.51 L^{-1}$ less ice is predicted at the CTT. Both C86 and (ACC) $< N_{ice(CTT)} < 1.31 L^{-1}$ (D10 do not reproduce the observed cloud liquid well) over the sea ice (Fig. 7i). D10 \times 0.1 produces reasonable agreement with the 6, 7). With reference to the observed N_{ice} and Q_{liq} observations at 7 (0.47 ± 0.86 h (Fig. S11); however, the rapidly increasing cloud top height and Q_{liq} with time are not also representative of the observations. As discussed in Sect. 5.3, large-scale subsidence may help to constrain these properties. ACC provides good agreement with both L^{-1} , Table 2), the upper limit proposed here is more than twice the mean value, but is still within one standard deviation. In case 2, the low temperatures modelled affect our recommendation. The best predictions of N_{ice} and Q_{liq} – when not considering the shattering event at cloud base (with comparison to our observations (0.35 ± 0.20 , Table 2) are obtained with C86 ($0.23 L^{-1}$) and D10 ($0.34 L^{-1}$) when considering the observed CTT. However, the most comparable microphysical representation (from Fig. 47e(b, e) – where 0.54 is achieved when using ACC, which predicts an N_{ice} of $0.17 L^{-1}$ is predicted at the case 3 CTT. This is in very good agreement with the ice number concentration observed (0.55 ± 0.95 at the observed CTT but produces a peak N_{isg} of $0.36 L^{-1}$, Table 2). The N_{ice} values predicted in D10 and at the colder modelled temperatures. We suggest that C86 and/or D10 \times 0.1 produced a microphysical structure with enhanced precipitation, which may lead to cloud break up after time. Steady would perform better than ACC if the modelled temperature was more comparable with observations in this case. Finally, steady mixed-phase conditions were only simulated when implementing ACC and/or D10 \times 0.5 – in case 3. Therefore, to simulate a consistent cloud layer over the ocean in case 3, $0.54 L^{-1}$ (ACC) $< N_{ice(CTT)} < 1.04 L^{-1}$ (D10 \times 0.5) is required.

From these three cases, it is clear that small differences in the predicted N_{ice} can produce significant microphysical impacts on the modelled clouds. The best prediction of N_{ice} for each case is different; however, they are of a similar order of magnitude and vary only a little between each case. Case 2 requires the least N_{ice} due to the comparatively warmer CTT ($-12.7^\circ C$, Table 1), whereas cases 1 and 3 – with similar CTTs (approximately $-20^\circ C$) – require N_{ice} over a similar range (approximately $0.5 L^{-1}$ to $1.3 L^{-1}$) to produce a sustained, mixed-phase cloud layer with $N_{ice-isg}$ and Q_{liq} in approximate agreement with in situ observations. These limitations are based upon the parameterisations chosen in this study (C86, D10, ACC, D10 \times 0.1,

and $D10 \times 10$); therefore, further work should be conducted to test other relationships and constrain the identified limitations in each case. ~~These~~ Nevertheless, these concentrations compare well with springtime INP measurements made at the Alert station (Canadian Arctic, Mason et al., 2016), where mean INP number concentrations of 0.05 L^{-1} , 0.2 L^{-1} and 1 L^{-1} were measured at -15°C , -20°C , and -25°C respectively. Additionally, these results are in accordance with Ovchinnikov et al. (2011), whose modelled springtime Arctic MPS glaciated when an ice number concentration of 2 L^{-1} was imposed, whilst 0.5 L^{-1} produced mixed-phase conditions with both consistent LWP and IWPs attained after ~ 3.5 h. ~~Given~~ However, given these are idealised simulations (with constant SW radiation and no INP depletion), the ability of the model to simulate realistic conditions should be inferred with caution. ~~results~~ Results from this study can simply conclude that modelled microphysics is sensitive to ice number concentrations, surface fluxes, and BL humidity (see Supplement), and that small increases in the modelled ice crystal number concentration can cause persistent mixed-phase clouds to glaciate.

6 Conclusions

In this study, we have used large eddy simulations to investigate the microphysical sensitivity of Arctic mixed-phase clouds to primary ice number concentrations and surface conditions. The Large Eddy Model (LEM, UK Met Office, Gray et al., 2001) was used to simulate cloud structure and evolution over the sea ice, marginal ice zone (MIZ), and ocean. Aircraft observations of cloud microphysics from the Aerosol-Cloud Coupling and Climate Interactions in the Arctic (ACCACIA) campaign were used as a guide to indicate which simulations gave the most realistic microphysical representation. We used two primary ice nucleation parameterisations (Cooper, 1986; DeMott et al., 2010, abbreviated to C86 and D10 respectively), one derived from ACCACIA observations (ACC, Eq. 3), and an upper and lower sensitivity test ($D10 \times 10$ and $D10 \times 0.1$) to produce ice crystal number concentrations within the modelled clouds.

Three main sensitivities arise from the three considered cases.

- C86 cannot reproduce the sea ice cloud (case 1) under the conditions commonly used in the Weather Research and Forecasting (WRF) model with the Morrison et al. (2005) microphysics scheme (Fig. 5). However, these criteria do allow for a mixed-phase layer to form in cases 2 and 3, when the ocean provides strong sensible heat fluxes to the BL. This result demonstrates that deposition ice nucleation is not wholly representative of ice nucleation in the Arctic springtime clouds observed during the ACCACIA campaign. Ice nucleation in water-saturated conditions must be implemented to create a mixed-phase cloud layer in our three considered cases (Figs. 6, 9, and 10).
- Warm supercooled mixed-phase clouds over the MIZ (case 2) can be modelled to reasonable accuracy by using the C86 and D10 parameterisations (Figs. 6, 7). At the cloud top temperature attained by case 2 (Fig. 9b, c). Temperatures modelled in this case are lower than observed, leading to a much greater peak N_{s+g} when using these parameterisations (1.09 L^{-1} and 1.03 L^{-1} respectively) than would be expected from their predictions (0.23 L^{-1} and 0.34 L^{-1} respectively, Table 1) at the observed CTT (-12.7°C), the difference between the C86 and D10 parameterisations is small (Fig. 1, Table 1). ~~These parameterisations~~ However, we suggest that C86 and D10 would perform the best out of those parameterisations

considered if the modelled temperature was in better agreement with our observations. However, C86 and D10 significantly overpredict the ice number concentrations at the colder temperatures modelled in cases 1 and 3 (approximately -20 °C). ACC is modulated to have a weakened temperature-dependence; therefore, and it allows for persistent, mixed-phase cloud layers are to be modelled in all three cases using this relationship.

5 – Results shown here illustrate that microphysical structure of MPS is particularly sensitive to the modelled ice crystal number concentration when simulating clouds over an ocean surface. With marginally too much ice (e.g. 2.43 L⁻¹, C86, Table 1), cloud glaciation occurs. Slightly less ice (2.07 L⁻¹, D10, Table 1) allows for persistent mixed-phase conditions for some time (approximately 24 h); however, convective cells form with heightened snow-precipitation number concentrations of snow particles, which may promote cloud break up. Conversely, too much liquid and very few ice crystals (0.21 L⁻¹, D10×0.1, Table 1) may also promote cloud break up via precipitation-as-rain the development of large liquid (rain) particles. Case 3 simulations show that there is a "sweet spot" for simulating ice in ocean-based single-layer Arctic MPS (attained by ACC and D10×0.5), where the number concentration of ice is low enough to sustain a reasonable Q_{liq} through vertical motions and high enough to suppress the liquid phase and restrict efficient collision-coalescence and rain formation. In this narrow limit, the influence of the WBF mechanism is depleted. The fact that this "sweet spot" can be attained by halving the D10 prediction of INP number concentration – yet it is overshot with D10×0.1 – illustrates just how sensitive the cloud structure is to the ice phase. Therefore, we suggest that the method of parameterising the primary ice number concentration in bulk microphysical models is very important, as small differences in the predicted ice concentration can have substantial effects on the microphysical structure and lifetime of Arctic MPS.

20 These idealised simulations assume an infinite source of INPs to the modelled clouds; here, INP-INPs are not depleted by activation or precipitation. An infinite source of INPs is likely unrepresentative of the Arctic environment (Pinto, 1998), as there are few in situ sources of INPs (e.g. mineral dusts, Murray et al., 2012). Although Young et al. (2016b) identified mineral dusts during all flights of the ACCACIA campaign, further work should include prognosing INPs in such simulations to investigate how their depletion could affect the microphysical structure of these clouds. Several studies have previously identified INP depletion as an important process to represent in modelling Arctic MPS (Harrington et al., 1999; Harrington and Olsson, 2001, amongst others).

30 Additionally, the Morrison et al. (2005) microphysics scheme has been used for its detailed representation of microphysical interactions, such as ice aggregation and growth, but it can be utilised further to represent aerosol particle properties. Size distributions can be prescribed; therefore, the D10 parameterisation could be developed to give a spatially-dependent INP prediction based on aerosol particle observations, likely leading to a more comprehensive treatment of INP variability throughout the domain.

Acknowledgements. This work was funded as part of the ACCACIA campaign (grant NE/I028696/1) by the National Environment Research Council (NERC). G. Young was supported by a NERC PhD studentship. We would like to thank A. Hill and B. Shipway for advising on the microphysics scheme, and [K. Bower, M. Gallagher, and J. Crosier for their helpful advice.](#) Airborne data were obtained using the BAe-146-301 Atmospheric Research Aircraft [ARA] flown by Directflight Ltd and managed by the Facility for Airborne Atmospheric Measurements [FAAM], which is a joint entity of the Natural Environment Research Council [NERC] and the Met Office. Sea ice data were obtained from the National Snow and Ice Data Centre (NSIDC).

References

- ACIA: Arctic Climate Impact Assessment, pp. 990–1020, Cambridge University Press, 2005.
- Bigg, E. K.: The formation of atmospheric ice crystals by the freezing of droplets, *Quarterly Journal of the Royal Meteorological Society*, 79, 510–519, doi:10.1002/qj.49707934207, 1953.
- 5 Bigg, E. K. and Leck, C.: Cloud-active particles over the central Arctic Ocean, *Journal of Geophysical Research*, 106, 32 155, doi:10.1029/1999JD901152, 2001.
- Boucher, O., Randall, D., Artaxo, P., Bretherton, C., Feingold, G., Forster, P., Kerminen, V. M., Kondo, Y., Liao, H., Lohmann, U., Rasch, P., Satheesh, S. K., Sherwood, S., Stevens, B., and Zhang, X. Y.: Clouds and Aerosols, in: *Climate Change 2013: The Physical Science Basis. Contribution of Working Group I to the Fifth Assessment Report of the Intergovernmental Panel on Climate Change*, edited by: Stocker, T. F., Qin, D., Plattner, G. K., Tignor, M., Allen, S. K., Boschung, J., Nauels, A., Xia, Y., Bex, V., and Midgley, P. M., Cambridge University Press, Cambridge, United Kingdom and New York, NY, USA, doi:10.1017/CBO9781107415324.016, 2013.
- 10 Cooper, W. A.: Ice Initiation in Natural Clouds, *Meteorological Monographs*, 21, 29–32, doi:10.1175/0065-9401-21.43.29, 1986.
- Courant, R., Friedrichs, K., and Lewy, H.: On the Partial Difference Equations of Mathematical Physics, *IBM J. Res. Dev.*, 11, 215–234, doi:10.1147/rd.112.0215, 1967.
- 15 Crosier, J., Bower, K. N., Choulaton, T. W., Westbrook, C. D., Connolly, P. J., Cui, Z. Q., Crawford, I. P., Capes, G. L., Coe, H., Dorsey, J. R., Williams, P. I., Illingworth, A. J., Gallagher, M. W., and Blyth, A. M.: Observations of ice multiplication in a weakly convective cell embedded in supercooled mid-level stratus, *Atmospheric Chemistry & Physics*, 11, 257–273, doi:10.5194/acp-11-257-2011, 2011.
- Crosier, J., Choulaton, T. W., Westbrook, C. D., Blyth, A. M., Bower, K. N., Connolly, P. J., Dearden, C., Gallagher, M. W., Cui, Z., and Nicol, J. C.: Microphysical properties of cold frontal rainbands, *Quarterly Journal of the Royal Meteorological Society*, 140, 1257–1268, doi:10.1002/qj.2206, 2014.
- 20 Curry, J. A., Rossow, W. B., Randall, D., and Schramm, J. L.: Overview of Arctic Cloud and Radiation Characteristics., *Journal of Climate*, 9, 1731–1764, doi:10.1175/1520-0442(1996)009<1731:OOACAR>2.0.CO;2, 1996.
- de Boer, G., Hashino, T., and Tripoli, G. J.: Ice nucleation through immersion freezing in mixed-phase stratiform clouds: Theory and numerical simulations, *Atmospheric Research*, 96, 315–324, doi:10.1016/j.atmosres.2009.09.012, 2010.
- 25 de Boer, G., Morrison, H., Shupe, M. D., and Hildner, R.: Evidence of liquid dependent ice nucleation in high-latitude stratiform clouds from surface remote sensors, *Geophysics Research Letters*, 38, L01803, doi:10.1029/2010GL046016, 2011.
- de Boer, G., Shupe, M. D., Caldwell, P. M., Bauer, S. E., Persson, O., Boyle, J. S., Kelley, M., Klein, S. A., and Tjernström, M.: Near-surface meteorology during the Arctic Summer Cloud Ocean Study (ASCOS): evaluation of reanalyses and global climate models, *Atmospheric Chemistry & Physics*, 14, 427–445, doi:10.5194/acp-14-427-2014, 2014.
- 30 DeMott, P. J., Prenni, A. J., Liu, X., Kreidenweis, S. M., Petters, M. D., Twohy, C. H., Richardson, M. S., Eidhammer, T., and Rogers, D. C.: Predicting global atmospheric ice nuclei distributions and their impacts on climate, *Proceedings of the National Academy of Sciences*, doi:10.1073/pnas.0910818107, 2010.
- Edwards, J. M. and Slingo, A.: Studies with a flexible new radiation code. I: Choosing a configuration for a large-scale model, *Quarterly Journal of the Royal Meteorological Society*, 122, 689–719, doi:10.1002/qj.49712253107, 1996.
- 35 Fan, J., Wang, Y., Rosenfeld, D., and Liu, X.: Review of Aerosol–Cloud Interactions: Mechanisms, Significance, and Challenges, *Journal of the Atmospheric Sciences*, 73, 4221–4252, doi:10.1175/JAS-D-16-0037.1, 2016.

- Gray, M. E. B., Petch, J. C., Derbyshire, S. H., Brown, A. R., Lock, A. P., Swann, H. A., and Brown, P. R. A.: Version 2.3 of the Met Office Large Eddy Model: Part II. Scientific Documentation., Tech. rep., 2001.
- Hallett, J. and Mossop, S. C.: Production of Secondary Ice Particles during the Riming Process, *Nature*, 249, 26–28, doi:10.1038/249026a0, 1974.
- 5 Harrington, J. Y. and Olsson, P. Q.: On the potential influence of ice nuclei on surface-forced marine stratocumulus cloud dynamics, *Journal of Geophysical Research: Atmospheres*, 106, 27 473–27 484, doi:10.1029/2000JD000236, 2001.
- Harrington, J. Y., Reisin, T., Cotton, W. R., and Kreidenweis, S. M.: Cloud resolving simulations of Arctic stratus. Part II: Transition-season clouds, *Atmospheric Research*, 51, 45–75, doi:10.1016/S0169-8095(98)00098-2, 1999.
- Hartmann, J., Kottmeier, C., and Raasch, S.: Roll Vortices and Boundary-Layer Development during a Cold Air Outbreak, *Boundary-Layer Meteorology*, 84, 45–65, doi:10.1023/A:1000392931768, 1997.
- 10 Hobbs, P. V. and Rangno, A. L.: Microstructures of low and middle-level clouds over the Beaufort Sea, *Quarterly Journal of the Royal Meteorological Society*, 124, 2035–2071, doi:10.1002/qj.49712455012, 1998.
- Jackson, R. C., McFarquhar, G. M., Korolev, A. V., Earle, M. E., Liu, P. S. K., Lawson, R. P., Brooks, S., Wolde, M., Laskin, A., and Freer, M.: The dependence of ice microphysics on aerosol concentration in arctic mixed-phase stratus clouds during ISDAC and M-PACE, *Journal of Geophysical Research (Atmospheres)*, 117, D15207, doi:10.1029/2012JD017668, 2012.
- 15 Klein, S. A., McCoy, R. B., Morrison, H., Ackerman, A. S., Avramov, A., Boer, G. d., Chen, M., Cole, J. N. S., Del Genio, A. D., Falk, M., Foster, M. J., Fridlind, A., Golaz, J.-C., Hashino, T., Harrington, J. Y., Hoose, C., Khairoutdinov, M. F., Larson, V. E., Liu, X., Luo, Y., McFarquhar, G. M., Menon, S., Neggers, R. A. J., Park, S., Poellot, M. R., Schmidt, J. M., Sednev, I., Shipway, B. J., Shupe, M. D., Spangenberg, D. A., Sud, Y. C., Turner, D. D., Veron, D. E., Salzen, K. v., Walker, G. K., Wang, Z., Wolf, A. B., Xie, S., Xu, K.-M., Yang, F., and Zhang, G.: Intercomparison of model simulations of mixed-phase clouds observed during the ARM Mixed-Phase Arctic Cloud Experiment. I: single-layer cloud, *Quarterly Journal of the Royal Meteorological Society*, 135, 979–1002, doi:10.1002/qj.416, 2009.
- 20 Korolev, A. and Isaac, G.: Phase transformation of mixed-phase clouds, *Quarterly Journal of the Royal Meteorological Society*, 129, 19–38, doi:10.1256/qj.01.203, 2003.
- Lance, S., Brock, C. A., Rogers, D., and Gordon, J. A.: Water droplet calibration of the Cloud Droplet Probe (CDP) and in-flight performance in liquid, ice and mixed-phase clouds during ARCPAC, *Atmospheric Measurement Techniques*, 3, 1683–1706, doi:10.5194/amt-3-1683-2010, 2010.
- Lawson, R. P., O'Connor, D., Zmarzly, P., Weaver, K., Baker, B., Mo, Q., and Jonsson, H.: The 2D-S (Stereo) Probe: Design and Preliminary Tests of a New Airborne, High-Speed, High-Resolution Particle Imaging Probe, *Journal of Atmospheric and Oceanic Technology*, 23, 1462, doi:10.1175/JTECH1927.1, 2006.
- 30 Lloyd, G., Choullarton, T. W., Bower, K. N., Crosier, J., Jones, H., Dorsey, J. R., Gallagher, M. W., Connolly, P., Kirchgaessner, A. C. R., and Lachlan-Cope, T.: Observations and comparisons of cloud microphysical properties in spring and summertime Arctic stratocumulus during the ACCACIA campaign, *Atmospheric Chemistry & Physics*, 15, 3719–3737, doi:10.5194/acp-15-3719-2015, 2015.
- Mason, B. J.: Growth Habits and Growth Rates of Snow Crystals, *Proceedings of the Royal Society of London Series A*, 441, 3–16, doi:10.1098/rspa.1993.0045, 1993.
- 35 Mason, R. H., Si, M., Chou, C., Irish, V. E., Dickie, R., Elizondo, P., Wong, R., Brintnell, M., Elsasser, M., Lassar, W. M., Pierce, K. M., Leaitch, W. R., MacDonald, A. M., Platt, A., Toom-Sauntry, D., Sarda-Estève, R., Schiller, C. L., Suski, K. J., Hill, T. C. J., Abbatt, J. P. D., Huffman, J. A., DeMott, P. J., and Bertram, A. K.: Size-resolved measurements of ice-nucleating particles at six locations in North America and one in Europe, *Atmospheric Chemistry and Physics*, 16, 1637–1651, doi:10.5194/acp-16-1637-2016, 2016.

- McFarquhar, G. M., Ghan, S., Verlinde, J., Korolev, A., Strapp, J. W., Schmid, B., Tomlinson, J. M., Wolde, M., Brooks, S. D., Cziczo, D., Dubey, M. K., Fan, J., Flynn, C., Gultepe, I., Hubbe, J., Gilles, M. K., Laskin, A., Lawson, P., Leaitch, W. R., Liu, P., Liu, X., Lubin, D., Mazzoleni, C., MacDonald, A.-M., Moffet, R. C., Morrison, H., Ovchinnikov, M., Shupe, M. D., Turner, D. D., Xie, S., Zelenyuk, A., Bae, K., Freer, M., and Glen, A.: Indirect and Semi-direct Aerosol Campaign: The Impact of Arctic Aerosols on Clouds., *Bull. Am. Meteorol. Soc.*, 92, 183–201, doi:10.1175/2010BAMS2935.1, 2011.
- 5 Meyers, M. P., Demott, P. J., and Cotton, W. R.: New Primary Ice-Nucleation Parameterizations in an Explicit Cloud Model., *Journal of Applied Meteorology*, 31, 708–721, doi:10.1175/1520-0450(1992)031<0708:NPINPI>2.0.CO;2, 1992.
- Möhler, O., Benz, S., Saathoff, H., Schnaiter, M., Wagner, R., Schneider, J., Walter, S., Ebert, V., and Wagner, S.: The effect of organic coating on the heterogeneous ice nucleation efficiency of mineral dust aerosols, *Environmental Research Letters*, 3, 025007, doi:10.1088/1748-9326/3/2/025007, 2008.
- 10 Morrison, H., Curry, J. A., and Khvorostyanov, V. I.: A New Double-Moment Microphysics Parameterization for Application in Cloud and Climate Models. Part I: Description., *Journal of Atmospheric Sciences*, 62, 1665–1677, doi:10.1175/JAS3446.1, 2005.
- Morrison, H., Pinto, J. O., Curry, J. A., and McFarquhar, G. M.: Sensitivity of modeled arctic mixed-phase stratocumulus to cloud condensation and ice nuclei over regionally varying surface conditions, *Journal of Geophysical Research (Atmospheres)*, 113, D05203, doi:10.1029/2007JD008729, 2008.
- 15 Morrison, H., McCoy, R. B., Klein, S. A., Xie, S., Luo, Y., Avramov, A., Chen, M., Cole, J. N. S., Falk, M., Foster, M. J., Del Genio, A. D., Harrington, J. Y., Hoose, C., Khairoutdinov, M. F., Larson, V. E., Liu, X., McFarquhar, G. M., Poellot, M. R., von Salzen, K., Shipway, B. J., Shupe, M. D., Sud, Y. C., Turner, D. D., Veron, D. E., Walker, G. K., Wang, Z., Wolf, A. B., Xu, K.-M., Yang, F., and Zhang, G.: Intercomparison of model simulations of mixed-phase clouds observed during the ARM Mixed-Phase Arctic Cloud Experiment. II: Multilayer cloud, *Quarterly Journal of the Royal Meteorological Society*, 135, 1003–1019, doi:10.1002/qj.415, 2009.
- 20 Morrison, H., Zuidema, P., Ackerman, A. S., Avramov, A., de Boer, G., Fan, J., Fridlind, A. M., Hashino, T., Harrington, J. Y., Luo, Y., Ovchinnikov, M., and Shipway, B.: Intercomparison of cloud model simulations of Arctic mixed-phase boundary layer clouds observed during SHEBA/FIRE-ACE, *Journal of Advances in Modeling Earth Systems*, 3, M06003, doi:10.1029/2011MS000066, 2011.
- Morrison, H., de Boer, G., Feingold, G., Harrington, J., Shupe, M. D., and Sulia, K.: Resilience of persistent Arctic mixed-phase clouds, *Nature Geoscience*, 5, 11–17, doi:10.1038/ngeo1332, 2012.
- 25 Murray, B. J., O’Sullivan, D., Atkinson, J. D., and Webb, M. E.: Ice nucleation by particles immersed in supercooled cloud droplets., *Chem Soc Rev.*, 41, 6519–54, doi:10.1039/c2cs35200a, 2012.
- Ovchinnikov, M., Korolev, A., and Fan, J.: Effects of ice number concentration on dynamics of a shallow mixed-phase stratiform cloud, *Journal of Geophysical Research: Atmospheres*, 116, doi:10.1029/2011JD015888, d00T06, 2011.
- 30 Pinto, J. O.: Autumnal Mixed-Phase Cloudy Boundary Layers in the Arctic., *Journal of Atmospheric Sciences*, 55, 2016–2038, doi:10.1175/1520-0469(1998)055<2016:AMPCBL>2.0.CO;2, 1998.
- Prenni, A. J., Harrington, J. Y., Tjernström, M., Demott, P. J., Avramov, A., Long, C. N., Kreidenweis, S. M., Olsson, P. Q., and Verlinde, J.: Can Ice-Nucleating Aerosols Affect Arctic Seasonal Climate?, *Bulletin of the American Meteorological Society*, 88, 541, doi:10.1175/BAMS-88-4-541, 2007.
- 35 Primm, K. M., Schill, G. P., Veghte, D. P., Freedman, M. A., and Tolbert, M. A.: Depositional ice nucleation on NX illite and mixtures of NX illite with organic acids, *Journal of Atmospheric Chemistry*, pp. 1–15, doi:10.1007/s10874-016-9340-x, 2016.
- Pruppacher, H. R. and Klett, J. D.: *Microphysics of Clouds and Precipitation*, Kluwer Academic Publishers, 1997.

- Rangno, A. L. and Hobbs, P. V.: Ice particles in stratiform clouds in the Arctic and possible mechanisms for the production of high ice concentrations, *Journal of Geophysical Research: Atmospheres*, 106, 15 065–15 075, doi:10.1029/2000JD900286, 2001.
- Rosenberg, P. D., Dean, A. R., Williams, P. I., Dorsey, J. R., Minikin, A., Pickering, M. A., and Petzold, A.: Particle sizing calibration with refractive index correction for light scattering optical particle counters and impacts upon PCASP and CDP data collected during the Fennec campaign, *Atmospheric Measurement Techniques*, 5, 1147–1163, doi:10.5194/amt-5-1147-2012, 2012.
- Serreze, M. C. and Barry, R. G.: Processes and impacts of Arctic amplification: A research synthesis, *Global and Planetary Change*, 77, 85 – 96, doi:dx.doi.org/10.1016/j.gloplacha.2011.03.004, 2011.
- Shupe, M. D., Matrosov, S. Y., and Uttal, T.: Arctic Mixed-Phase Cloud Properties Derived from Surface-Based Sensors at SHEBA., *Journal of Atmospheric Sciences*, 63, 697–711, doi:10.1175/JAS3659.1, 2006.
- Shupe, M. D., Daniel, J. S., de Boer, G., Eloranta, E. W., Kollias, P., Long, C. N., Luke, E. P., Turner, D. D., and Verlinde, J.: A Focus On Mixed-Phase Clouds, *Bulletin of the American Meteorological Society*, 89, 1549, doi:10.1175/2008BAMS2378.1, 2008a.
- Shupe, M. D., Kollias, P., Persson, P. O. G., and McFarquhar, G. M.: Vertical Motions in Arctic Mixed-Phase Stratiform Clouds, *Journal of Atmospheric Sciences*, 65, 1304, doi:10.1175/2007JAS2479.1, 2008b.
- Shupe, M. D., Walden, V. P., Eloranta, E., Uttal, T., Campbell, J. R., Starkweather, S. M., and Shiobara, M.: Clouds at Arctic Atmospheric Observatories. Part I: Occurrence and Macrophysical Properties, *Journal of Applied Meteorology and Climatology*, 50, 626–644, doi:10.1175/2010JAMC2467.1, 2011.
- Solomon, A., Feingold, G., and Shupe, M. D.: The role of ice nuclei recycling in the maintenance of cloud ice in Arctic mixed-phase stratocumulus, *Atmospheric Chemistry and Physics*, 15, 10 631–10 643, doi:10.5194/acp-15-10631-2015, 2015.
- Sotiropoulou, G., Sedlar, J., Tjernström, M., Shupe, M. D., Brooks, I. M., and Persson, P. O. G.: The thermodynamic structure of summer Arctic stratocumulus and the dynamic coupling to the surface, *Atmospheric Chemistry and Physics*, 14, 12 573–12 592, doi:10.5194/acp-14-12573-2014, 2014.
- Stocker, T., Qin, D., Plattner, G.-K., Alexander, L., Allen, S., Bindoff, N., Bréon, F.-M., Church, J., Cubasch, U., Emori, S., Forster, P., Friedlingstein, P., Gillett, N., Gregory, J., Hartmann, D., Jansen, E., Kirtman, B., Knutti, R., Krishna Kumar, K., Lemke, P., Marotzke, J., Masson-Delmotte, V., Meehl, G., Mokhov, I., Piao, S., Ramaswamy, V., Randall, D., Rhein, M., Rojas, M., Sabine, C., Shindell, D., Talley, L., Vaughan, D., and Xie, S.-P.: Technical Summary, in: *Climate Change 2013: The Physical Science Basis. Contribution of Working Group I to the Fifth Assessment Report of the Intergovernmental Panel on Climate Change*, edited by: Stocker, T.F., D. Qin, G.-K. Plattner, M. Tignor, S.K. Allen, J. Boschung, A. Nauels, Y. Xia, V. Bex and P.M. Midgley, Cambridge University Press, Cambridge, United Kingdom and New York, NY, USA, doi:10.1017/CBO9781107415324.005, 2013.
- Taylor, J. W., Choulaton, T. W., Blyth, A. M., Liu, Z., Bower, K. N., Crosier, J., Gallagher, M. W., Williams, P. I., Dorsey, J. R., Flynn, M. J., Bennett, L. J., Huang, Y., French, J., Korolev, A., and Brown, P. R. A.: Observations of cloud microphysics and ice formation during COPE, *Atmospheric Chemistry and Physics*, 16, 799–826, doi:10.5194/acp-16-799-2016, 2016.
- Tjernström, M., Sedlar, J., and Shupe, M. D.: How Well Do Regional Climate Models Reproduce Radiation and Clouds in the Arctic? An Evaluation of ARCMIP Simulations, *Journal of Applied Meteorology and Climatology*, 47, 2405, doi:10.1175/2008JAMC1845.1, 2008.
- Verlinde, J., Harrington, J. Y., McFarquhar, G. M., Yannuzzi, V. T., Avramov, A., Greenberg, S., Johnson, N., Zhang, G., Poellot, M. R., Mather, J. H., Turner, D. D., Eloranta, E. W., Zak, B. D., Prenni, A. J., Daniel, J. S., Kok, G. L., Tobin, D. C., Holz, R., Sassen, K., Spangenberg, D., Minnis, P., Tooman, T. P., Ivey, M. D., Richardson, S. J., Bahrmann, C. P., Shupe, M., Demott, P. J., Heymsfield, A. J., and Schofield, R.: The Mixed-Phase Arctic Cloud Experiment, *Bulletin of the American Meteorological Society*, 88, 205, doi:10.1175/BAMS-88-2-205, 2007.

- Vihma, T., Pirazzini, R., Fer, I., Renfrew, I. A., Sedlar, J., Tjernström, M., Lüpkes, C., Nygård, T., Notz, D., Weiss, J., Marsan, D., Cheng, B., Birnbaum, G., Gerland, S., Chechin, D., and Gascard, J. C.: Advances in understanding and parameterization of small-scale physical processes in the marine Arctic climate system: a review, *Atmospheric Chemistry & Physics*, 14, 9403–9450, doi:10.5194/acp-14-9403-2014, 2014.
- 5 Young, G., Jones, H. M., Choulaton, T. W., Crosier, J., Bower, K. N., Gallagher, M. W., Davies, R. S., Renfrew, I. A., Elvidge, A. D., Darbyshire, E., Marengo, F., Brown, P. R. A., Ricketts, H. M. A., Connolly, P. J., Lloyd, G., Williams, P. I., Allan, J. D., Taylor, J. W., Liu, D., and Flynn, M. J.: Observed microphysical changes in Arctic mixed-phase clouds when transitioning from sea ice to open ocean, *Atmospheric Chemistry and Physics*, 16, 13945–13967, doi:10.5194/acp-16-13945-2016, 2016a.
- Young, G., Jones, H. M., Darbyshire, E., Baustian, K. J., McQuaid, J. B., Bower, K. N., Connolly, P. J., Gallagher, M. W., and Choulaton, T. W.: Size-segregated compositional analysis of aerosol particles collected in the European Arctic during the ACCACIA campaign, *Atmospheric Chemistry and Physics*, 16, 4063–4079, doi:10.5194/acp-16-4063-2016, 2016b.
- 10 Young, K. C.: The Role of Contact Nucleation in Ice Phase Initiation in Clouds, *Journal of the Atmospheric Sciences*, 31, 768–776, doi:10.1175/1520-0469(1974)031<0768:TROCNI>2.0.CO;2, 1974.

Supplementary Material

Drosonde dry bias

5 A possible dry bias was influencing the dropsonde data used to initialise the LEM, producing a drier boundary layer than was observed. Of the data used to initialise the model, only the q_{vap} field (as shown in Fig. 3) was affected. Cloud fields are initialised with an adiabatic liquid water mixing ratio profile; therefore, this bias only has a small effect on the modelled cloud structure. However, the rate at which precipitation develops is affected and highlights an additional sensitivity of cloud structure to the humidity of the boundary layer in each case.

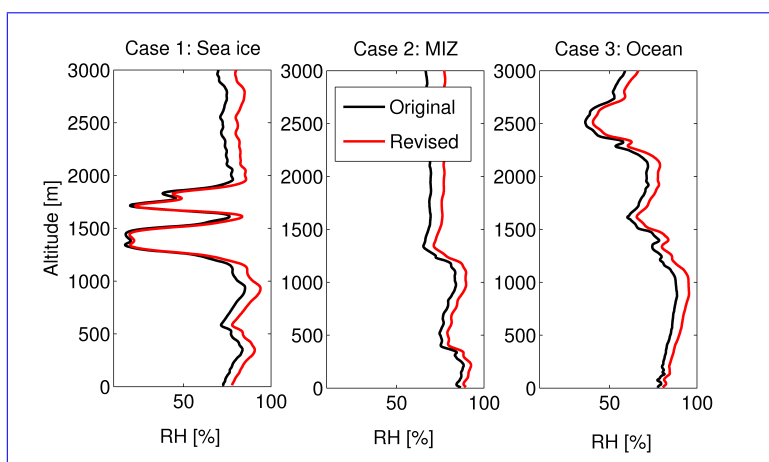


Figure S1. Relative humidity (RH) dropsonde measurements. Original data (black) was used to initialise the LEM in the presented simulations. Revised data is shown in red.

10 Figures illustrating the extent of this dry bias are included as follows. Relative humidity data are shown in Fig. S1. An equivalent version of Fig. 3 is included to demonstrate the revised q_{vap} profiles (Fig. S2). Additionally, an example test simulation with revised dropsonde profiles from each case is included for justification.

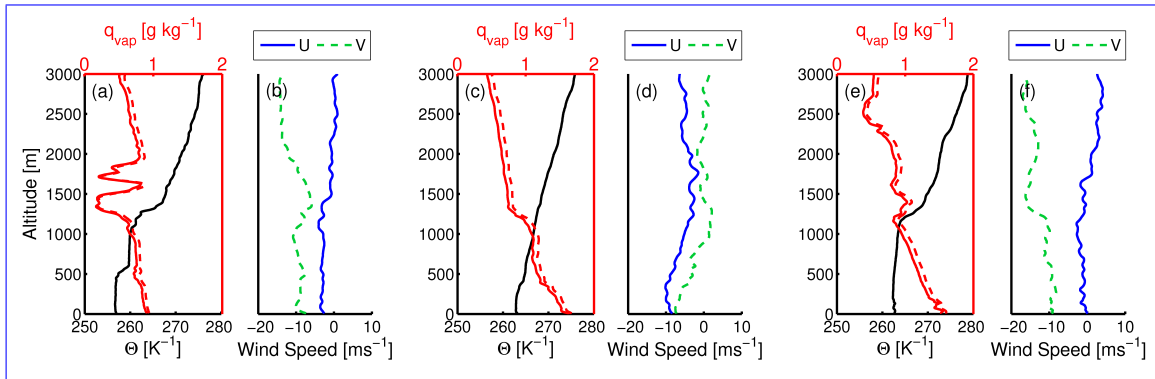


Figure S2. As Fig. 3 with revised q_{vap} data shown by a dashed (red) line in panels a, c, and e.

Figure S3 shows the equivalent simulation to Fig. 5(a) with the revised humidity profiles. Our conclusions remain unchanged with this new data: using C86 under the deposition-condensation conditions commonly used in WRF causes the production of an ice cloud with complete suppression of the liquid phase. The mixed-phase conditions observed are inadequately reproduced using these criteria.

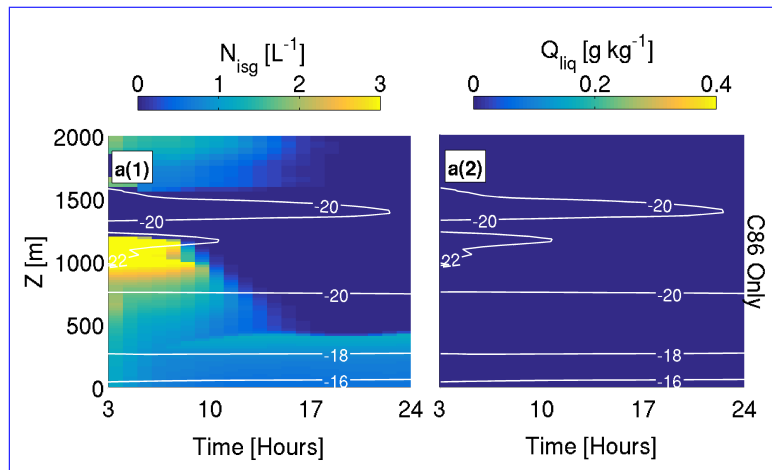


Figure S3. As Fig. 5(a) with revised dropsonde initialisation conditions.

- 5 Figure S4 illustrates that increasing the humidity of the boundary layer quickens the formation of the mixed-phase cloud layer in case 2. Cloud top increases to higher altitudes than in the drier case (Fig. 9(c)), and reaches colder temperatures, due to the development of precipitation. The increased humidity allows for more efficient precipitation development, which acts to deplete the liquid phase of the cloud.

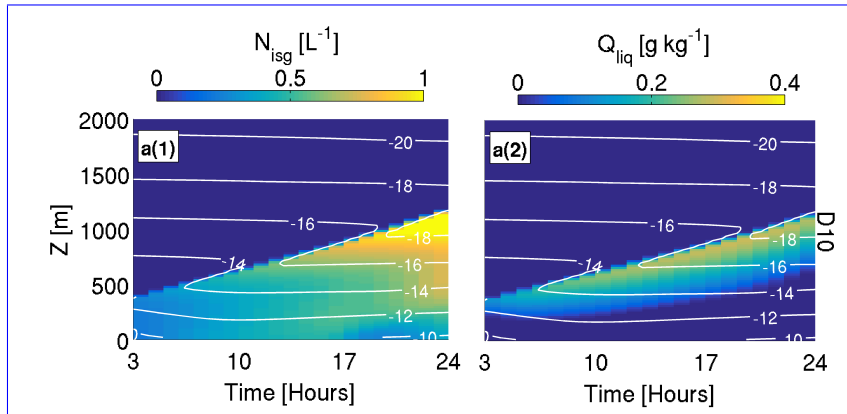


Figure S4. As Fig. 9(c) with revised dropsonde initialisation conditions.

Figure S5 shows the D10 ocean simulation (as Fig. 10(c)) with the revised initialisation profiles. In contrast to the drier conditions, this cloud glaciates by 22 h and all ice falls out of the cloud by 24 h. No convective features form as the precipitation which forms does so more efficiently with increased humidity, leading to complete cloud break up. Greater number concentrations of large solid hydrometeors (snow and graupel) are simulated at earlier times, leading to cloud break up with no convection development.

5

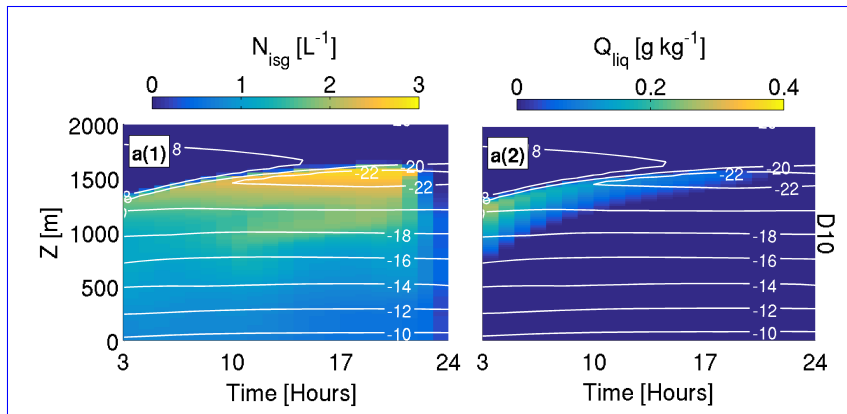


Figure S5. As Fig. 10(c) with revised dropsonde initialisation conditions.

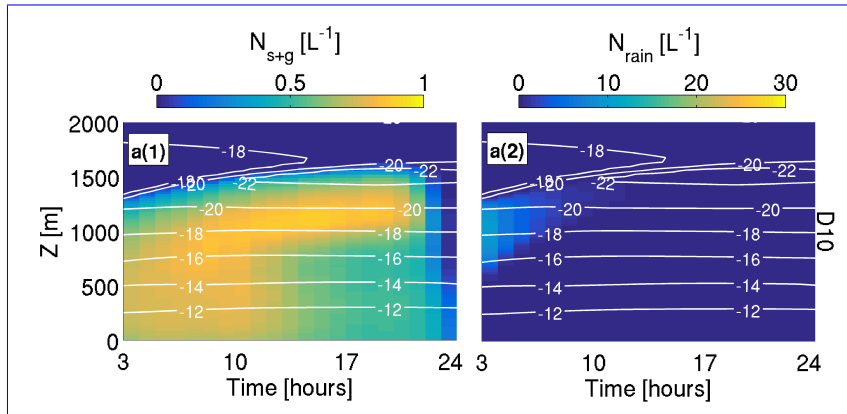


Figure S6. As Fig. 12(a) with revised droplet initialisation conditions.

Bigg immersion-freezing and Meyers contact-freezing

The influence of immersion- and contact-freezing within the Morrison et al. (2005) microphysics scheme was tested to quantify their contribution to $N_{ice,sg}$. Simulations with contact-freezing (Meyers et al. 1992 - hereafter, M92) and immersion-freezing (Bigg 1953 - hereafter, B53) switched either on or off are shown in Fig. S7. The addition of B53 and M92 produces a significantly larger ice crystal number concentration (up to $3 L^{-1}$, $1.5 L^{-1}$, and $10 L^{-1}$ in cases 1, 2, and 3 respectively) than the mean observed ($0.47 \pm 0.86 L^{-1}$, $0.35 \pm 0.20 L^{-1}$, and $0.55 \pm 0.95 L^{-1}$ respectively, Table 2).

Modelled ice number concentrations with and without B53 and M92 active are similar in case 1. Both representations cause glaciation, and liquid water is not modelled at any point during the simulations. No improvement can be seen in the liquid water mixing ratio when both the B53 and M92 nucleation mechanisms are disabled. Modelled ice number concentrations for case 2 peak at $\sim 1.5 L^{-1}$ and $\sim 0.8 L^{-1}$ with and without both B53 immersion- and M92 contact-freezing nucleation active. Both scenarios allow for liquid water to form in the cloud, with $\sim 0.2 g kg^{-1}$ modelled. When B53 and M92 are active in case 3, high ice number concentrations are rapidly simulated at approximately 12 h-14 h. This event causes the evaporation of all simulated liquid water, and the region of high ice number concentration dissipates back to the original sustained concentration of $\sim 2 L^{-1}$ afterwards. This event is not simulated when B53 and M92 are disabled, suggesting these additional sources of ice number are the cause of this phenomenon.

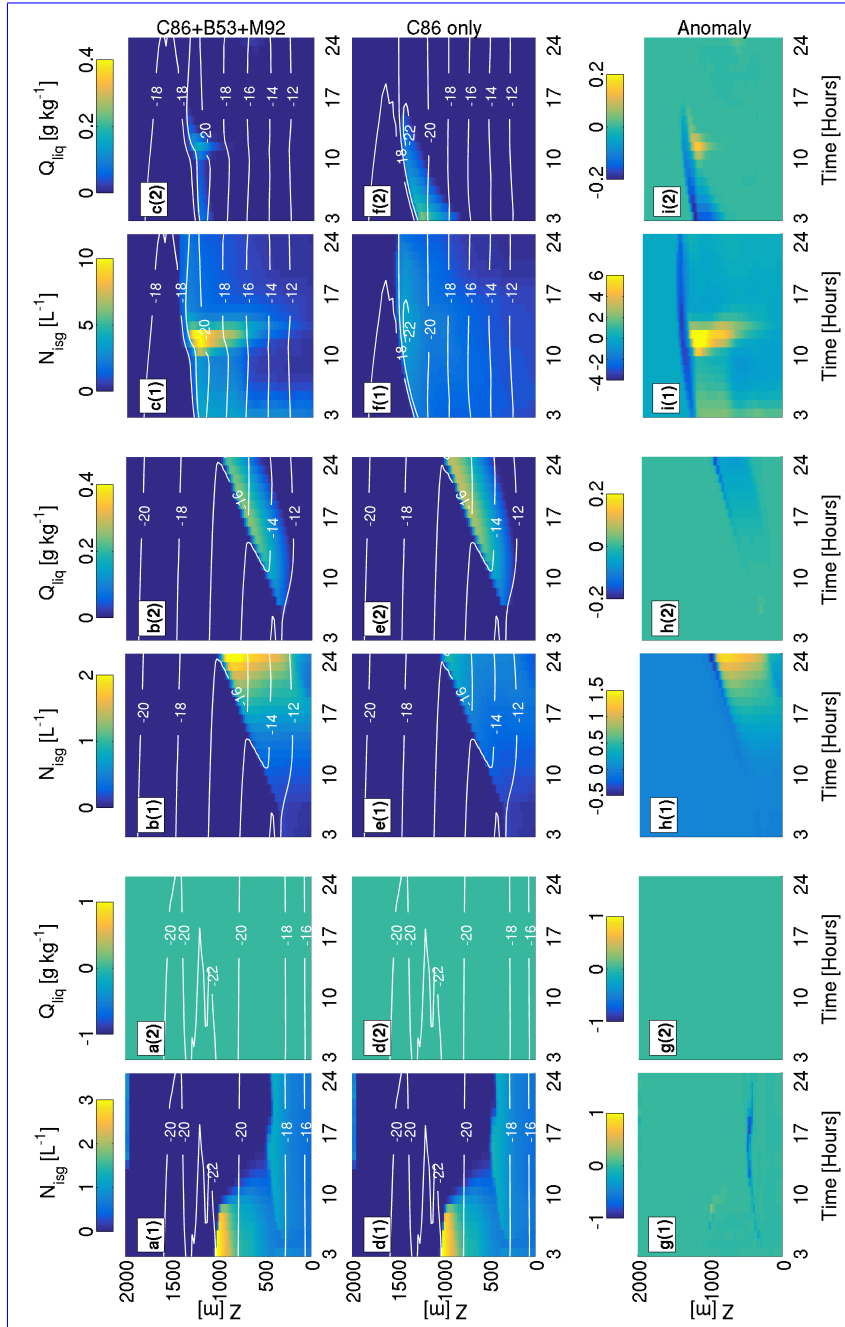


Figure S7. Simulated ice number concentrations (N_{ice} , **columns 1, 3, and 5**) and liquid water mixing ratios (Q_{liq} , **columns 2, 4, and 6**) using the Cooper (1986) parameterisation under default WRF conditions ($T < -8^{\circ}\text{C}$, $S_w > 0.999$ or $S_i > 1.08$). **Top row:** (a, b, c): B53, M92, and C86 active. **Middle row:** (d, e, f): C86 deposition-condensation freezing nucleation only. **Bottom row:** (g, h, i): Anomaly between simulations including B53 and M92 and those using C86 only. **Column 1-2:** (a, d, g): Sea ice (case 1), **Column 3-4:** (b, e, h): MIZ (case 2), **Column 5-6:** (c, f, i): Ocean (case 3). Run length 24 hours. Temperature ($^{\circ}\text{C}$) contours are overlaid in white. Note changing colour bars for each subfigure.

Supplementary figures

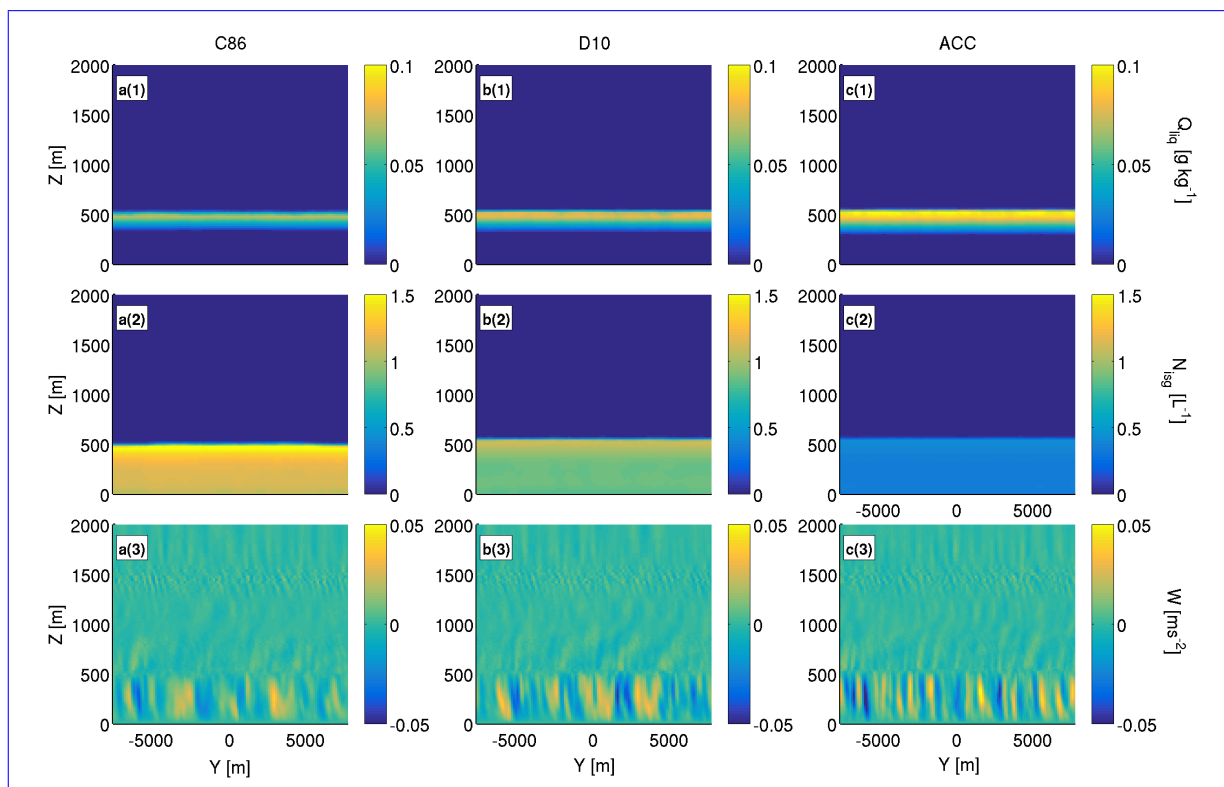


Figure S8. Z-Y slice of modelled Q_{liq} (**top row**), $N_{ice-ice}$ (**middle row**), and vertical velocity (**bottom row**) at 21 h over the sea ice (case 1). The $N_{ice-ice}$ and Q_{liq} fields are homogeneous, with liquid layer at cloud top and ice formation throughout. Enhanced turbulent activity, due to the comparatively larger liquid water content, is modelled with ACC (**panel c**). Note changing colour bars for each subfigure.

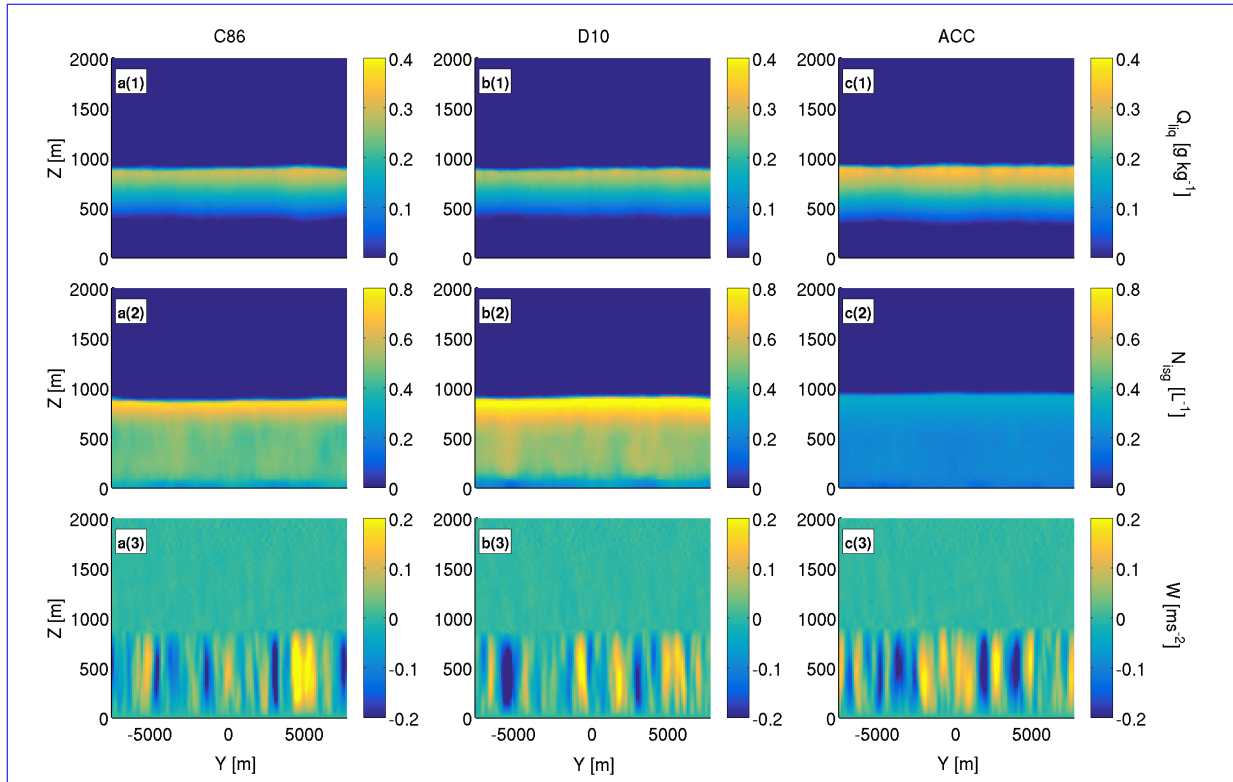


Figure S9. Z-Y slice of modelled Q_{liq} (**top row**), N_{ice_isg} (**middle row**), and vertical velocity (**bottom row**) at 21 h over the MIZ (case 2). Significant turbulence is simulated within the cloudy layer (bottom row). With comparison to the sea ice case, the liquid layer at cloud top is more heterogeneous in all cases. This is particularly clear in the D10 simulations ([panel b](#)), where N_{ice_isg} is enhanced in downdraughts. [Note changing colour bars for each subfigure.](#)

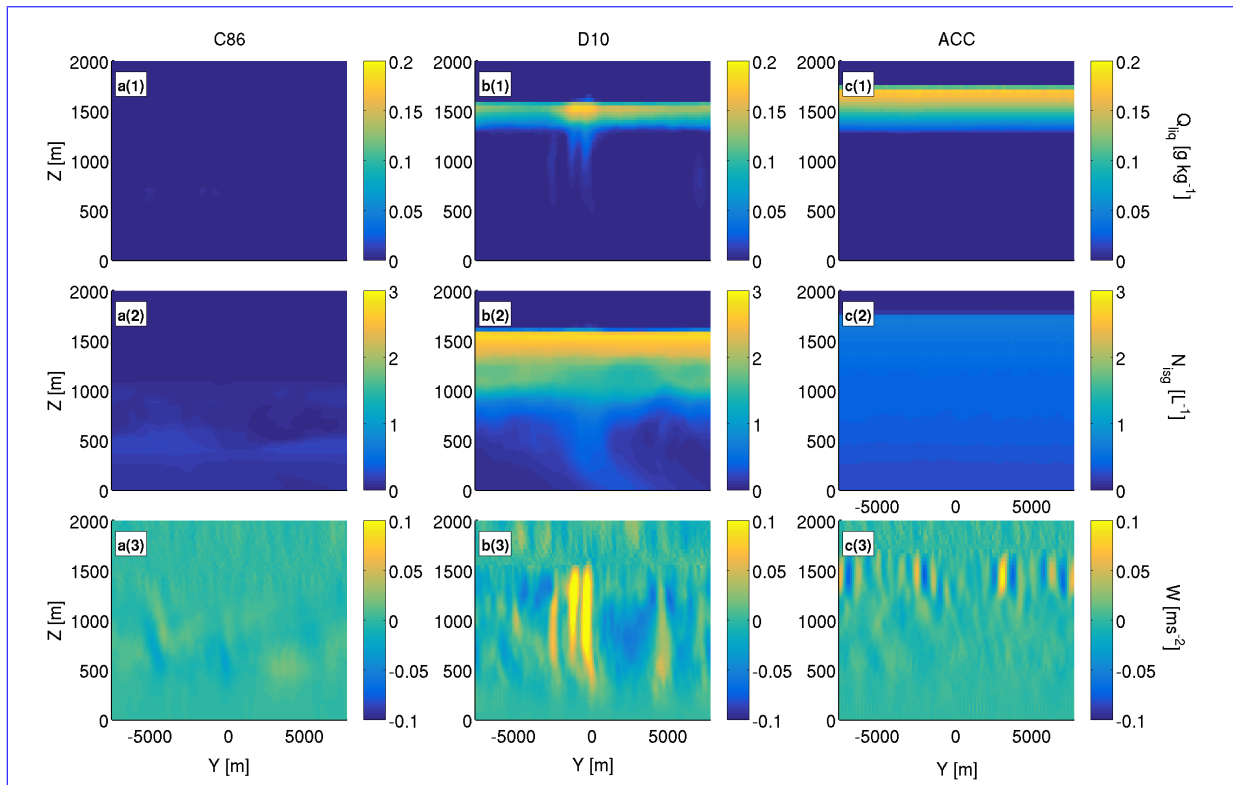


Figure S10. Z-Y slice of modelled Q_{liq} (top row), $N_{ice-issg}$ (middle row), and vertical velocity (bottom row) at 21 h over the ocean (case 3). Large updraught columns are simulated using D10, which correspond spatially with columns of high Q_{liq} . These updraughts are co-located with a precipitating (snow) region, evident from the $N_{ice-issg}$ figures (second row). C86 (panel a) had dissipated by 21 h; therefore, little activity can be seen in this simulation. Similar to cases 1 and 2, ACC produces a homogeneous liquid layer at cloud top, with ice below (panel c). Note changing colour bars for each subfigure.

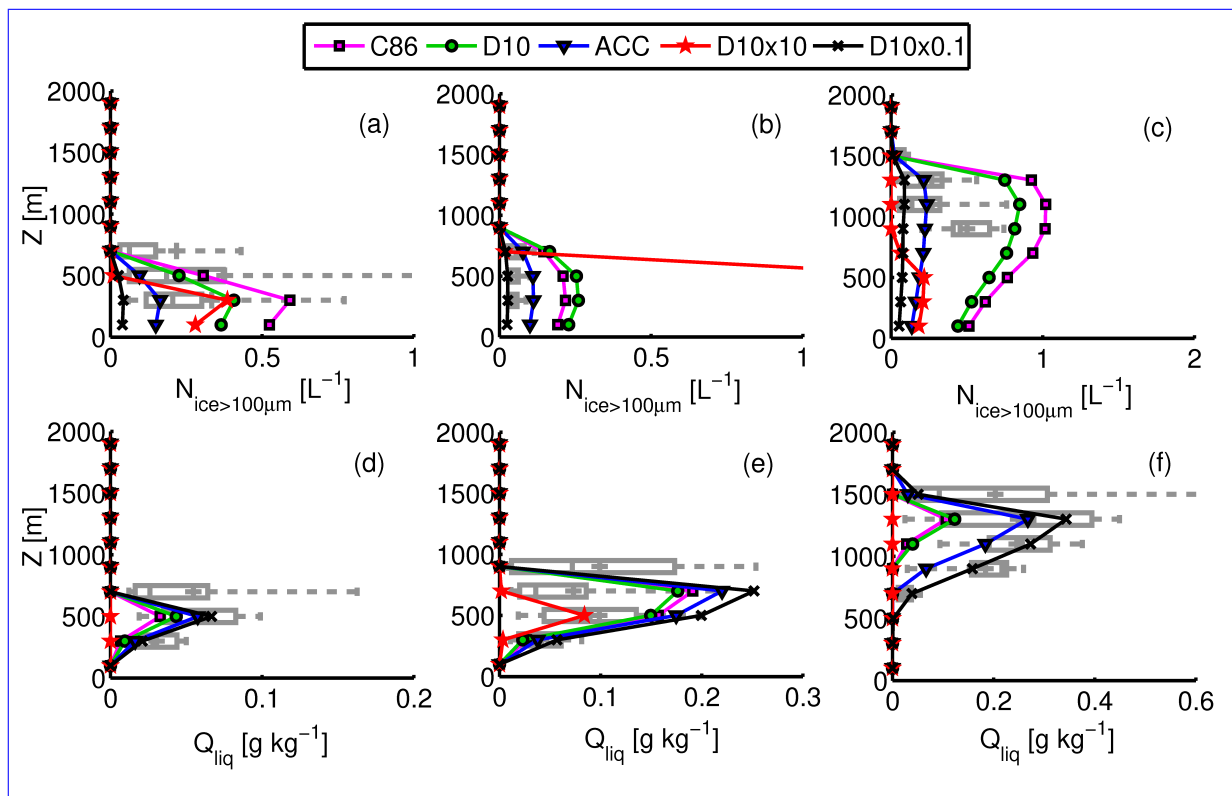


Figure S11. Observed N_{ice} , $N_{ice>100\mu m}$ (top row), $N_{ice>100\mu m}$ (middle row), and Q_{liq} (bottom row) for the sea ice (column 1), MIZ (column 2) and ocean (column 3) cases. Observations are shown as grey boxes. These boxes illustrate data similarly to those in Fig. 7. Modelled N_{ice} , $N_{ice>100\mu m}$, and Q_{liq} are overlaid from the C86 (magenta), D10 (green), ACC (blue), D10x10 (red), and D10x0.1 (black) simulations. Model time steps of 21 h, 17 h, and 7 h are again used for comparison with the sea ice, MIZ, and ocean observations respectively.

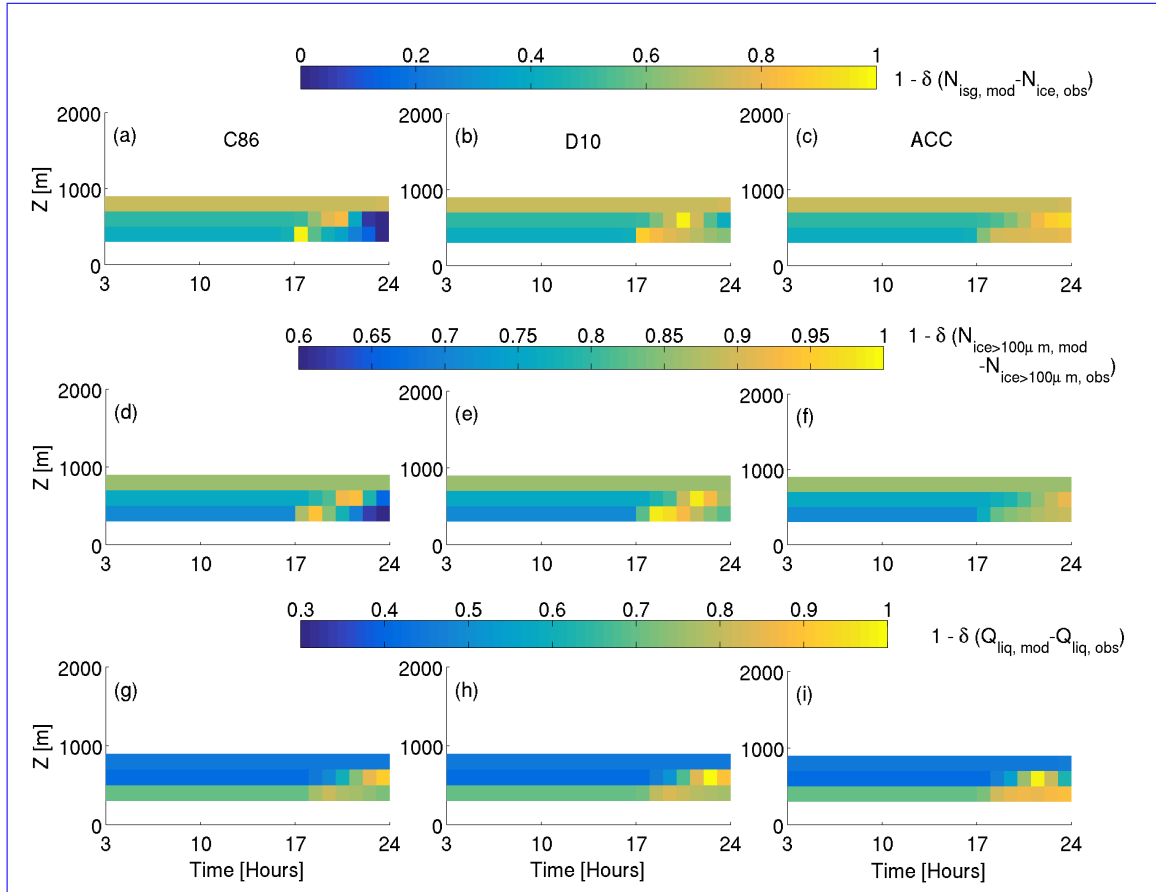


Figure S12. Residual comparison of modelled and observed $N_{ice, isg}$ (**top row**), $N_{ice > 100 \mu m}$ (**middle row**), and Q_{liq} (**bottom row**) in case 1 (sea ice) for each model time step. At each altitude bin, the mean observed quantity is subtracted from the mean modelled. The absolute magnitude of this fraction is then subtracted from 1. Therefore, better agreement between the mean observed and mean modelled values gives a larger fraction (with a maximum of 1). When two of the three parameterisations give good agreement with the $N_{ice, isg}$ observations at the same time step, that time step has been selected for comparison with the observations in Fig. 7. For the sea ice simulations, the chosen time step was 21 h. [Note changing colour bars for each row.](#)

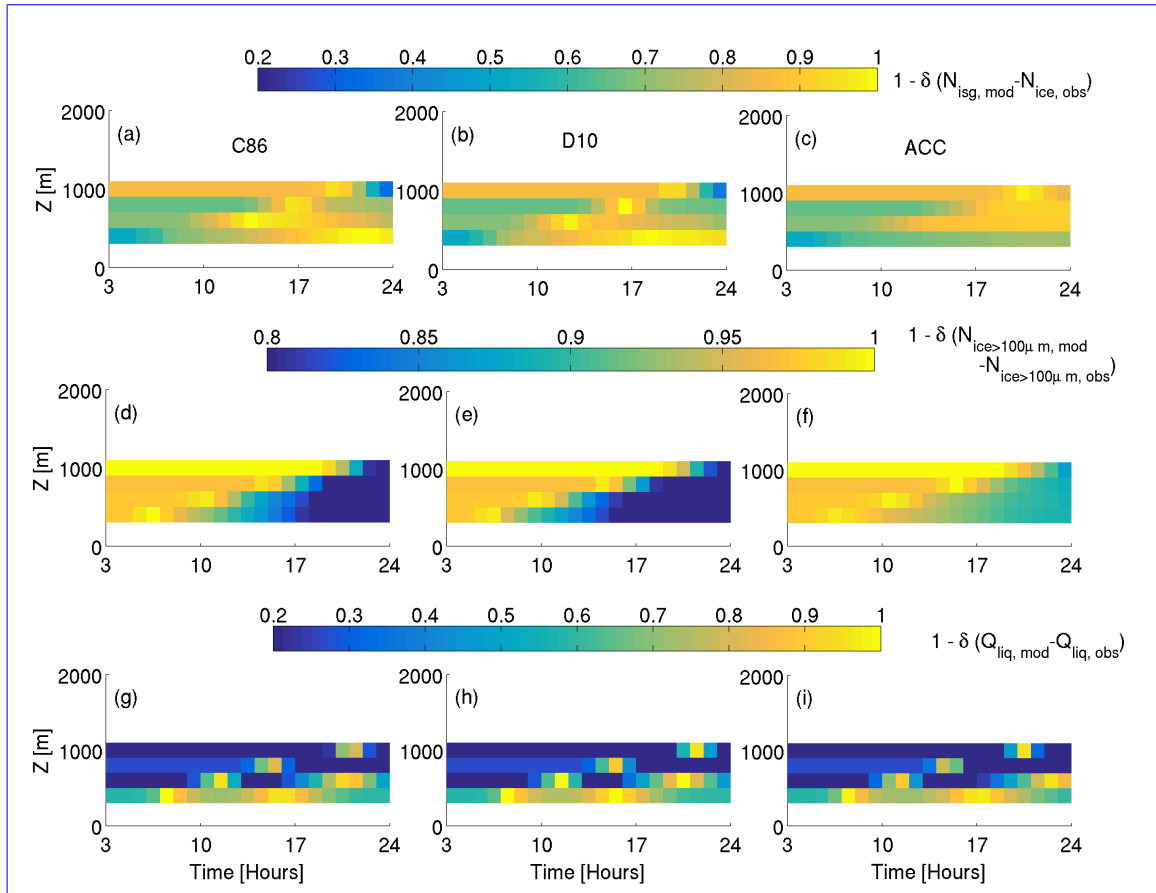


Figure S13. Residual comparison of modelled and observed $N_{ice-isc}$ (top row), $N_{ice>100\mu m}$ (middle row), and Q_{liq} (bottom row) in case 2 (MIZ) for each model time step. As with Fig. S12, better agreement with the mean observed value gives a larger fraction (with a maximum of 1). For the MIZ simulations, the chosen time step was 17 h. [Note changing colour bars for each row.](#)

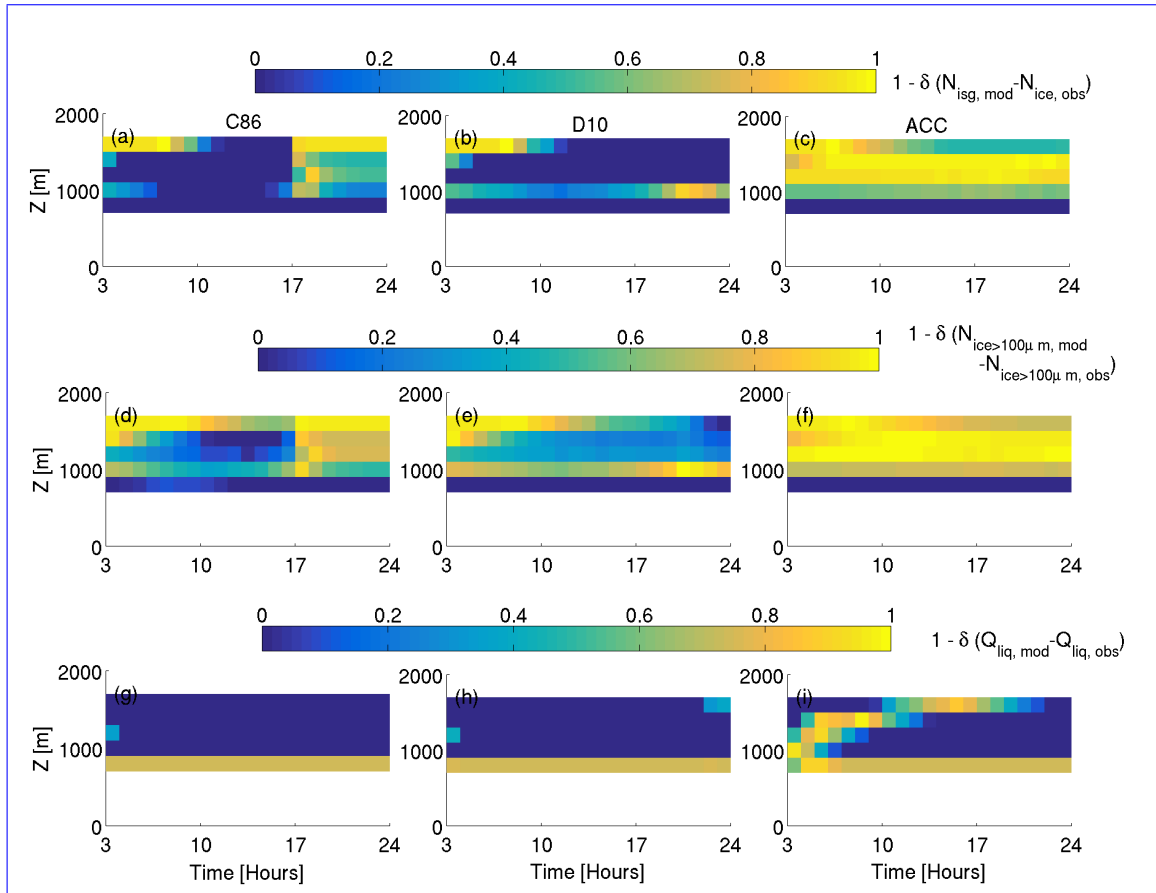


Figure S14. Residual comparison of modelled and observed $N_{ice-IsG}$ (**top row**), $N_{ice>100\mu m}$ (**middle row**), and Q_{liq} (**bottom row**) in case 3 (ocean) for each model time step. As with Fig. S12, better agreement with the mean observed value gives a larger fraction (with a maximum of 1). For the MIZ simulations, the chosen time step was 7 h. [Note changing colour bars for each row.](#)

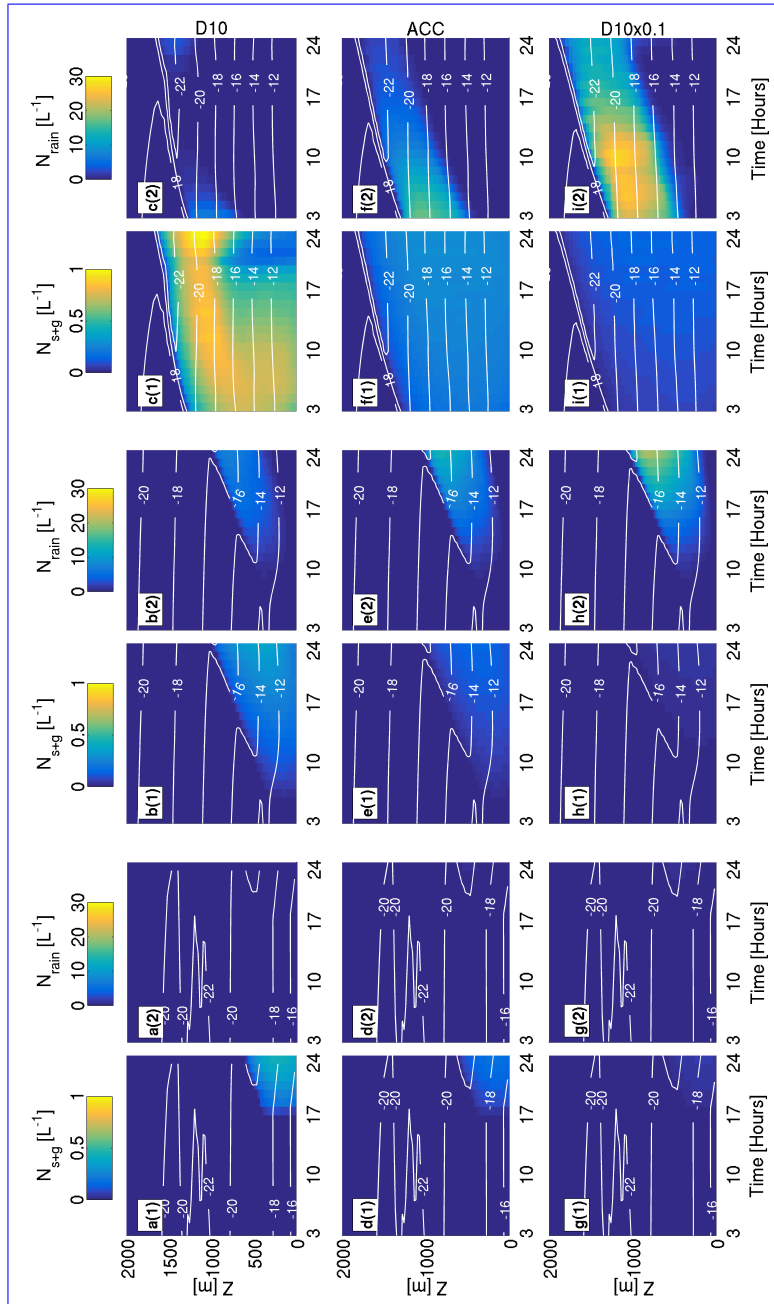


Figure S15. Summed snow and graupel number concentrations (N_{s+g} , **columns 1, 3, and 5**) and rain number concentration (N_{liq} , **columns 2, 4, and 6**) using D10 (**top row**), ACC (**middle row**) and D10 \times 0.1 (**bottom row**). **Column 1-2: (a, d, g):** Sea ice (case 1), **Column 3-4: (b, e, h):** MIZ (case 2), **Column 5-6: (c, f, i):** Ocean (case 3). Run length 24 hours. Solid precipitation increases Number concentrations of solid precipitable particles increase with simulation time in all cases when using D10, and the rain number concentration behaves similarly in case 2 when applying D10 \times 0.1. Overall, little small concentrations of large solid and liquid precipitation is hydrometeors are modelled during the ACC simulations (**panels d, e, f**), and almost no precipitation is precipitable particles are modelled in case 1 with D10 \times 0.1 (**panel g**). Note changing colour bar for each column.

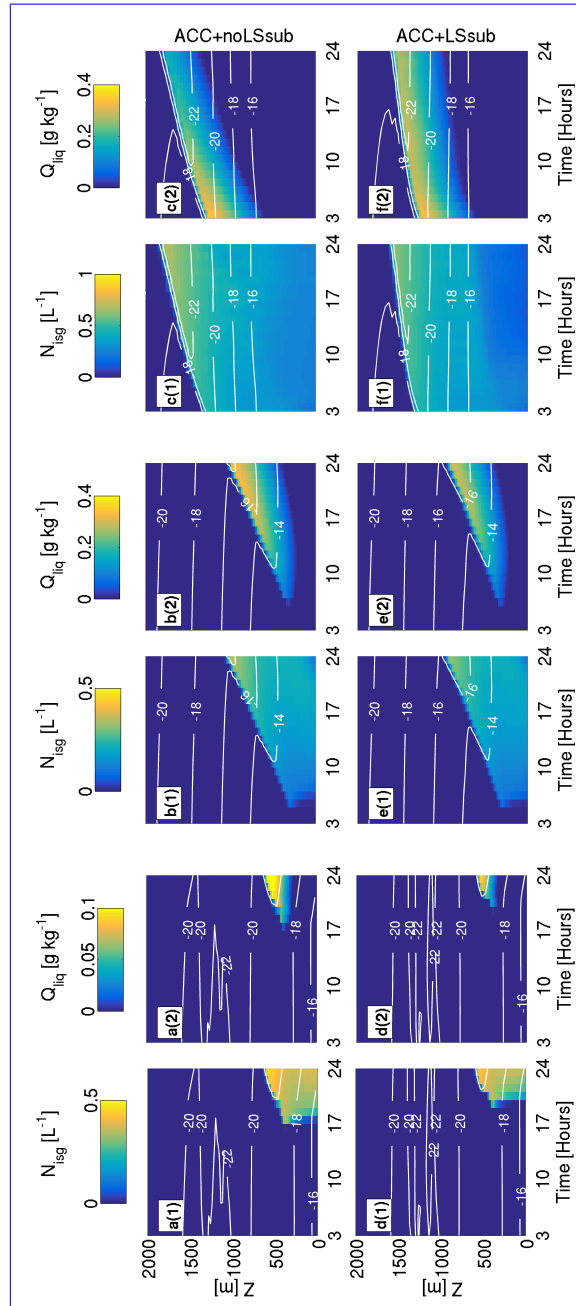


Figure S16. Simulated ice number concentrations ($N_{ice,lg}$, **columns 1, 3, and 5**) and liquid water mixing ratios (Q_{liq} , **columns 2, 4, and 6**) using ACC without large-scale subsidence (**top row**) and with an imposed subsidence of $2.5 \times 10^{-6} \text{ s}^{-1}$ (**bottom row**, as in Solomon et al., 2015). All are restricted to water-saturation. **Column 1-2: (a, d):** Sea ice (case 1), **Column 3-4: (b, e):** MIZ (case 2), **Column 5-6: (c, f):** Ocean (case 3). Run length 24 hours. In all cases, cloud top height and Q_{liq} is suppressed when large-scale subsidence is imposed. Temperatures are also warmer; however, case 2 is still too cold with comparison to the observations. [Note changing colour bars for each subfigure.](#)

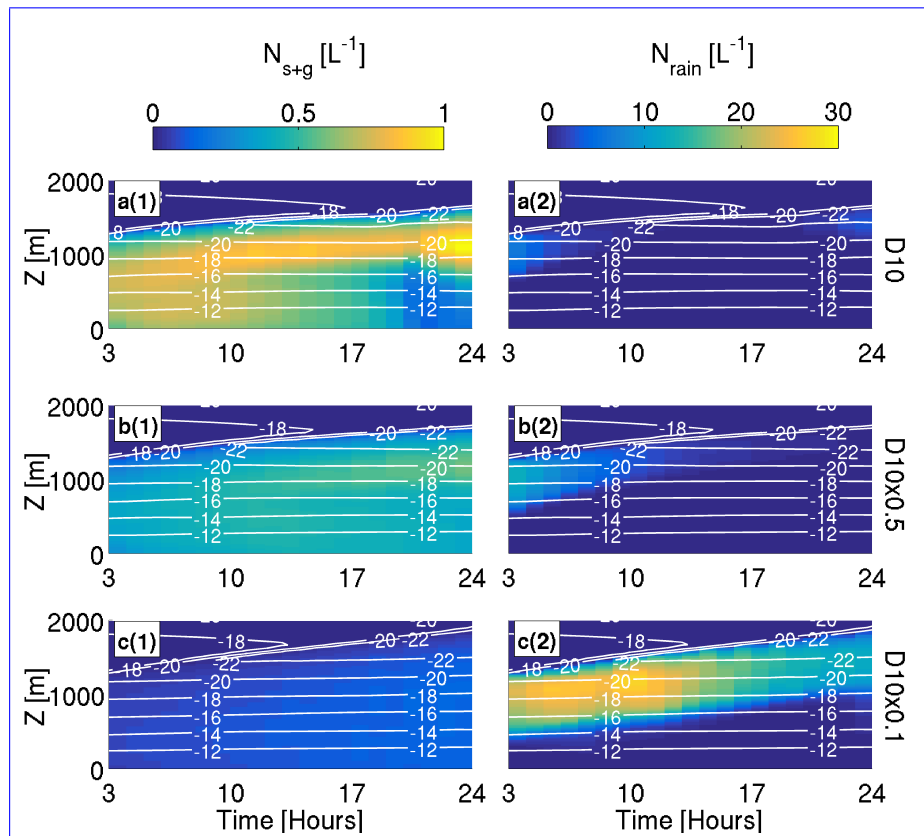


Figure S17. Number concentrations of solid (snow + graupel, N_{s+g} , **left-column1**) and liquid (rain, N_{rain} , **right-column2**) precipitation precipitable particles modelled during the **(a)** D10, **(b)** D10 \times 0.5, and **(c)** D10 \times 0.1 simulations over the ocean (case 3). Note changing colour bars for each subfigure.

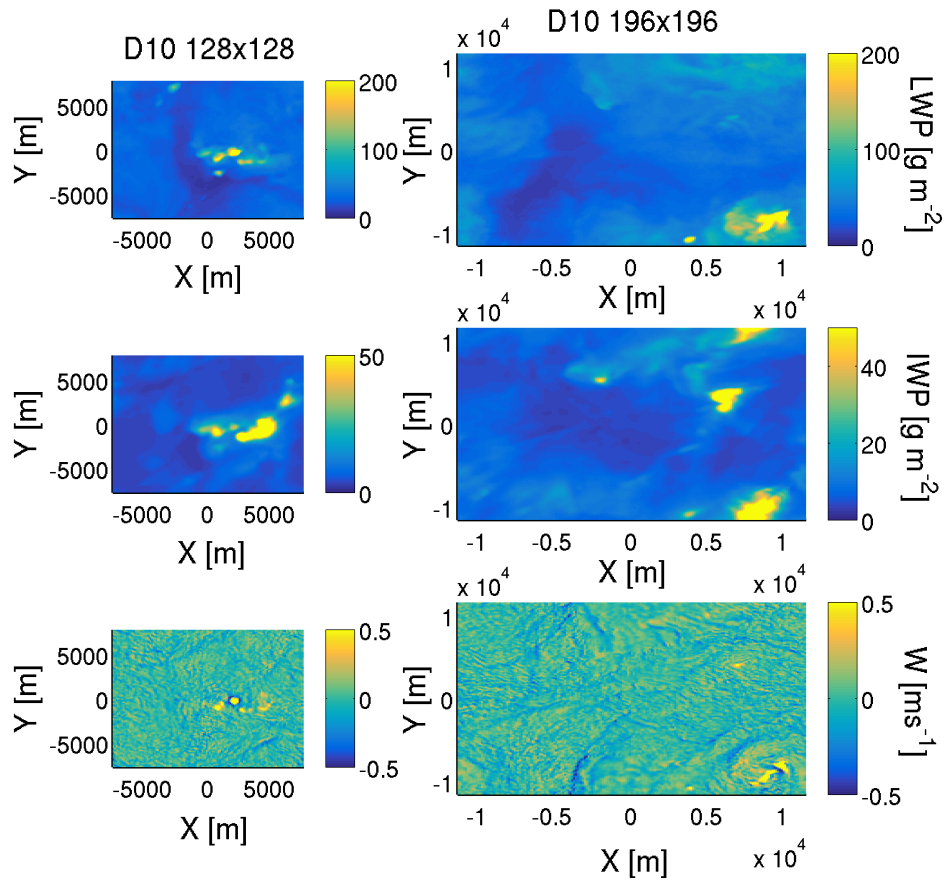


Figure S18. Modelled LWP (top row), IWP (second row), and W (at approximately 1500 m, bottom row) for domain sizes 128×128 grid points (left column) and 196×196 grid points (right column) at 21 h into the simulations. Both domains use X/Y resolution of 120 m and use the same vertical domain size and resolution; the only difference is the domain size in X/Y. Convective cells – as shown by the hot-spots in LWP, IWP, and W – form in both cases, suggesting that these phenomena were not a result of the original domain specifications. [Note changing colour bars for each subfigure.](#)

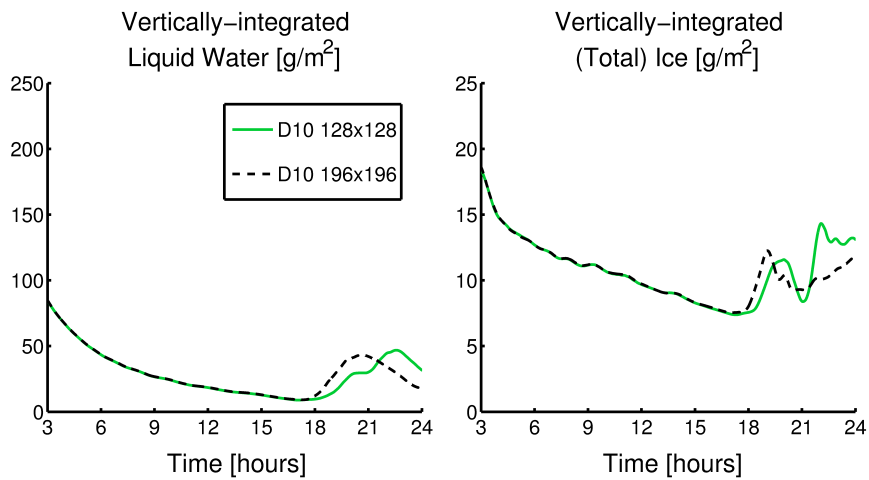


Figure S19. Modelled LWP (**left panel**) and IWP (**right panel**) with time for the original domain size (128×128 grid points, **green**) and the larger domain size (196×196 grid points, **black**) over the ocean (case 3). These traces diverge at approximately 18 h; however, similar trends are seen. The feedbacks associated with convection and precipitation formation affect the evolution of the cloud properties, leading to different LWP and IWPs. These differences are due to the influence of the domain size on, for example, cloud radiative cooling and entrainment, leading to the formation of different convective cells, of different sizes, to the original domain.

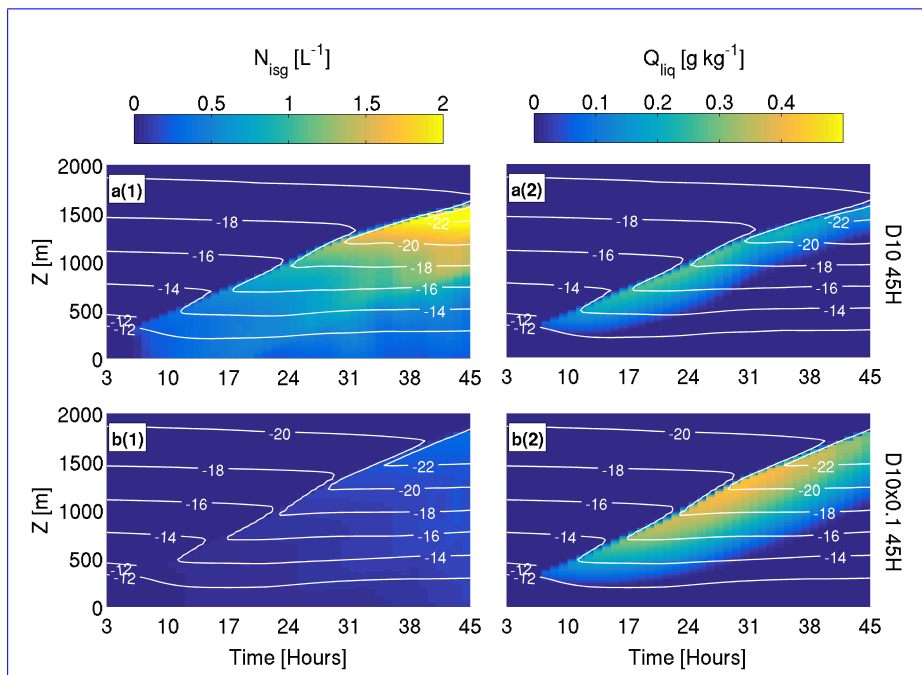


Figure S20. Modelled N_{ice} (**left column 1**) and Q_{liq} (**right column 2**) when using **(a)** D10 (**top row**) and **(b)** D10 \times 0.1 (**bottom row**) to simulate case 2 over an extended run time of 45 h. Note changing colour bars for each subfigure.

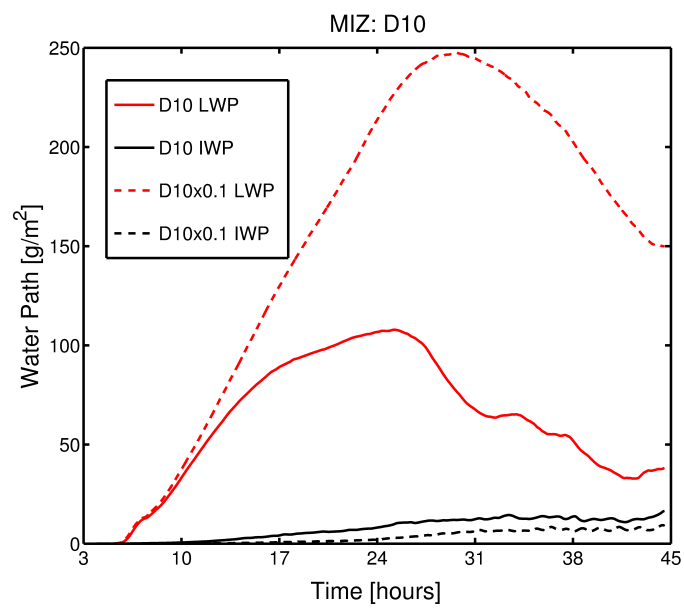


Figure S21. Modelled LWP (red) and IWP (black) when using D10 (**solid**) and D10×0.1 (**dashed**) to simulate case 2 over an extended run time of 45 h.

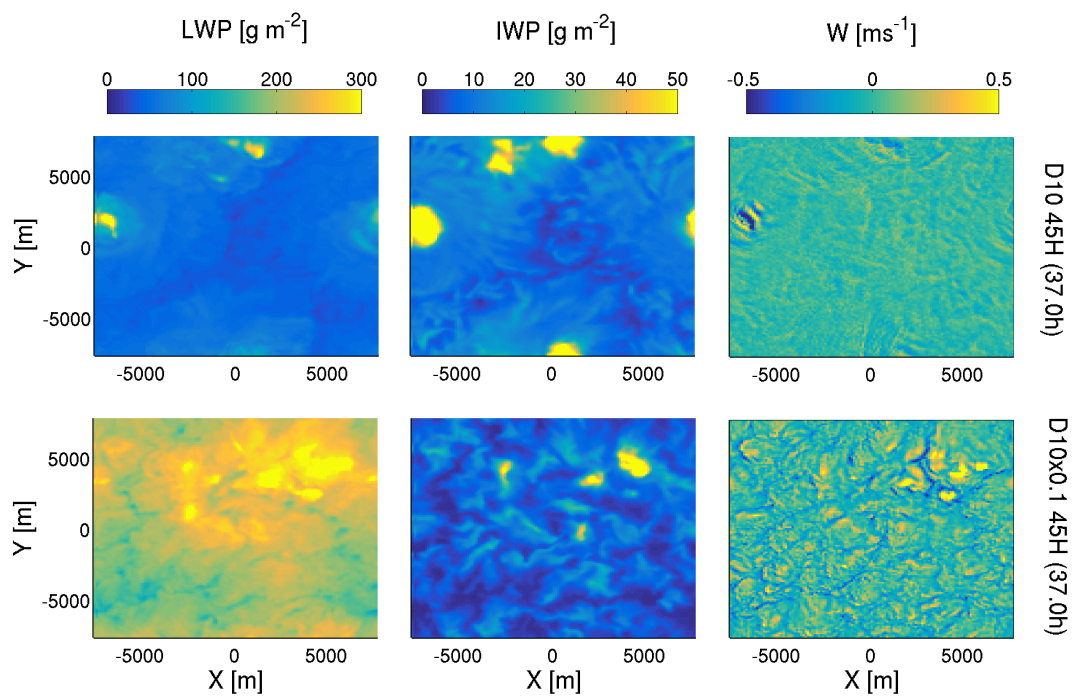


Figure S22. Modelled LWP (first column), IWP (second column), and vertical velocity (third column) at approximately 1500 m using D10 (top row) and D10×0.1 (bottom row) to simulate case 2. Planar X-Y slices are shown at 37 h. [Note changing colour bars for each subfigure.](#)

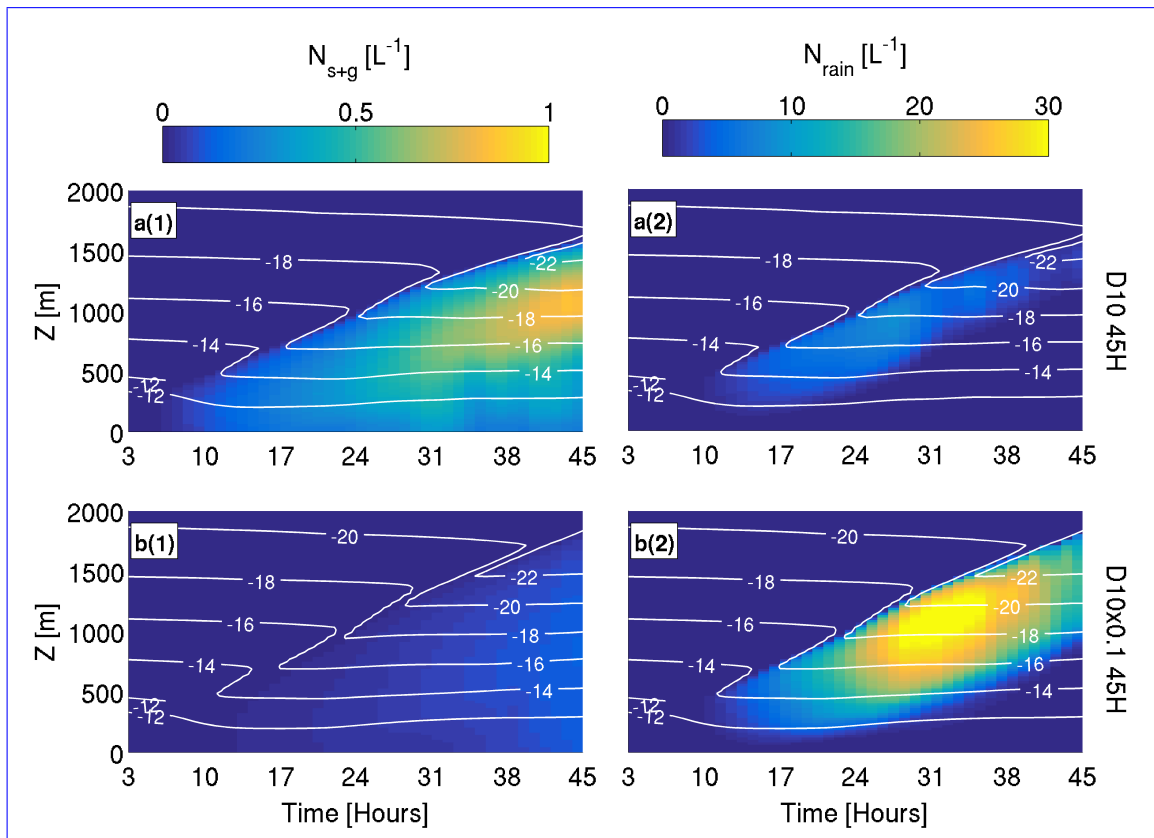


Figure S23. Modelled number concentrations of solid (N_{s+g} , **left column 1**) and liquid (N_{rain} , **right column 2**) precipitation-precipitable particles when using **(a)** D10 (**top row**) and **(b)** D10 \times 0.1 (**bottom row**) to simulate case 2 over an extended run time of 45 h. Note changing colour bars for each subfigure.